034796-4-T

Parallel Electromagnetic Solvers for High Frequency Antenna and Circuit Design

Linda P.B. Katehi

January 1999

Parallel Electromagnetic Solvers for High Frequency Antenna and Circuit Design

Graduate Students : Donghoon Chen and Eray Yasan

Research Fellow : Jong-Gwan Yook

Principal Investigator : Linda Katehi

Radiation Laboratory

Department of Electrical Engineering and Computer Science

The University of Michigan, Ann Arbor, MI 48109-2122, U. S. A.

Project Leader: : Leo DiDomenico and Dr. Barry Perlman

Applied Communications-Electronics Laboratory

US Army Communications-Electronics Command (CECOM)

Command Control & Systems Integration Directorate

AMSEL-RD-C2, Ft. Monmouth, N.J. 07703

Contents

1 Introduction

This report summarizes the effort on the development of accurate and computationally efficient codes for large scale electromagnetic problems with emphasis on three-dimensional monolithic circuits for high-frequency applications. This development will be successfully accomplished by two approaches:

- increasingly sparse matrix techniques also known as near matrix diagonalization (NMD) techniques

- code parallelization using Massage Passing Interface (MPI).

In the following, description of CHSSI scalable software project goals and progress summaries for various efforts are provided.

2 Project Goal

High-frequency radar systems for communication, detection and surveillance incorporate MMIC modules which are characterized by high density and substantial geometrical complexity. In most cases these modules are packaged for electrical and/or environmental protection and the resulting 3D structures exhibit a considerable complexity that impedes design and influences electrical performance due to unwanted parasitics. The design of these complex three-dimensional monolithic circuit (MMIC modules) with hundreds of vias and lines interconnecting a large number of active and passive circuit components to a rather large number of radiating elements, has been a problem of critical importance to DoD. The design and characterization of these circuits requires numerical approaches which can fully characterize the excited electromagnetic fields. Among the various techniques, the method of moments has demonstrated superiority in solving radiation problems but it has been hindered by long computational times and is limited, for this reason, to small circuits not exceeding more than a few components and interconnecting lines.

In this study, we have concentrated on the development of codes which have the capability to accelerate numerical computations in electromagnetic problems with large computational domains and/or computationally intensive tasks. Among the existing full-wave methods which have been developed for the solution of EM problems are the Integral Equation Technique (IE) and Finite Element Method (FEM). These methods are numerical techniques which solve Maxwell's Equations in the frequency domain using large computational volumes and intensive numerical calculations which have to be performed repeatedly at all frequency points of interest. In addition to these problems, the numerical solution of Maxwell's Equations results in full (IE case) and huge sparse (FEM case) matrices which further limit applicability of the technique. With

regards to substantially increasing the computational efficiency of these techniques, we concentrate on improving IE method through near-matrix diagonalization techniques(multiresolution analysis) as well as code parallelization and FEM through task parallelization.

The project leverages on existing synergism between DOD and the University of Michigan efforts on large-scale simulations of advanced software systems. The team will concentrate on the development, validation, documentation, visualization, and demonstration of scaleable algorithms for modeling critical DOD problems in high frequency electromagnetic circuits. Technology transfer to the DOD user community is an integral component of the project. In addition, cross-platform portability and software reusability will be emphasized using the Message-Passing Interface (MPI) standard.

In our effort, the developement of scalable softwaresis based on the IE and FEM techniques to sustain the high accuracy capability while, at the same time, solve complex planar circuits including their packages in very short times, allowing for real time simulations. Such softwares can eventually lead to real time design and optimization.

3   Integral Equation with Multiresolution Analysis [1, 2]

From our previous study, it has been indicated that the use of Multiresolution expansions in integral based formulations leads to the generation of highly sparse linear systems whose numerical solution is fast and efficient with minimal memory usage. This finding allows us to believe that application of wavelet techniques to the method of moments has made the modeling of large scale electromagnetic problems possible. The capability of the multiresolution analysis (MRA) to compete with the fastest up-to-date techniques, such as the Fast Multipole Method (FMM) and Multilevel Fast Multipole Method (MFMM) has been demonstrated through very thorough computer experiments. We expect this trend to sustain as the size of matrix increases to hundreds of thousands or millions.

The roof top multiresolution basis is used for the expansion of planar currents, in a way that the relevant boundary and edge conditions are satisfied to an appropriate degree of accuracy. Through this project it is shown that wavelet-dominated expansion bases generate highly sparse moment matrices and the resulting sparse linear systems can be solved numerically using very efficient computational tools. The fast wavelet transform is exploited for the numerical integration of the Green's function to speed up the matrix fill process. This work is emphasizing results for microstrip patch antenna and finite size arrays of such antennas. In addition, special emphasis is being placed on the solution of large-scale problems, which could not otherwise be handled by conventional moment method implementations. These efforts should yield a unique design capability for maintaining technology leadership.

The MRA allows the analysis software to perform a thresholding process on the entire ma-

trix. An additional benefit in the development of this software will be the available theoretical foundation for the thresholding required for matrix sparsification. The result of this code development will be the use of scaleable parallel high performance computing systems to solve electrically large electromagnetics problems of critical importance to DOD. While in these problems we have been able to provide matrix sparsities of the order of 99.9% (a perfectly diagonal matrix has a sparsity of $(1 - 1/N)\%$ which is equal to 99.99% for $N = 1000$), numerical computations have become more complex and lengthy. A large portion of these computations are in the form of multiple nested loops where similar types of intensive numerical computations are repeated. Furthermore, a large number of branched or cascaded loops are performed in a serial fashion. Parallelization of these code segments improves the speed and efficiency to a large extend. Another approach to improve the computation time is through the fast wavelet algorithm. This algorithm performs all the computations at the highest resolution level only once and then reconstructs the rest of the computations in the remain resolution levels very efficiently. In addition to code parallelization, domain decomposition techniques and task parallelization have a great potential with this technique and are applied in addition to near-matrix diagonlization.

Demonstration of scaleable simulations will address the critical DOD applications area of electrically large antennas integrated to multi-layer RF front end electronics which will itself be electrically large. Such systems need to be analyzed at the phenomenological level at one time in order to understand the details of device performance in the large subsystems environment.

4   Parallelized FEM for MMIC Simulation [1, 2, 5]

The numerical analysis of MMIC using parallel computer becomes powerful especially in FEM-based codes. The frequency parallelization of FEM achieves linearly scaleable performance with the number of processors being used. The frequency parallelization is completed using MPI standards for distributed memory machines such as IBM SP2. The application of frequency parallelized FEM code to microstrip feeding network for patch array antenna is accomplished and its field plot is available by a recently developed post field plotting Matlab file. Parallelization schemes will be further applied to the patch antenna structures including their microstrip feeding network using a hybrid method(MoM/FEM). This work will involve the parallelization of matrix generation for this hybrid method, the parallelization of far field calculation for each array antenna and the development of post-processor files for radiation patterns. The parallelized FEM scheme is also appropriate to the characterization of a microwave/millimeterwave package.

As efficient packaging technologies are emphasized for high frequency and high performance microwave/millimeter-wave circuits, it is very important to provide design rules to avoid unwanted electromagnetic effects of the package on the circuit performance. In this study, the electromagnetic effects of a via fense on a microstrip/stripline and the suppression of higher order

4

modes in the cavity are investigated.

In this study, three different types of via fences are considered: continuous metal filled via fence on both sides of the circuits, short section of a via fence on both sides of the circuits, and via fence cross to the circuits. In each case, the fence is moved between $1h$ to $4h$ from the circuit where h is the height between the ground plane and the center conductor of the circuit. As the scattering parameters and radiation loss of the circuits do not vary by more than a few percent over the simulation frequency (10 GHz - 40 GHz), average values over this frequency range are calculated for each case. Moreover, field distributions are also generated. The result shows that when the via fence is closer to the circuits the EM effects are stronger resulting in increased reflection coefficient, insertion and radiation loss. Furthermore, the results show that the closely spaced via fence confines more electric field than the wider spaced via fence giving less radiation loss. It is noted that the stripline shows better EM performance than microstrip over the via fence in the package.

The suppression of higher order packaging modes is studied for the cavity with two different types of striplines: (a) cavity with two isolated striplines and (b) cavity with one bent stripline. In the former case, via fence is placed between two isolated striplines and via gaps are changed from $57.228h$ to $13.932h$. In order to visualize the suppression of higher order modes in a quantitative way, only one stripline is excited and the ratio, maximum magnitude of total electric field on the unexcited stripline over the one on the excited stripline, is calculated. Results show that the via gap should be less than $0.394 \lambda_c$ for a of $1h \times 1h$ via to suppress unwanted cavity mode under -50 dB, where λ_c is the cutoff wavelength of the dominant mode in the cavity. The field distribution over the cavity is shown in the result. The cavity with bent stripline is simulated for different via gaps, from $56.76h$ to $2.6h$. The scattering paramenters of the stripline are calculated for each case and field distributions over the cavity are presented. It is seen that the via gap should not greater than $0.248 \lambda_c$ for a $1h \times 1h$ via to suppress cavity mode in the package.

All simulations have been carried out by a parallelized 3D-FEM. The frequency parallelization scheme is implemented in this study, due to the independent nature of the problem in the frequency domain. The parallel computer used for the simulation is the distributed memory IBM SP2 at the University of Michigan. The performance of the parallelized 3-D FEM program is near linearly improved with respect to the number of processes that are used.

This study shows the electromagnetic effects of a via fence on microstrip/stripline and the suppression of higher order modes in the package. The result can be used as guide lines for designing high performance and high frequency packages.

5 Active Circuits in FEM [6, 7]

Based on our previous research, we have launched an effort to analyze active as well as passive circuits, such as a mixer circuit (with 4 diodes), by use of FEM. This is an extension of our previous effort in the sense that we have added capability of handling nonlinear elements to our codes. Using the FEM, the Z parameters (or Y parameters) of the passive part of the circuit are computed and then these values are fed into a software such as Libra in the form of a linear data element with inner and outer ports. The linear or nonlinear elements are connected to inner ports and the whole circuit is analyzed by harmonic balance in order to find in/output characteristics.

The goal is to verify the experimental results of mixer circuits under consideration and make some further improvements. In the next step, the harmonic balance code will be integrated into the FEM method and will be parallelized. The direct inclusion of linear passive elements (resistors, capacitiors etc) into FEM code has already been accomplished.

A   User Manual for FEM part

A.1   Compilation and Execution

There are 2 important files, one for meshing and the other for FEM main program as illustrated in Fig. 1, and these files are written in high level language Fortran. The first file, `fem_mesh.f`, is a serial code, since it only takes a small fraction of overall solution process. However, the second Fortran code, `fem_main.f`, has been parallelized using Message Passing Interface (MPI) to enhance portability of the code on different parallel computer architectures and vendors.

Here are some examples of how to compile these 2 codes on parallel computers, for example, IBM SP2 and SGI Powerchallenge Array (PCA):

Compile meshing program	
conventional workstation	f77 -O -o fem_mesh.x fem_mesh.f

Compile main program	
on IBM SP2	mpxlf -us -O3 -lmpi -o fem_main.x fem_main.f
on SGI PCA	f77 -64 -O2 -o fem_main.x fem_main.f -L/usr/lib64 -lmpi

Executing these compiled codes is fairly straightforward for the meshing code, but not for the FEM main part. There are different methods for different parallel platforms. For IBM SP2, one can use LoadLeveler to submit jobs in a batch mode or can utilize interactive nodes for small size short running codes and for debugging purposes.

Here are some examples on executing the FEM main code on IBM and SGI machines:

Executing meshing program (phase I)	
conventional workstation	fem_mesh.x fem_mesh.f < input_mesh_file

Executing main program (phase II) with 8 CPUs	
on IBM SP2	fem_main.x -rmpool 0 -procs 8 < input_main_file
on SGI PCA	mpirun -np 8 fem_main.x < input_main_file

Note that these scripts are specific to the environment and operating systems. For example, Maui High Performance Computing Center (MHPCC) and Center for Parallel Computing (CPC) at the University of Michigan have similar IBM SP2 machines, but they have different batch systems and scheduling arrangements. Therefore, users need to be aware of what kind of system and environment they have to work with.
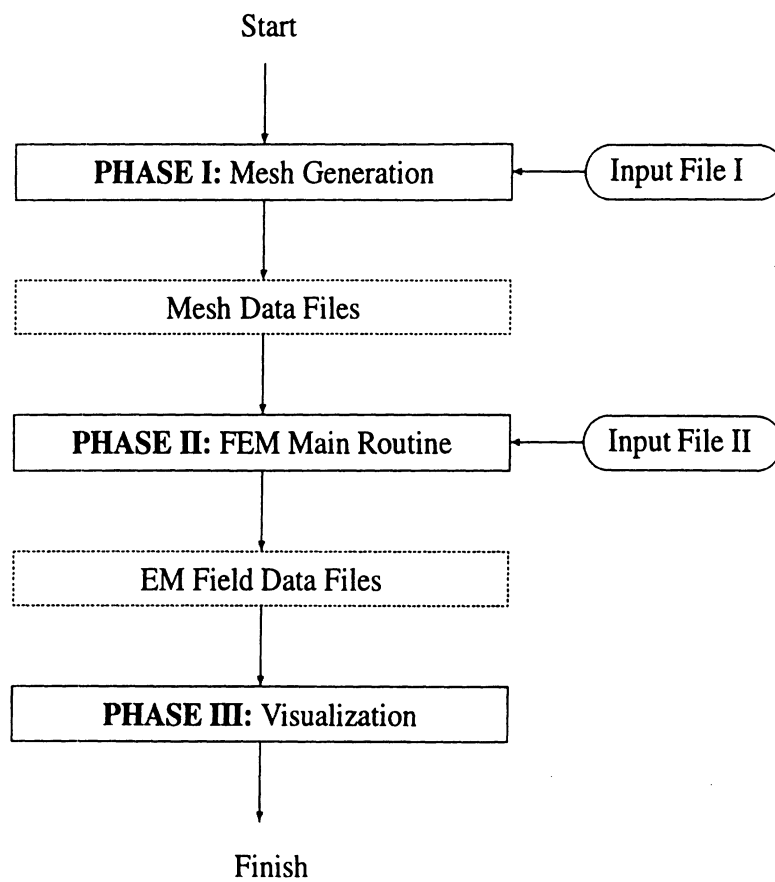
Start

PHASE I: Mesh Generation ← Input File I

Mesh Data Files

PHASE II: FEM Main Routine ← Input File II

EM Field Data Files

PHASE III: Visualization

Finish

Figure 1: Flow chart of the finite element method (FEM) solution process.

8

A.2 User Manual for Phase I - Mesh Generation

In this section, a brief description of the input file for **Phase I**, (mesh generation) is given. As an example, we have chosen to use a simple patch antenna on duroid substrate operating at 4.0 GHz. The schemetic of the antenna is shown in Fig. 2. To model this geometry, first, one needs to define an outer terminating boundary as shown in Fig. 3. This terminating boundary is crucial for mesh termination and control of the overall problem size. As shown in the figure, the distance of the boundary from the structure to be modeled, D_{side} and D_{top}, need to be at least 4 to 5 times greater than the substrate thickness or $0.2 \times \lambda_o$ for correct result. The outer boundaries are assigned to be perfect electric or magnetic (PEC or PMC) surface defending on the application.
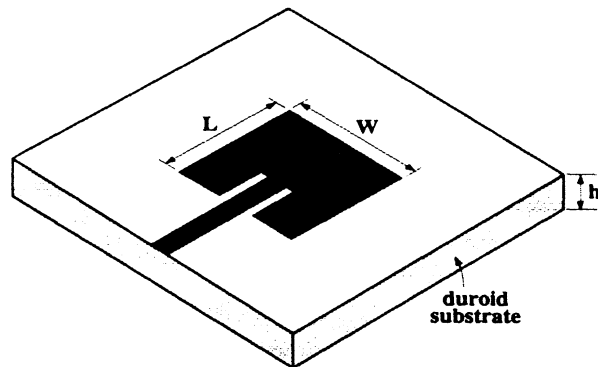

Figure 2: Single element patch antenna on duroid substrate: $L = 11.2$ mm, $W = 8.0$ mm, $h = 2.25$mm, $\epsilon_{duroid} = 10.8$

In addition, for simulation of open boundary problems, such as antennas, artificial absorbing materials need to be placed inside of the outer terminating boundaries as shown in Fig. 4. The material constants (ϵ_r and μ_r) are chosen to minimize the reflections at the interface and to maximize electromagnetic field attenuation in the material. Please refer to [3] for more details.

After the outer boundaries are defined, one needs to specify the location of the conducting surfaces, such as the antenna and its feeding network. As shown in Fig. 5, the antenna and feeding network are divided into number of rectangular sections that can be defined by any two diagonal points.
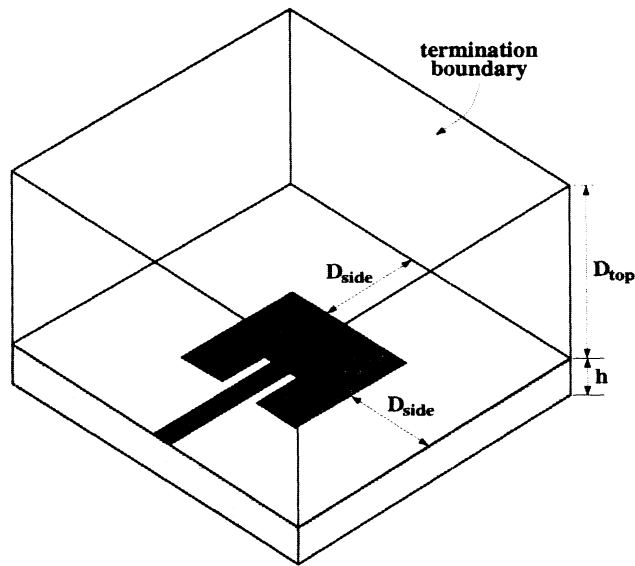
Figure 3: Illustration of total solution space and outer boundary.

Outer Boundary Definitions	
0.0, 24.0	x_{min}, x_{max}
-10.0, 54.0	y_{min}, y_{max}
0.0, 20.0	z_{min}, z_{max}

Note 1. One has to define all of the above parameters regardless of whether the solution space is an open or close boundary.

Note 2. For closed boundary problems, such as cavity problem, one can use all the outside surface as PEC.

Note 3. For open boundary problems, such as antenna problem, one needs to design and place artificial absorbing material inside of the outermost boundary.

Note 4. When there are symmetries in the problem, one can take advantage of the fact to reduce the overall problem size.
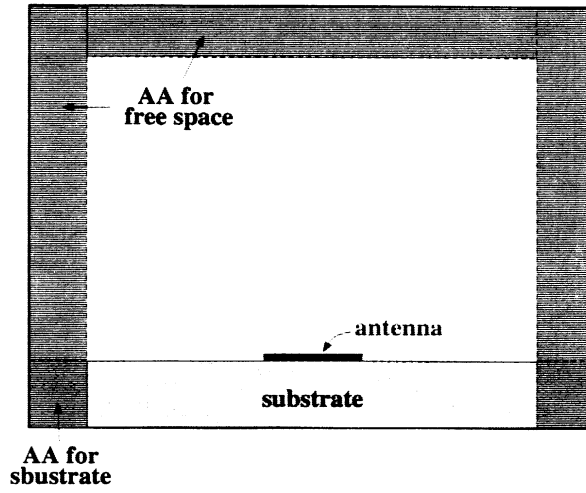
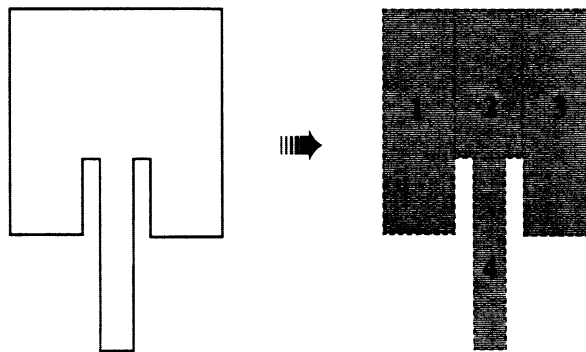Figure 4: Artificial absorbing layers for simulation of open boundary problem.

Figure 5: Example of surface boundary condition application with appropriate rectangulation.

Discretization	
2	discretization method :
	[1] uniform discretization
	[2] non-uniform discretization
5	number of divisions in x direction
1.00000, 4	$\Delta x_1, N_x^1$
1.00000, 16	$\Delta x_2, N_x^2$
0.80000, 3	$\Delta x_3, N_x^3$
0.50000, 1	$\Delta x_4, N_x^4$
0.55000, 2	$\Delta x_5, N_x^5$
6	number of divisions in y direction
1.00000, 4	$\Delta y_1, N_y^1$
1.00000, 26	$\Delta y_2, N_y^2$
0.76625, 8	$\Delta y_3, N_y^3$
0.84500, 6	$\Delta y_4, N_y^4$
0.94000, 20	$\Delta y_5, N_y^5$
1.00000, 4	$\Delta y_6, N_y^6$
3	number of divisions in z direction
0.85000, 3	$\Delta z_1, N_z^1$
1.24500, 10	$\Delta z_2, N_z^2$
1.00000, 5	$\Delta z_3, N_z^3$

Note. $\Delta x, y, z_i$: i^{th} *subsection size in* x, y, z-*direction.*
$N_{x,y,z}^i$: *number of* i^{th} *subsection.*

12

Material Property: Real and Imaginary Parts of Material	
9	number of material
10.8, 0.0	$Re(\epsilon_{r1})$, $Im(\epsilon_{r1})$: duroid substrate
1.0, 0.0	$Re(\mu_{r1})$, $Im(\mu_{r1})$
10.8, 15.0	$Re(\epsilon_{r2})$, $Im(\epsilon_{r2})$: AA for duroid substrate
1.0, 1.3889	$Re(\mu_{r2})$, $Im(\mu_{r2})$
10.8, 15.0	$Re(\epsilon_{r3})$, $Im(\epsilon_{r3})$: AA for duroid substrate
1.0, 1.3889	$Re(\mu_{r3})$, $Im(\mu_{r3})$
10.8, 15.0	$Re(\epsilon_{r4})$, $Im(\epsilon_{r4})$: AA for duroid substrate
1.0, 1.3889	$Re(\mu_{r4})$, $Im(\mu_{r4})$
1.0, 5.0	$Re(\epsilon_{r5})$, $Im(\epsilon_{r5})$: AA for free space
1.0, 5.0	$Re(\mu_{r5})$, $Im(\mu_{r5})$
1.0, 5.0	$Re(\epsilon_{r6})$, $Im(\epsilon_{r6})$: AA for free space
1.0, 5.0	$Re(\mu_{r6})$, $Im(\mu_{r6})$
1.0, 5.0	$Re(\epsilon_{r7})$, $Im(\epsilon_{r7})$: AA for free space
1.0, 5.0	$Re(\mu_{r7})$, $Im(\mu_{r7})$
1.0, 5.0	$Re(\epsilon_{r8})$, $Im(\epsilon_{r8})$: AA for free space
1.0, 5.0	$Re(\mu_{r8})$, $Im(\mu_{r8})$
1.0, 0.0	$Re(\epsilon_{r9})$, $Im(\epsilon_{r9})$: AA for free space
1.0, 0.0	$Re(\mu_{r9})$, $Im(\mu_{r9})$

Note 1. For each material, real and imaginary parts of the relative permitivity (ϵ_r) and permeability (μ_r) need to be defined as above.

Note 2. Artificial absorbers (AA) for free space and any arbitrary material have to be chosen by user. The formulars can be found in [3].

Material Allocations : $(x_{min}, y_{min}, z_{min})_i$ and $(x_{max}, y_{max}, z_{max})_i$ 2 points are diagonal of a cube containing given material	
4.0, -6.0, 0.0	$(x_{min}, y_{min}, z_{min})_1$
24.0, 50.0, 2.55	$(x_{max}, y_{max}, z_{max})_1$
0.0, -10.0, 0.0	$(x_{min}, y_{min}, z_{min})_2$
4.0, 54.0, 2.55	$(x_{max}, y_{max}, z_{max})_2$
4.0, -10.0, 0.0	$(x_{min}, y_{min}, z_{min})_3$
24.0, -6.0, 2.55	$(x_{max}, y_{max}, z_{max})_3$
4.0, 50.0, 0.0	$(x_{min}, y_{min}, z_{min})_4$
24.0, 54.0, 2.55	$(x_{max}, y_{max}, z_{max})_4$
0.0, -10.0, 2.55	$(x_{min}, y_{min}, z_{min})_5$
4.0, 54.0, 15.0	$(x_{max}, y_{max}, z_{max})_5$
4.0, -10.0, 2.55	$(x_{min}, y_{min}, z_{min})_6$
24.0, -6.0, 15.0	$(x_{max}, y_{max}, z_{max})_6$
4.0, 50.0, 2.55	$(x_{min}, y_{min}, z_{min})_7$
24.0, 54.0, 15.0	$(x_{max}, y_{max}, z_{max})_7$
0.0, -10.0, 15.0	$(x_{min}, y_{min}, z_{min})_8$
24.0, 54.0, 20.0	$(x_{max}, y_{max}, z_{max})_8$
4.0, -6.0, 2.55	$(x_{min}, y_{min}, z_{min})_9$
24.0, 50.0, 15.0	$(x_{max}, y_{max}, z_{max})_9$

Note. Any 2 diagonal points can be used to define a cube whose material property is homogeneous.

Surface Boundary Conditions : $(x_{min}, y_{min}, z_{min})_i$ and $(x_{max}, y_{max}, z_{max})_i$	
2 points define the diagonal of a rectangle for i^{th} surface	

20.0, 20.0, 2.55	$(x_{min}, y_{min}, z_{min})_1$: patch 1
22.4, 31.2, 2.55	$(x_{max}, y_{max}, z_{max})_1$
1	"1" for PEC, "0" for PMC
y	"y" for more surface, "n" for no more surface to define
22.4, 26.13, 2.55	$(x_{min}, y_{min}, z_{min})_2$: patch2
24.0, 31.2, 2.55	$(x_{max}, y_{max}, z_{max})_2$
1	PEC
y	more surface to define
22.7, -10.0, 2.55	$(x_{min}, y_{min}, z_{min})_3$: input feeding line
24.0, 26.13, 2.55	$(x_{max}, y_{max}, z_{max})_3$
1	PEC
y	more surface to define
0.0, -10.0, 0.0	$(x_{min}, y_{min}, z_{min})_4$: bottom surface
24.0, 54.0, 0.0	$(x_{max}, y_{max}, z_{max})_4$
1	PEC
y	more surface to define
0.0, -10.0, 20.0	$(x_{min}, y_{min}, z_{min})_5$: top surface
24.0, 54.0, 20.0	$(x_{max}, y_{max}, z_{max})_5$
1	PEC
y	more surface to define
0.0, -10.0, 0.0	$(x_{min}, y_{min}, z_{min})_6$: left surface
0.0, 54.0, 20.0	$(x_{max}, y_{max}, z_{max})_6$
1	PEC
y	more surface to define
0.0, -10.0, 0.0	$(x_{min}, y_{min}, z_{min})_7$: front surface
24.0, -10.0, 20.0	$(x_{max}, y_{max}, z_{max})_7$
1	PEC
y	more surface to define

Boundary Conditions (Surface) : continued	
`24.0, -10.0, 0.0`	$(x_{min}, y_{min}, z_{min})_8$: right surface
`24.0, 54.0, 20.0`	$(x_{max}, y_{max}, z_{max})_8$
`0`	PMC
`y`	more surface to define
`0.0, 54.0, 0.0`	$(x_{min}, y_{min}, z_{min})_9$: back surface
`24.0, 54.0, 20.0`	$(x_{max}, y_{max}, z_{max})_9$
`1`	PEC
`y`	more surface to define
`23.45, -5.0, 1.7`	$(x_{min}, y_{min}, z_{min})_{10}$: excitation place
`23.45, -5.0, 2.55`	$(x_{max}, y_{max}, z_{max})_{10}$
`1`	PEC
`n`	NO more surface to define

Note 1. PEC - Perfect electric conductor.

PMC - Perfect magnetic conductor.

Note 2. These boundary conditions can be utilized to define symmetric boundary conditions depending on the electromagnetic field distribution.

Excitation Points :	
define 2 end points $(x_{min}, y_{min}, z_{min})_i$ and $(x_{max}, y_{max}, z_{max})_i$	
`1`	number of excitation points
`23.45, -5.0, 1.7`	$(x_{min}, y_{min}, z_{min})_1$
`23.45, -5.0, 2.55`	$(x_{max}, y_{max}, z_{max})_1$

Note. One has to define a PEC line for excitation edges. You may need to define more than 1 line as it is in the case of coplanar waveguide (CPW).

Impedance Load Definition	
`0`	"0" for no impedance loads
	"1" for impedance loads

Note. One can use this option to define lumped circuit element, such as R, L, and C.

A.3 Sample Output Data Files for Phase I

In this section, the first few lines of each of the output data files are shown for better understanding. In general, the user does not need to modify or look into these mesh output data files. These files will be read from the FEM main program as described in phase II. In terms of storage space requirement, these output data files range from several Mega-byte to 100 Mega-byte depending on overall mesh size.

File Name : DAT_EDGY

Description : edge label and x, y, and z components of the edge vectors.

---

1   0.0000000000000000E+00   1.000000000000000   0.8500000000000000

2   1.000000000000000   1.000000000000000   0.0000000000000000E+00

...

File Name : DAT_EGLB

Description : material constants, number of nodes and tetrahedrons, and node labels for non-overlapping edges.

1

10.80000   0.0000000000000000E+00

1.000000   0.0000000000000000E+00

2

10.80000   15.00000000000000

1.000000   1.388900000000000

...

8

1.000000   5.000000000000000

1.000000   5.000000000000000

9

1.000000   0.0000000000000000E+00

1.000000   0.0000000000000000E+00

35397

159120

1   1 1 1891 2

1   2 1 29   2

1   3 1 28   2

...

File Name : DAT_ELMT
Description : element labels, 4 nodes for each tetrahedron, and material index.

1	1	1891	29	28	2
2	29	1891	1865	1892	2
3	1	2	29	1865	2
4	1	1891	1865	1864	2
5	1	1891	1865	29	2
6	29	1865	1893	1892	2
7	1865	3	1893	1866	2
8	29	1865	3	2	2
9	29	3	1893	30	2
10	29	3	1893	1865	2

. . .

File Name : DAT_ESUR
Description : surface edge definitions.

31996	6420	6421	1
32151	6420	6447	1
32004	6421	6422	1
32156	6421	6447	1
32158	6421	6448	1
32160	6421	6449	1
32328	6450	6477	1

. . .

File Name : DAT_EXCI
Description : excitation position definition.

28045

File Name : DAT_GRID
Description : surface edge definitions for later visualizations.

1	20.000000	20.000000	2.5500000	20.800000	20.000000	2.5500000
1	20.000000	20.000000	2.5500000	20.000000	20.766250	2.5500000

. . .

File Name : DAT_GRUP
Description : node labels on each surface definition.

PEC NODE ON SURFACE	1
1	60
1	6420
2	6421
3	6422
4	6423
5	6447

. . .

File Name : DAT_NODE
Description : node coordinate table.

1	0.00000000E+00	-10.000000	0.00000000E+00
2	1.0000000	-10.000000	0.00000000E+00
3	2.0000000	-10.000000	0.00000000E+00
4	3.0000000	-10.000000	0.00000000E+00

. . .

File Name : DAT_NUMB
Description : total number surface, edges and edges on surfaces.

9
201436
21181

A.4 User Manual for Phase II - FEM Main Program

In this section, a brief description of the input file for **Pahse II**, FEM main program, is given. This input file contains parameters for geometry selection and some other miscellaneous data as will be described below. Also, operating frequency range and output data file names for each frequency point are required. For electromagnetic field sampling in the solution domain, the user has to provide appropriate cross-section and coordinates for two diagonal points of the circuit cross-section. Finally, the user can select appropriate iterative solver convergence criteria to specify the residual norm. In most case, 10^{-3} to 10^{-4} will be enough.

Problem Definition	
1	What problem will be solved?
	[1] PEC/PMC/Artificial absorber
	[2] 1st order absorbing boundary condition
	[3] 2nd order absorbing boundary condition
1	What excitation mechanism (only for 2-port network)?
	[1] Even
	[2] Odd
	Note: For 1-port network, you can choose either 1 or 2.

Miscellaneous Parameters : These parameters provide optional information for discretization	
0.05	Global mesh size
0.5	Length of the structure
7.5	Approximate effective dielectric constant

Note: These parameters do not affect the accuracy and performance of the (parallel) FEM code

Operating Frequency Range and Output File Names	
`3.80`	Start frequency (f_{start})
`4.20`	Stop frequency (f_{stop})
`0.02`	Frequency step (Δf)
`ant-array-3.80ghz.m`	Output data file names
`ant-array-3.82ghz.m`	
`ant-array-3.84ghz.m`	
`ant-array-3.86ghz.m`	
`ant-array-3.88ghz.m`	
`ant-array-3.90ghz.m`	
`ant-array-3.92ghz.m`	
`ant-array-3.94ghz.m`	
`ant-array-3.96ghz.m`	
`ant-array-3.98ghz.m`	
`ant-array-4.00ghz.m`	
`ant-array-4.02ghz.m`	
`ant-array-4.04ghz.m`	
`ant-array-4.06ghz.m`	
`ant-array-4.08ghz.m`	
`ant-array-4.10ghz.m`	
`ant-array-4.12ghz.m`	
`ant-array-4.14ghz.m`	
`ant-array-4.16ghz.m`	
`ant-array-4.18ghz.m`	
`ant-array-4.20ghz.m`	

Note 1. The number of frequency points are determined by $(f_{stop} - f_{start})/\Delta f$.

Note 2. For task parallelization scheme, the best linear scalability can be achieved when the number of CPUs is equal to the number of frequency points.

Electromagnetic Field Sampling	
2	Which cross section do you want to cut?
	[1] X-Z plane(constant y plane)
	[2] X-Y plane(constant z plane)
	[3] Y-Z plane(constant x plane)
0.010, 23.99	x_{min}, x_{max}
-9.98, 55.99	y_{min}, y_{max}
2.56	Constant z

Note. If you choose [1], you need to provide (x_{min}, x_{max}) first, (z_{min}, z_{max}) second, and constant y.
If you choose [3], you need to provide (y_{min}, y_{max}) first, (z_{min}, z_{max}) second, and constant x.

Resistive Material	
2	Resistive material?
	[1] Yes, [2] No

Iterative Solver (BiCG or QMR) Convergence Criterion	
1.0^{-4}	Tolerence (residue) $\leq 10^{-4}$

B Benchmarking

In this section, some benchmarking examples of our parallel electromagnetic solvers are illustrated. As shown in Fig. 6, a 2-element patch array antenna has been simulated using different number of CPUs: 1 to 25. The direct output of the simulator provides electromagnetic field data as illustrated in Fig. 7. From thsese data, one can easily extract important circuits parameters, such as S-parameters, can be extracted as shown in Fig. 8.
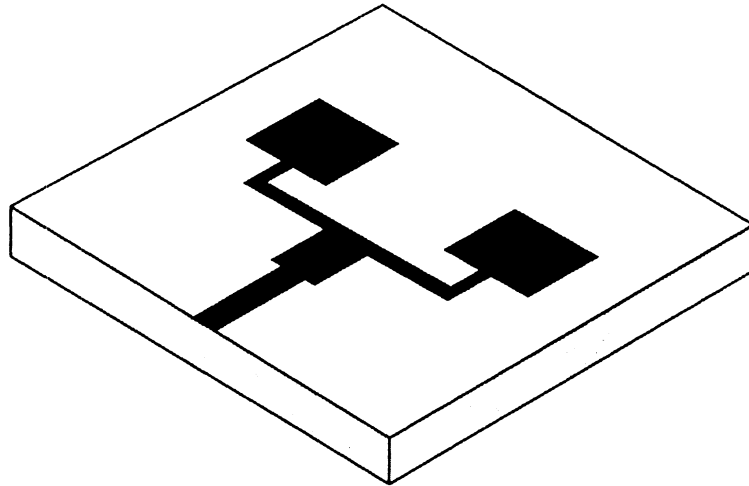
Figure 6: 2 element patch array antenna with corporate feeding network.
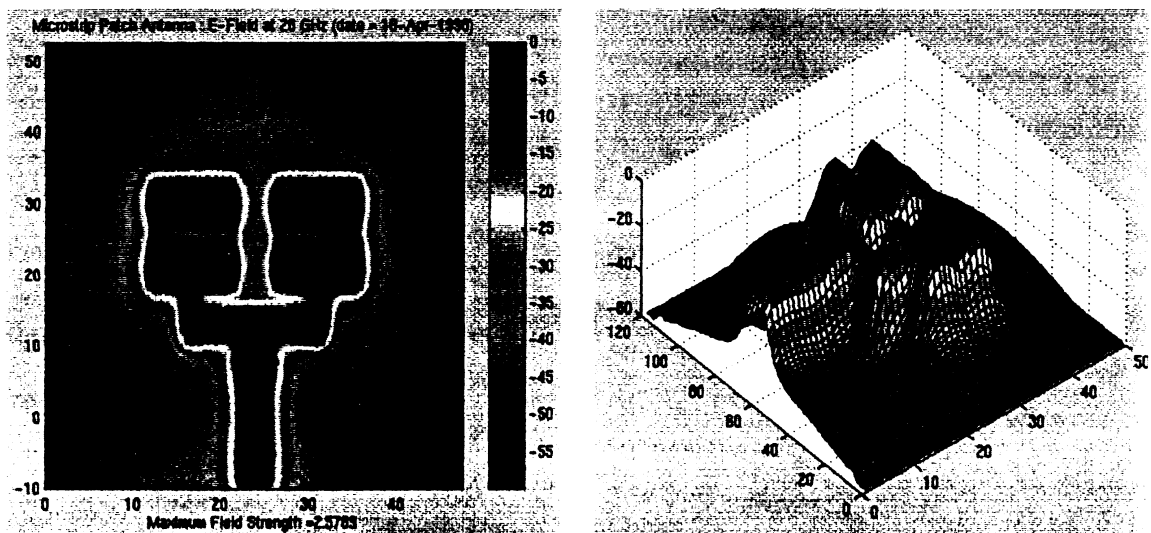
Figure 7: Electromagnetic field distributions for 2 element patch array antenna with corporate feeding network.
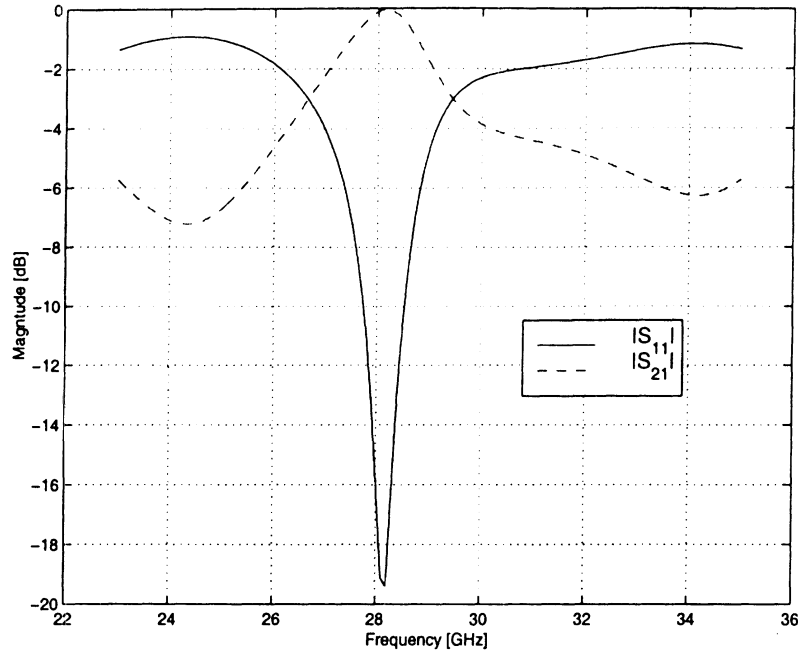
Figure 8: Scattering parameters for 2 element patch array antenna with corporate feeding network.

In this particular example, we have computed the electromagnetic field distribution at 25 different frequency points using our *task parallelized* solver and we also presented speedup curves for various number of CPUs(Fig. 9). As shown in the figure, we have achieved linear scalability on distributed memory machine using MPI (Message passing interace) standard. It needs to be pointed out that with our task parallelization strategy the best performance can be achieved when there are $p = M/2^n$ processors, where M is the total number of frequency points to be computed and $n = \{0, 1, 2, 3, \ldots\}$. When M is not a multiple of 2, $p = int(M/2^n) + mod(M, M/2^n)$.

The scalability of a parallelized code can be studied by examining the load balancing between different processors. As shown in 10, the best performance is achieved when we have good load balancing between those CPUs. For example, when one needs to obtain 40 frequency data, the best scalability can be achieved when there are 40 CPUs available. However, if there are only 30 CPUs available, the use of 30 or 20 CPUs will not make a big difference.

As a last example, Fig. 11 shows the coupling between two radiating antenna element in an array environment. For this study, conventional and micromachined silicon substrates are used as depicted in the figure. Apart from the coupling issues, this example demonstrates the capability of our parallel electromagnetic codes to solve and visualize very complicate electromagnetic field distributions. This will be greatly useful to RF circuit and antenna designers and even to engineers in DoD community.
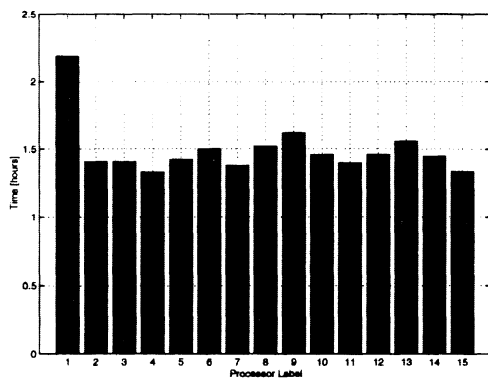
24
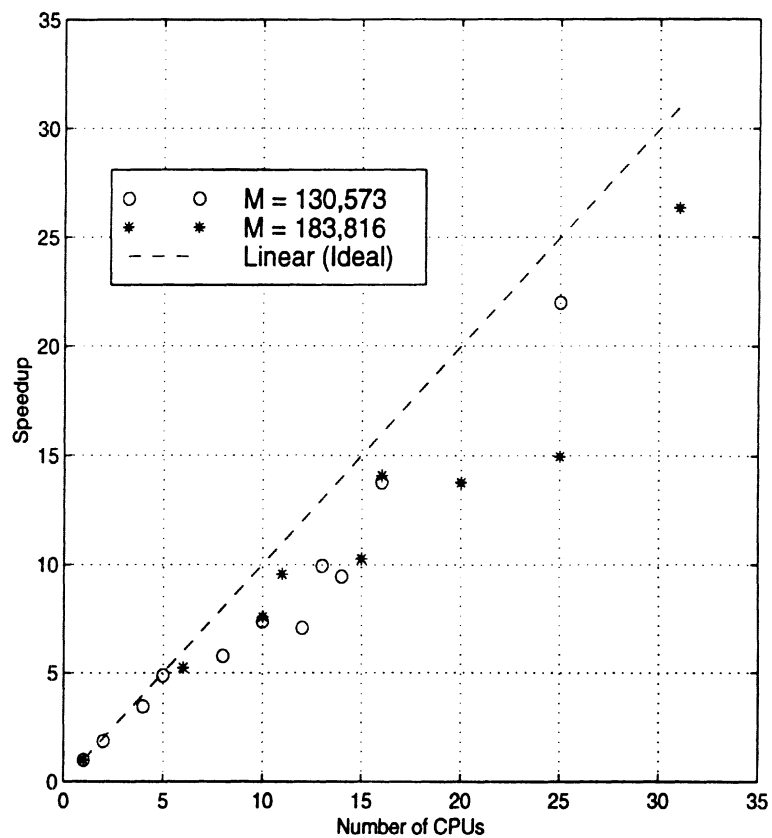
Figure 9: Speedup curves for two different problem sizes. M is the number of unknowns to be solved.
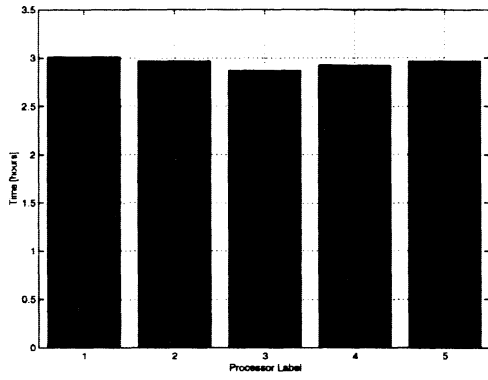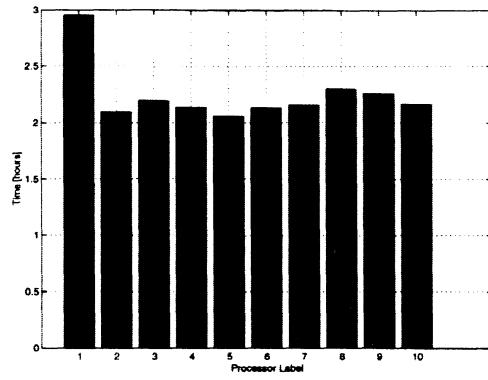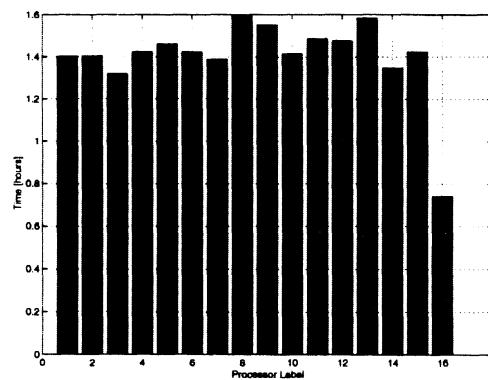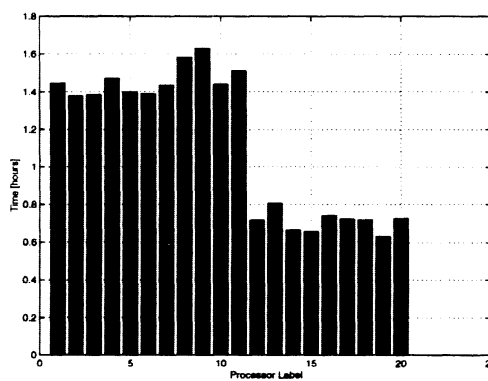
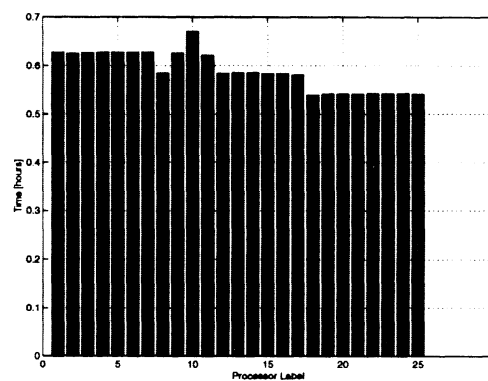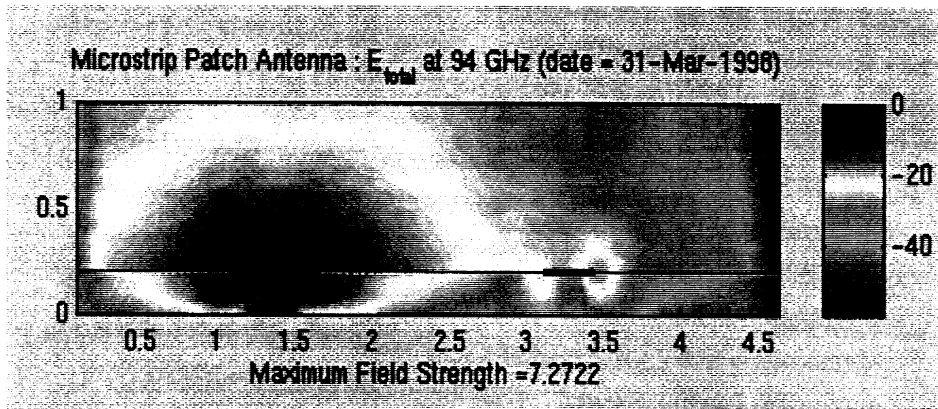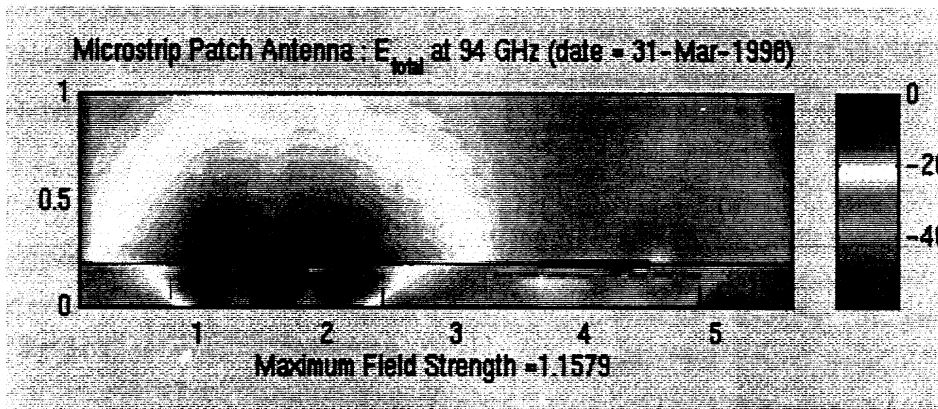Figure 10: Load balancing characteristics for different number of CPUs (N): (a) $N = 5$ (b) $N = 10$ (c) $N = 15$ (d) $N = 16$ (e) $N = 20$ (f) $N = 25$

Figure 11: Coupling between two adjcent radiating elements: (a) Antenna on conventional substrate. (b) Antenna on micromachined substrate.

C User Manual for Hybrid (FEM + MoM) Method

C.1 Procedure

In this section, a brief description of hybrid method is given. As can be seen in Fig. 12, the FEM and MoM solutions are combined to yield circuit parameters or electromagnetic field distribution.
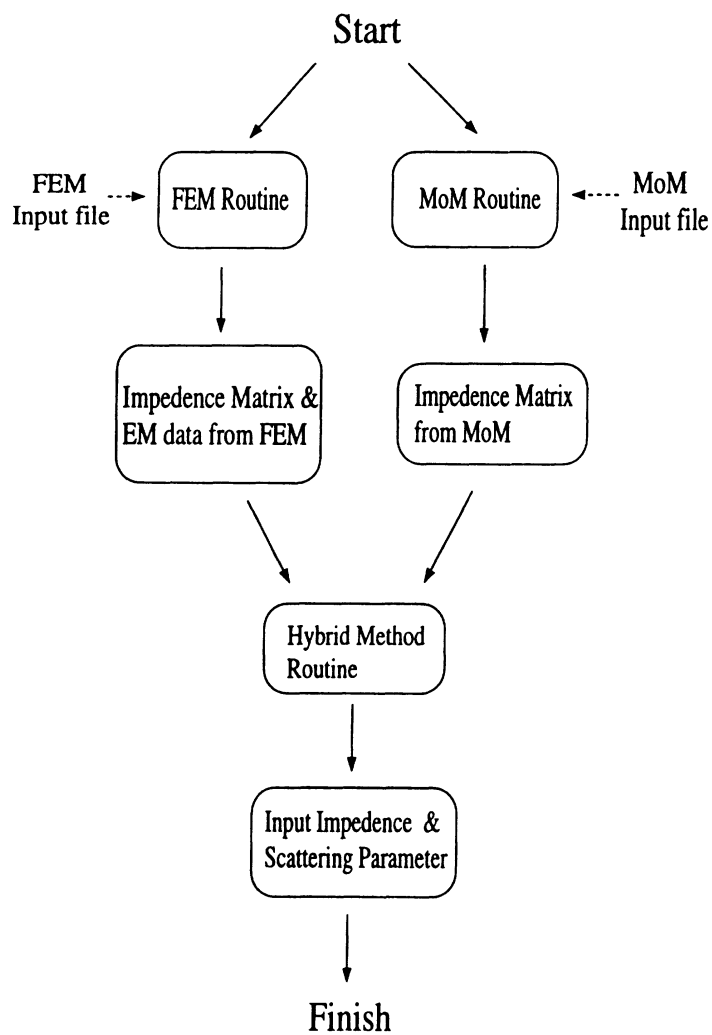
Figure 12: Flow chart of the hybrid method solution process.

C.2 File flow chart

The hybrid method requires several different input files for FEM and MoM solution processes as described in Fig. 13. Also, some of output files are used in the next stage or contain final solution.
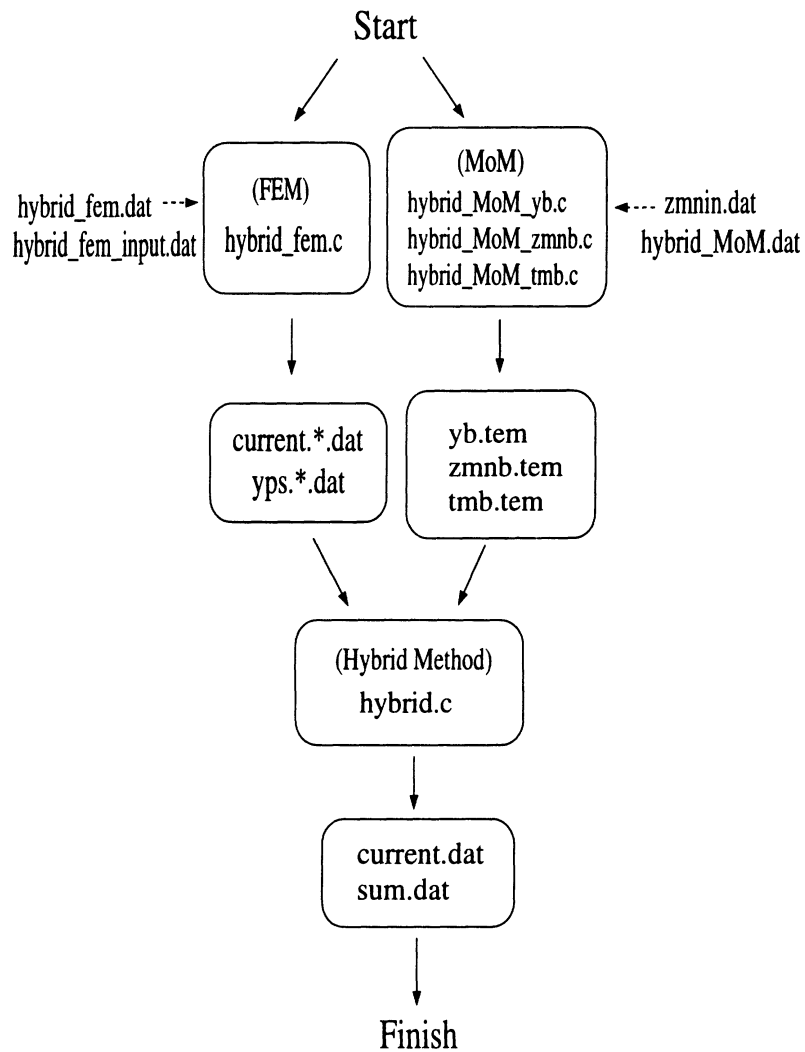
Figure 13: File flow chart of the hybrid method solution process.

C.3 File description

Here are descriptions of files, source codes, input and out files, for FEM, MoM, and hybrid method.

FEM file	
`hybrid_fem.dat`	FEM mesh input file.
`hybrid_fem_input.dat`	FEM input file.
`hybrid_fem.c`	FEM program.
`current.*.dat`	Output file : current information on microstrip for each excitation. File format: $Re(Ex), Im(Ex), Re(Ey), Im(Ey), Re(Ez), Im(Ez)$
`yps.*.tem`	Output file : Impedance matrix component for each excitation. *Note. * = 0,1,2,.... Numbered according to each excitation.*

MoM file	
`zmnin.dat`	MoM input file.
`hybrid_MoM.dat`	MoM input file.
`hybrid_MoM_yb.c`	MoM program for slot.
`hybrid_MoM_zmnb.c`	MoM program for patch.
`hybrid_MoM_tmnb.c`	MoM program for interaction between slot and patch.
`yb.tem`	Output file : Impedence matrix for slot.
`zmnb.tem`	Output file : Impedence matrix for patch.
`tmnb.tem`	Output file : Impedence matrix for interaction between slot and patch.

Hybrid method file	
`hybrid.c`	Hybrid program.
`current.dat`	Output file : current distribution on input microstrip, which is the final solution of the problem. Input impedence and scattering parameters are calculated with this information.
`sum.dat`	Output file : current profile on slot and patch. File format : Map is magnetic basis function profile on slot. Ib is current basis function profile on patch.

C.4 Compilation and Execution

In hybrid method there are 3 important steps. FEM, Method of Moment(MoM), and hybrid simulation which combines FEM and MoM results. All the programs are written in C++ language, which enables dynamic memory allocations and memory savings as a result. The programs are also parallelized using MPI to give portablility for different types of parallel computers.

As a first step, FEM program, hybrid_fem.c, is simulated using its data file, hybrid_fem.dat. Compilation and execution examples are shown as follows.

Compile FEM program
⋆ conventional workstation
g++ hybrid_fem.c −DDOMAINS −D_SUNC__ −o hybrid_fem.x −O2 −lm
⋆ IBM SP2
mpCC −+ hybrid_fem.c −DDOMAINS −DPARALLEL −D_GNUC__ −o hybrid_fem.x −O3 −lm

If the structure is symmetry, we can utilize it by adding option −DSYMMETY when compile in both conventional workstation and IBM SP2.

As mentioned before, FEM part of hybrid method can be simulated on two modes in IBM SP2, which is loadleveler mode and interactive mode. Here are some examples on executing the FEM code on conventional workstation and IBM SP2.

Executing FEM program
⋆ conventional workstation   hybrid_fem.x < hybrid_fem_input.dat (fem input file)

Executing FEM program with 8 CPUs
⋆ IBM SP2
hybrid_fem.x −rmpool 0 −procs 8 < hybrid_fem_input.dat (fem input file)

Compile MoM program
⋆ IBM SP2
mpCC −+ hybrid_MoM_yb.c −DPARALLEL −D_GNUC__ −o hybrid_MoM_yb.x −O3 −lm
mpCC −+ hybrid_MoM_zmnb.c −DPARALLEL −D_GNUC__ −o hybrid_MoM_zmnb.x −O3 −lm
mpCC −+ hybrid_MoM_tmb.c −DPARALLEL −D_GNUC__ −o hybrid_MoM_tmb.x −O3 −lm

Executing MoM program with 4 CPUs	
⋆ IBM SP2	hybrid_MoM_yb.x −rmpool 0 −procs 4 < zmnin.dat
	(MoM input file)
	hybrid_MoM_zmnb.x −rmpool 0 −procs 4 < zmnin.dat
	hybrid_MoM_tmb.x −rmpool 0 −procs 4 < zmnin.dat
Compile Hybrid program	
⋆ conventional workstation	g++ hybrid.c −D_SUNC__ −o hybrid.x −lm
⋆ IBM SP2	mpCC −+ hybrid.c −DPARALLEL −D_GNUC__ −o
	hybrid.x −O3 −lm
Executing Hybrid program	
⋆ conventional workstation	hybrid.x
⋆ IBM SP2	hybrid.x −rmpool 0 −procs 1

The structure, as an example, to be solved using hybrid method are shown below. FEM is used for microstrip feeding network where analytic Green's function is not known. Method of momentum(MoM) is used for patch antenna using Green's function. By combing the results from FEM and MoM, we can solve the whole structure, which is hybrid method.
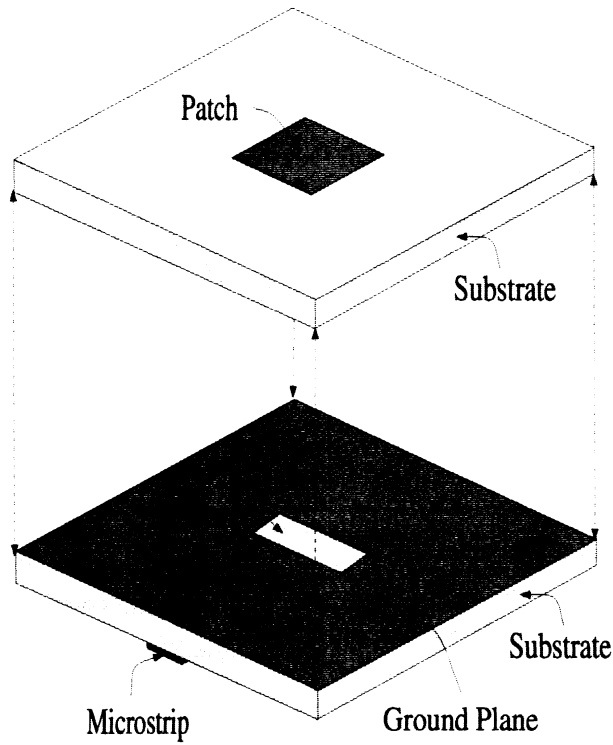

Figure 14: Single patch antenna with microstrip feeding network.

C.5   User Manual for FEM Mesh

In this section, a brief description of input files for FEM simulation is given.
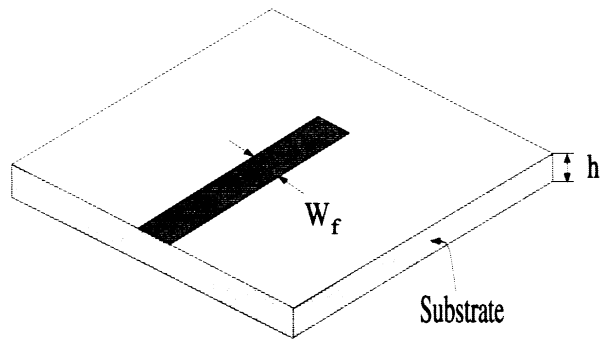
Figure 15: Microstrip feeding network.
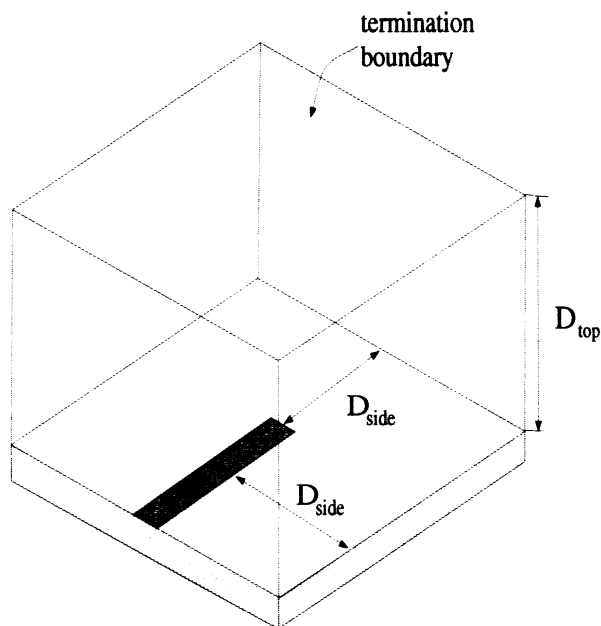
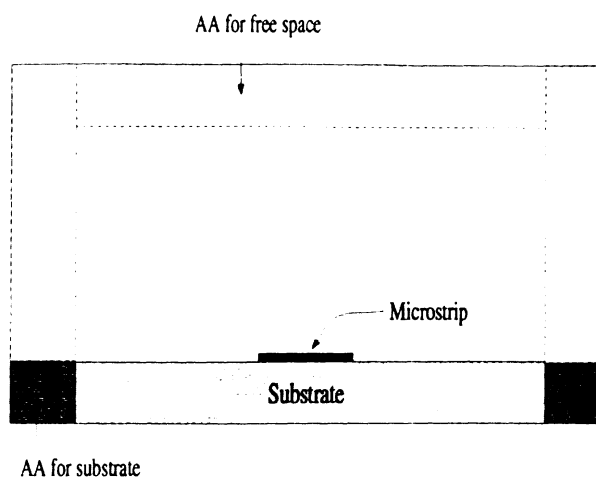Figure 16: Illustration of total solution space and outer boundary.

AA for free space

Microstrip

Substrate

AA for substrate

Figure 17: Artificial absorbing layers for simulation of open boundary problem.

Top mesh

Bottom mesh
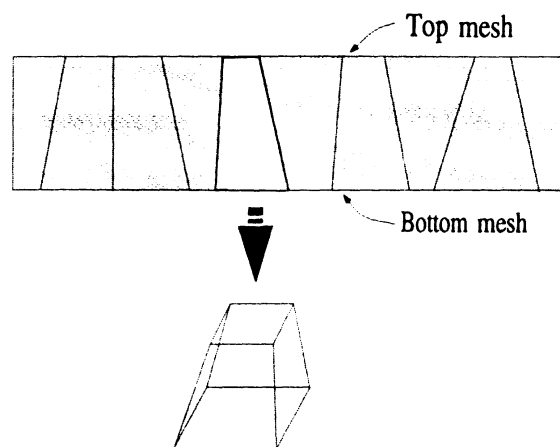
Figure 18: Meshing schemes for each layer.

FEM Part	
Discretization : file name (hybrid_fem.dat)	
2	Number of layer.
	⋆ Mesh the bottom section of first layer. ⋆
5	NS^1_{bx}
-39.45e-3 -27.45e-3	$x^1_{b1}, ...$
-6e-3 6e-3	.....
27.45e-3	$..., x^1_{b5}$
39.45e-3	x_{max}, End position
5 8 16 8 5	$N^1_{bx1}, ... , N^1_{bx5}$
6	NS^1_{by}
-202.55e-3	$y^1_{b1}, ...$
-182.55e-3	
-0.55e-3 0.55e-3	.....
20e-3 42e-3	$..., y^1_{b6}$
54e-3	y_{max}, End position.
5 70 2 8 8 5	$N^1_{by1}, ... , N^1_{by6}$
1	NS^1_{bz}
0	z^1_{b1}
1.6e-3	z_{max}, End position.
2	N^1_{bz1}
	⋆Mesh the top section of first layer.⋆
7	NS^1_{tx}
-39.45e-3 -27.45e-3	$x^1_{t1}, ...$
-6e-3 -2.475e-3	.....
2.475e-3 6e-3	.....
27.45e-3	x^1_{t7}
39.45e-3	x_{max}, End position.
5 8 5 6 5 8 5	$N^1_{tx1}, ... , N^1_{tx7}$
6	NS^1_{ty}
-202.55e-3	$y^1_{t1}, ...$
-182.55e-3	
-0.55e-3 0.55e-3	.....
20e-3 42e-3	$....., y^1_{t6}$
54e-3	y_{max}, End position.
5 70 2 8 8 5	$N^1_{ty1}, ... , N^1_{ty6}$

Discretization (continue)	
	★Mesh the bottom section of second layer.★
7	NS^2_{bx}
-39.45e-3 -27.45e-3	$x^2_{b1}, ...$
-6e-3 -2.475e-3	.....
2.475e-3 6e-3	.....
27.45e-3	x^2_{b7}
39.45e-3	x_{max}, End position.
5 8 5 6 5 8 5	$N^2_{bx1}, ... , N^2_{bx7}$
6	NS^2_{by}
-202.55e-3	$y^2_{b1}, ...$
-182.55e-3	
-0.55e-3 0.55e-3	.....
20e-3 42e-3	y^2_{b6}
54e-3	y_{max}, End position.
2	NS^1_{bz}
1.6e-3 22.4e-3	z^1_{b1}, z^1_{b2}
34.4e-3	z_{max}, End position.
8 5	N^1_{bz1}, N^1_{bz2}
	Mesh the top section of second layer.
7	NS^2_{tx}
-39.45e-3 -27.45e-3	$x^2_{t1}, ...$
6e-3 -2.475e-3	.....
2.475e-3 6e-3	.....
27.45e-3	x^2_{t7}
39.45e-3	x_{max}, End position.
5 8 5 6 5 8 5	$N^2_{tx1}, ... , N^2_{tx7}$
6	NS^2_{ty}
-202.55e-3	$y^2_{t1}, ...$
-182.55e-3	
-0.55e-3 0.55e-3	.....
20e-3 42e-3	....., y^2_{t6}
54e-3	y_{max}, End position.
5 70 2 8 8 5	$N^2_{ty1}, ... , N^2_{ty6}$

Note 1. $NS^i_{bx,by,bz} / NS^i_{tx,ty,tz}$: *Number of uniform mesh subsection of bottom/top for* i^{th} *layer in* x, y, z-*direction.*

37

Note 2. $x, y, z^i_{bj}/x, y, z^i_{tj}$: *Starting position of jth uniform mesh subsection in x,y,z-direction for bottom/top of ith layer.*

Note 3. $N^i_{bxj,byj,bzj}/N^i_{txj,tyj,tzj}$: *Number of division of jth uniform mesh subsection in x, y, z-direction for bottom/top of ith layer.*

Note 4. Top section and bottom section should be meshed for each layer and number of top mesh should be equal to the number of bottom mesh.

Note 5. For open boundary problems, such as antenna problem, one need to design and place artificial absorbing material inside of the outermost boundary.

Note 6. When there are symmetry in the problem, one can take advantage of the fact to reduce overall problem size.

Surface Boundary Conditions : $(x_{min}, x_{max}, y_{min}, y_{max}, z)_i$ 2 points are diagonal of a rectangle for i^{th} x-y surface	
1	Number of connected PEC domain
1	Number of PEC subdomain per connected PEC domain
-2.475e-3 2.475e-3	$(x_{min}, x_{max})_1$: microstrip
-200e-3 20e-3	$(y_{min}, y_{max})_1$
1.6e-3	z
1	Add edge above PEC domain (default)

Material Allocations : $(x_{min}, x_{max})_i$, $(y_{min}, y_{max})_i$, and $(z_{min}, z_{max})_i$ 2 points are diagonal of a cube containing given materal Material Property: Real and Imaginary Parts of Material $Re(\epsilon_{r1}), Im(\epsilon_{r1}), Re(\mu_{r1}), Im(\mu_{r1})$	
11	number of material
-27.45e-3 27.45e-3	$(x_{min}, x_{max})_1$
-182.55e-3 42e-3	$(y_{min}, y_{max})_1$
0 1.6e-3	$(z_{min}, z_{max})_1$
2.54 0.0	$Re(\epsilon_{r1}), Im(\epsilon_{r1})$: substrate
1.0, 0.0	$Re(\mu_{r1}), Im(\mu_{r1})$
-27.45e-3 27.45e-3	$(x_{min}, x_{max})_2$
-182.55e-3 42e-3	$(y_{min}, y_{max})_2$
1.6e-3 22.4e-3	$(z_{min}, z_{max})_2$
1.0 0.0	$Re(\epsilon_{r2}), Im(\epsilon_{r2})$: Free space
1.0, 0.0	$Re(\mu_{r2}), Im(\mu_{r2})$

-39.45e-3 39.45e-3	$(x_{min}, x_{max})_3$
-202.55e-3 54e-3	$(y_{min}, y_{max})_3$
22.4e-3 34.4e-3	$(z_{min}, z_{max})_3$
1.0 -5.0	$Re(\epsilon_{r3}), Im(\epsilon_{r3})$: AA for free space
1.0, -5.0	$Re(\mu_{r3}), Im(\mu_{r3})$
-39.45e-3 -27.45e-3	$(x_{min}, x_{max})_4$
-202.55e-3 54e-3	$(y_{min}, y_{max})_4$
0 1.6e-3	$(z_{min}, z_{max})_4$
2.54 -8	$Re(\epsilon_{r4}), Im(\epsilon_{r4})$: AA for substrate
1 -3.14961	$Re(\mu_{r4}), Im(\mu_{r4})$
27.45e-3 39.45e-3	$(x_{min}, x_{max})_5$
-202.55e-3 54e-3	$(y_{min}, y_{max})_5$
0 1.6e-3	$(z_{min}, z_{max})_5$
2.54 -8	$Re(\epsilon_{r5}), Im(\epsilon_{r5})$: AA for substrate
1 -3.14961	$Re(\mu_{r5}), Im(\mu_{r5})$
-27.45e-3 27.45e-3	$(x_{min}, x_{max})_6$
-202.55e-3	$(y_{min}, y_{max})_6$
-182.55e-3	
0 1.6e-3	$(z_{min}, z_{max})_6$
2.54 -8	$Re(\epsilon_{r6}), Im(\epsilon_{r6})$: AA for substrate
1 -3.14961	$Re(\mu_{r6}), Im(\mu_{r6})$
-27.45e-3 27.45e-3	$(x_{min}, x_{max})_7$
42e-3 54e-3	$(y_{min}, y_{max})_7$
0 1.6e-3	$(z_{min}, z_{max})_7$
2.54 -8	$Re(\epsilon_{r7}), Im(\epsilon_{r7})$: AA for substrate
1 -3.14961	$Re(\mu_{r7}), Im(\mu_{r7})$
-39.45e-3 -27.45e-3	$(x_{min}, x_{max})_8$
-202.55e-3 54e-3	$(y_{min}, y_{max})_8$
1.6e-3 22.4e-3	$(z_{min}, z_{max})_8$
1 -5	$Re(\epsilon_{r8}), Im(\epsilon_{r8})$: AA for free space
1 -5	$Re(\mu_{r8}), Im(\mu_{r8})$
27.45e-3 39.45e-3	$(x_{min}, x_{max})_9$
-202.55e-3 54e-3	$(y_{min}, y_{max})_9$
1.6e-3 22.4e-3	$(z_{min}, z_{max})_9$
1 -5	$Re(\epsilon_{r9}), Im(\epsilon_{r9})$: AA for free space

Surface Boundary Conditions (continue)	
1 -5	$Re(\mu_{r9})$, $Im(\mu_{r9})$
-27.45e-3 27.45e-3	$(x_{min}, x_{max})_{10}$
-202.55e-3	$(y_{min}, y_{max})_{10}$
-182.55e-3	
1.6e-3 22.4e-3	$(z_{min}, z_{max})_{10}$
1 -5	$Re(\epsilon_{r10})$, $Im(\epsilon_{r10})$: AA for free space
1 -5	$Re(\mu_{r10})$, $Im(\mu_{r10})$
-27.45e-3 27.45e-3	$(x_{min}, x_{max})_{11}$
42e-3 54e-3	$(y_{min}, y_{max})_{11}$
1.6e-3 22.4e-3	$(z_{min}, z_{max})_{11}$
1 -5	$Re(\epsilon_{r11})$, $Im(\epsilon_{r11})$: AA for free space
1 -5	$Re(\mu_{r11})$, $Im(\mu_{r11})$

Note. Any 2 diagonal points can be used to define a cube whose material property is homogeneous.

Note 2. Artificial absorbers (AA) for free space and any arbitrary material have to be chosen by user. The formulars can be found in the Dr. Yook's Ph.D. thesis.

Field Interpolation : define 2 end points $(x_{min}, y_{min}, z_{min})_i$ and $(x_{max}, y_{max}, z_{max})_i$	
70	Number of interpolation points.
0.001e-3 -162e-3	$(x_{min}, y_{min}, z_{min})_1$
0.801e-3	
0.001e-3 19.9e-3	$(x_{max}, y_{max}, z_{max})_1$
0.801e-3	

Excitation Points : define source as ractangular patch : $(x_{center}, y_{center})_i$ and $(\Delta x, \Delta y)_i$	
0 -177.35e-3	$(x_{center}, y_{center})_i$: center of the source
6e-3 5.2e-3	$(\Delta x, \Delta y)_i$: width of the source

FEM input file : file name (hybrid_fem_input.dat)	
1e-3	Tolerence of integration routine
1e-5	Tolerence of iterative solver
50000	Maximum number of iteration

C.6 User Manual - MoM

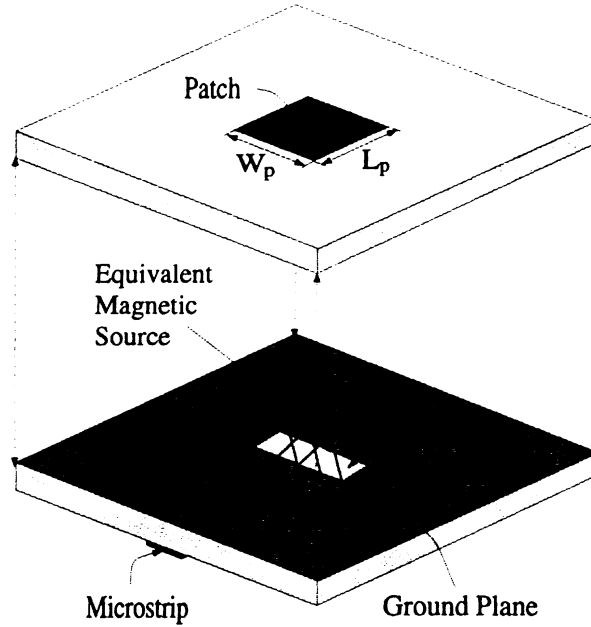In this section, a brief description of input files for MoM simulation is given.

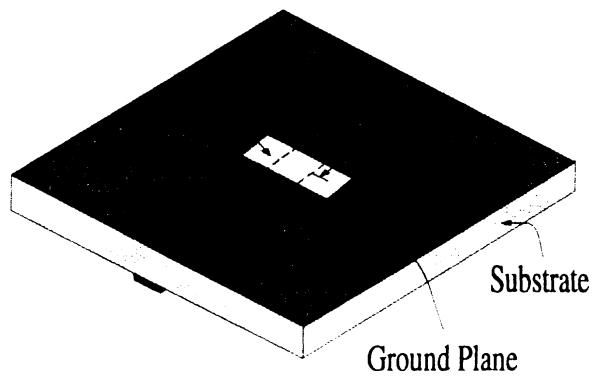Figure 19: Geometry and parameters of patch antenna.

Figure 20: Dimension parameters of slot.

41

MoM Part : file name (hybrid_MoM.dat)	
5	Nb : Number of basis on a patch.
3	Nap : Number of basis on a slot.
2.54	Erb : $Re(\epsilon_{rs})$ of substrate in microstrip
1.6e-3	db : Substrate thickness of microstrip
40e-3	Lp : Patch length
30e-3	Wap : Patch width
0 0	Xos, Yos : Center position of the patch
12e-3	Lap : Slot length
1.1e-3	Wap : Slot width
20e-3	Ls : Distance between center the slot and microstrip end
4.95e-3	Wf : Width of microstrip
2.225e9	freq : Simulation frequency

MoM Part : file name (zmnin.dat)	
1e-5	Integration tolerence
1000	Maximum number of division for integration
1	Integration parameter : default
150	Truncate integration range at $150k_o$ for ∞
3	Use $3\lambda_g$ for input traveling wave in microstrip
5	Integration parameter : default

D   Application of Parallel Computing in MoM

D.1   Introduction

Due to advance in semiconductor industry, the price of high performance processors falls rapidly, making it economical to build parallel computers with large number of processors. The need of high performance computing not achievable by single processor also drives the development of parallel computing technology. During the past decade we saw a lot of commercial parallel computers made by IBM, SGI and INTEL, to name a few. Parallel computers are no longer the proprieties of government or university research laboratories, but a reality. However, there is one cause hindering its widespread adoption. To tap into the power of parallel computing, the user has to modify his program according to the programming interface provided by the vender. Every time the user changes the parallel computer he used, he will need to modify his program again. There is no common programming interface among parallel computers until the Message Passing Interface (MPI) was standardized in 1994. Since then, MPI has been widely adopted by the computer industry.

To utilize parallel computers, first a programmer needs to design a parallelization model for his program. The idea of parallelization is to divide a single task to many independent jobs. A simple and easy way to implement is the Single Program Multiple Data (SPMD) model. In this model, different data sets are executed by the same program on different processors. These data sets have to be independent of each other, otherwise they cannot be executed in parallel. One simple example in electromagnetic problems is frequency response. In FEM or MoM, the computation process at each frequency point will not effect the outcome of other frequencies. Thus, we can simply submit the whole computation process of one frequency point to one processor. However, this may not achieve the best efficiency in terms of processor utilization. For instance, if there are 8 frequency points and 7 processors, when the last frequency point is computed on one processor, all other 6 processors will be idling. To achieve better efficiency, it is necessary to go to the inside of the computation process to seek out other independent operations which can be parallelized.

Many numerical techniques for solving electromagnetic problems have utilized parallel computers. Especially, the FDTD has attracted a lot of effort in parallelization due to its computer-intensive nature. A comprehensive study of its implementation can be found. A detailed description of a parallelized implementation of a MoM code is presented. A comparison of linear equation solvers for integral-equation formulations can be found.

In the following sections, two processes in MoM are parallelized using MPI. One is the impedance

matrix fill process; the other is the FWT process. The detail of the implementation and the measurement of the turn around time are included.

D.2 Parallelization Model of MoM Matrix Fill Process

The formulation of MoM always leads to a matrix equation as follows

$$Ax = B, \tag{1}$$

where A is a two-dimensional matrix, B is a column vector, and x is the unknown column vector we want to solve by direct inversion of A or by an iterative linear equation solver. The elements of matrix A are often the result of numerical integration of two basis functions with an integration kernel. The following equation is an example in one-dimensional space:

$$a_{ij} = \int \int f_i(x)\, g(x, x')\, f_j(x)\, dx\, dx'$$

where a_{ij} is the element of the matrix at i-th row and j-th column, $f_i(x)$ and $f_j(x)$ are the basis functions, and $g(x, x')$ is the kernel. Depending on the form and the distance between the basis functions, the time needed to perform the numerical integration of one element may vary greatly. To fully utilize the processors of a parallel computer, a dynamical job allocation scheme is necessary. As shown in ??, a processor is reserved as a dispatcher to send jobs and receive results from the workers. Other processors are served as workers to perform the numerical computation. 4 types of messages are passed between the dispatcher and workers. They are

FREE: sent by a worker to inform the dispatcher that it is ready to accept new jobs,

RESULT: sent by a worker to the dispatcher, containing the result of numerical integration,

TERMINATION: sent by the dispatcher to inform the worker that all jobs are sent.

JOB: send by the dispatcher, containing the information of a job.

Following are the procedures performed by the dispatcher:

1. create a list of the unique elements,

2. wait for messages from the workers,

3. if the message is a RESULT message, store the result, otherwise the message is a FREE message and a JOB message is sent to the worker,

4. repeat step 2 and 3 until all jobs are sent and returned,

5. send TERMINATION message to inform each worker to quit.

44

For the worker, the procedures are:

1. send FREE message to the dispatcher,

2. wait for messages from the dispatcher,

3. if it is a JOB message, perform the numerical integration and return the result, otherwise it is a TERMINATION message and the worker quits.

4. goto step 2.

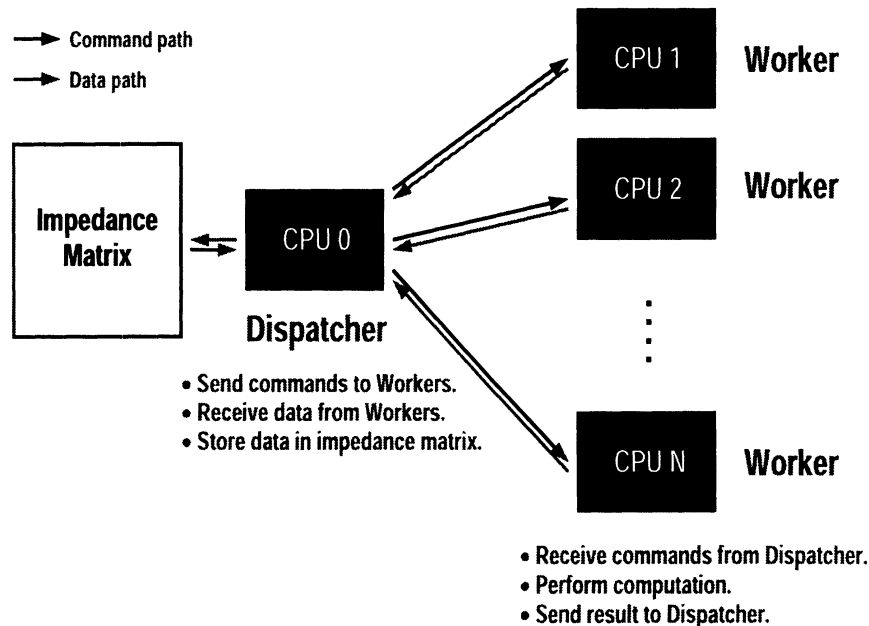## Parallelization Model of Impedance Matrix Fill

Figure 21: A dynamical allocation scheme for matrix fill process.

1 shows the flow chart of the above process. The dashed lines in the figure indicate the communication paths. Two kinds of processes, dispatcher and worker, are concurrently executed. First, the process of the dispatcher sorts out the unique matrix elements and builds a job list after it starts and reads in the necessary parameters. Then, it enters a loop waiting for messages from the workers. The loop terminates only after all the jobs are sent and all the data are collected from the workers. Inside the loop, the dispatcher checks the messages from the workers. If the message contains data, the dispatcher will store it and then wait for new messages. If the message is a FREE message, the dispatcher checks if all the jobs have been sent. If not, the dispatcher will send a job to the worker which sends the message. If all jobs have been sent, the

45
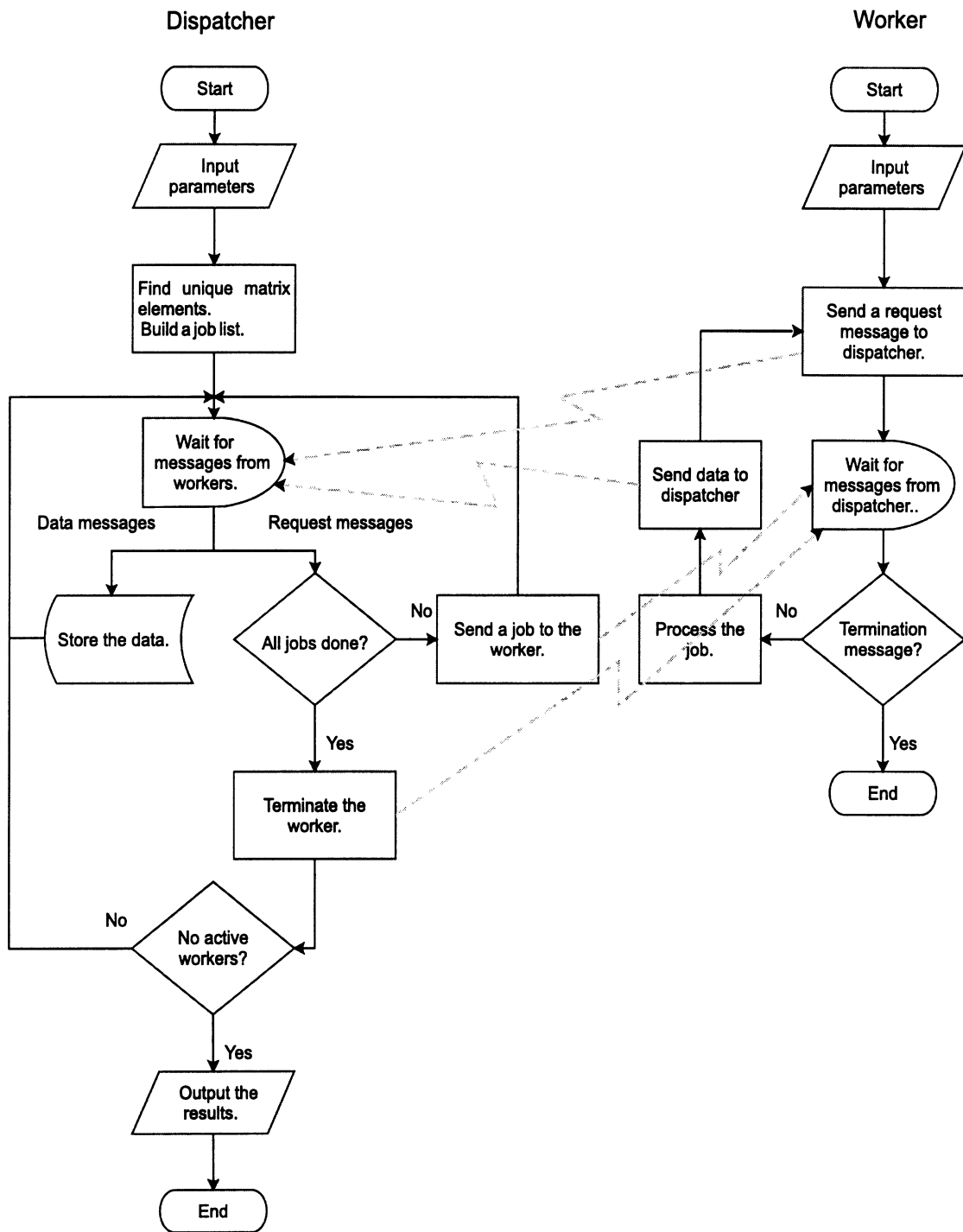
Figure 22: The flow chart of a dynamical allocation scheme for matrix fill process.

dispatcher will send a TERMINATION message to the worker. If all worker have been terminated, the dispatcher exits the loop, outputs the results and quits. If there are still active workers, the dispatcher will continue waiting for new messages.

The worker process, after starts and reads in the necessary parameters, sends a FREE message to the dispatcher to indicate that it is ready to accept new job. Then, it waits for a reply from the dispatcher. If the reply is a TERMINATION message, the worker quits. Otherwise, the message contains a job and the worker starts to execute it. After the worker has finished the job, the result is sent back to the dispatcher via a RESULT message. After sending the RESULT message, the worker sends a FREE message to the dispatcher and waits for the reply from the dispatcher again. A short program section is included in ?? to reveal the detail of implementation.

A measurement of turn around time v.s. number of processors is shown in ??. Here the "turn around time" means the elapsed time from the start of the program until completion. The measurement is performed on a 48 processor IBM SP2 machine. In the figure, the theoretical result is curve-fitted to the experimental result according to the following formula

$$\text{time}(i) = P + \text{Comm} \times n + \text{Comp}/(i - 1), \quad \text{for } i > 1 \tag{2}$$

where

time(i)	:	turn around time,
P	:	preprocessing time,
Comm	:	communication time per message,
Comp	:	total computation time of the jobs,
i	:	number of processors,
n	:	number of transmitted messages.

Note that Comm includes the communication latency and the actual transmission time of one message. Since the message size is fixed , Comm is a constant. Let N be the total number of the jobs. From the flow chart, there are $N + i - 1$ FREE, , N JOB, N RESULT, and $i - 1$ TERMINATION messages. Thus, the total number of transmitted messages is $3 \times N + 2(i - 1)$. When N is much larger than i, the total communication time is proportional to N.

From ??, it is seen that when the number of processors increases, only the third term in the formula decreases. This means that the preprocessing time plus the total communication time governs the limit. The formula also indicates that the curve of the turn around time should approximate a hyperbola when N is much larger than i. The measured results show very good agreement with the above theoretical model. The improvement of turn around time is larger when the number of processors is small. However, when the number of processors is large, only a small improvement is achieved because the preprocessing and communication time dominate. Note that the turn around time of 2 processors is higher than 1 processor. This is due to the higher preprocessing time of parallelized program and the communication cost. Also note that, due to the programming model, one processor is always reserved for coordinating other processors.

When the communication cost is small, this processor will mostly be idle. It is possible to also utilize the idle time on this processor to perform numerical integration by more sophisticated programming.

D.3 Parallelization Model of FWT

As discussed in ??, the FWT process transforms the matrix derived in MoM from one set of basis to another. ?? and ?? are repeated below for convenience.

$$\phi'_i = \sum_{j=1}^{N} p_{ij} \phi_j \tag{3}$$

$$[Z'] = [P]^{\dagger}[Z][P] \tag{4}$$

In ??, ϕ_i and ϕ'_i are the members of the basis Φ and Φ' respectively, and N is the rank of the basis. In ??, $[Z]$ and $[Z']$ are the MoM matrices evaluated in bases Φ and Φ' respectively. The p_{ij} in ?? is the i-th row, j-th column element of matrix $[P]$ in ??. Let z'_{mn} be the m-th row, n-th column element of $[Z']$, from the above two equations, we can derive

$$z'_{ij} = \sum_{m=1}^{N} \sum_{n=1}^{N} p_{mi} z_{mn} p_{nj}, \tag{5}$$

which is the form of the single operation in the FWT.

The process of FWT fits to the SPMD model which is characterized by repeating the same operation, for example, ??, on different data. Comparing to the previous matrix-fill process, each operation of FWT is shorter and fixed, however the total number of operations is much larger. If the same algorithm as the previous one is used, the overhead of communication will be too great. In stead, a fixed job-allocation scheme as shown in ?? is devised. At the beginning, each processor computes the job list and equally divides it to the total number of processors. Each processor can determines its share of jobs by his "rank"[1]. The only communication that takes place is when each processor sends its final computed results to one designated processor for post-processing.

Following are the procedures performed by each processor:

1. create a list of the operations,

2. divide the list equally into n shares, where n is the total number of processors,

3. use the rank of the processor as an index to determine which share belongs to itself,

4. perform the FWT,

---

[1]A terminology used by MPI to number the processors. If there is n processors, the rank of the processors will be 0, 1, 2, ..., n.

5. send the computed result to the processor with rank equal to 0.

1 shows the flow chart of the above process. A short program section is included in ?? to reveal the details of the implementation.

A measurement of turn around time v.s. number of processors is shown in ??. The definition of "turn around time" is the same as in the previous section. The measurement is also performed on the same parallel computer. In the figure, the theoretical result is curve-fitted to the experiment result according to the following formula

$$\text{time}(i) = P + \text{Tran} \times N + L \times i + \text{Comp} \times N/i, \tag{6}$$

where

time(i)	:	turn around time,
P	:	preprocessing time,
Tran	:	actual transmission time of one unit of data,
L	:	communication latency,
Comp	:	computation time,
i	:	number of processors,
N	:	number of unique matrix elements.

Since each processor only sends computed results once, the total latency time equals to $L \times i$. Comparing to other terms in ?? the total latency is negligible since the latency of SP2 is only 40 μS.

As in the previous section, when the number of processors increases, only the last term in the formula decreases, while the first and second terms remain the same. This means that the preprocessing time and the total communication time is the limit. The formula also indicates that the curve of the turn around time should be a hyperbola. The measured results show very good agreement with the above theoretical model. The improvement of turn around time is larger when the number of processors is small. However, when the number of processors is large, only diminishing returns are obtained because the preprocessing and communication time dominates.

D.4 Conclusion

In this section, the matrix-fill process and FWT in MoM are parallelized. The measured improvement is consistent to the theoretical model of the turn around time. Another bottleneck not addressed in this chapter is the process of solving ??. When the size of matrix A is large, direct inversion of A becomes impossible. Thus, iterative solvers need to be used. An iterative solver by nature is sequential. Each iteration relies on the result of last iteration. In this dissertation, a bi-conjugate gradient [?] iterative solver is used when the matrix size is large. In this solver, the most time-consuming part is the multiplication of a matrix with a column vector. Every iteration produces an improved guess of the solution vector. Thus, the communication overhead of

at least one solution vector in every iteration is not avoidable. When the dimension of the matrix is large, this communication overhead outweighs the improvement incurred by parallelizing the linear solver, since the communication speed is much slower than computation speed. This problem still needs to be addressed if further improvement on the speed of MoM is necessary.

E   The Implementation of Parallel Programming in C++

The following two sections show the implementation of the parallel programming of dynamic and static job allocation schemes in C++ language. The definition of the MPI functions can be found in [?, ?].

E.1   Dynamic job allocation

```
int rank, process_size;
mpidata mdata; /* common buffer for MPI messages */


MPI_Comm_rank(MPI_COMM_WORLD, &rank);
if (rank==0)
{
    /* Dispatcher Process */
    int send_count=0, receive_count=0, actual_count;
    int *process=new int[process_size-1];
    /* for storing the status of processors */
    for (int i=0;i<process_size-1;i++) process[i]=0;

    intpair* ip;/* pointer to the job list */
    int finished=0;
    do
    {
        MPI_Status status;
        /* receive message from workers */
        MPI_Recv(&mdata, sizeof(mdata), MPI_BYTE, MPI_ANY_SOURCE,
            MPI_ANY_TAG, MPI_COMM_WORLD, &status);
        int sent=0;
        switch (status.tag) /* check message type */
        {
        case TAG_REQUEST: /* request for job */
            if (finished) /* inform the work to end */
            {
                MPI_Send(&mdata, sizeof(mdata), MPI_BYTE, status.source,
```

```
                    TAG_END, MPI_COMM_WORLD);
                process[status.source-1]=1;
                sent=1;
            };
            while (!finished && !sent) /* send job to the worker */
            {
                mdata.job=ip[send_count]
                mdata.i=send_count++;
                MPI_Send(&mdata, sizeof(mdata), MPI_BYTE, status.source,
                    TAG_DATA, MPI_COMM_WORLD);
                actual_count++;
                if (send_count>=count)
                {
                    finished=1;
                };
                sent=1;
            };
            break;
        case TAG_DATA: /* returned results */
            ip[mdata.i].v=mdata.v;
            receive_count++;
            break;
        };
} while (receive_count<actual_count || finished==0);
/* inform workers to end */
for (int i=1;i<process_size;i++)
{
    MPI_Status status;
    if (process[i-1]==0)
    {
        MPI_Recv(&mdata, sizeof(mdata), MPI_BYTE, i, TAG_REQUEST,
            MPI_COMM_WORLD,&status);
        MPI_Send(&mdata, sizeof(mdata), MPI_BYTE, i, TAG_END,
            MPI_COMM_WORLD);
    };
};
/* output the results */
```

52

```
}
else
{
    /* Work Process */
    MPI_Status status;
    while (
        MPI_Send(&mdata, sizeof(mdata), MPI_BYTE, 0, TAG_REQUEST,
            MPI_COMM_WORLD),
        MPI_Recv(&mdata, sizeof(mdata), MPI_BYTE, 0, MPI_ANY_TAG,
            MPI_COMM_WORLD, &status),
        status.tag==TAG_DATA)
    {
        /* compute the job stored in mdata.job */
        /* store the result in mdata.v*/
        /* return the result in mdata.v */
        MPI_Send(&mdata, sizeof(mdata), MPI_BYTE, 0, TAG_DATA,
            MPI_COMM_WORLD);
    };
};
MPI_Finalize();
```

E.2   Static Job Allocation

```
int size; /* total number of jobs */
int rank, process_size;
mpidata mdata; /* common buffer for MPI messages */
MPI_Comm_rank(MPI_COMM_WORLD, &rank);
MPI_Comm_size(MPI_COMM_WORLD, &process_size);

/* compute the size of jobs for each processors */
int count=size/process_size;
int remain=size % process_size; /* remaining jobs */
int *recvcount, *displs, offset;
if (rank==0)
{
    /* processor 0 is also in charge of collecting
        the results, so it needs to prepare the
        place to store them */
```

```
        recvcount=new int[process_size];
        displs=new int[process_size];
        for (int i=0; i<process_size; i++)
        {
            if (i<remain)
            {
                displs[i]=i*(count+1)*sizeof(intpair);
                recvcount[i]=(count+1)*sizeof(intpair);
            }
            else
            {
                displs[i]=(i*count+remain)*sizeof(intpair);
            };
        };
    };


/* adjustment for the remaining jobs */
if (rank<remain)
{
    count++;
    offset=count*rank;
}
else
{
    offset=count*rank+remain;
};
/* compute the jobs */
/* return the results */
MPI_Gatherv(&(z.ia[offset]),count*sizeof(intpair),MPI_BYTE,&(z.ia[0]),
    recvcount, displs, MPI_BYTE, 0, MPI_COMM_WORLD);
if (rank==0)
{
    /* processor 0 output the total results */
};
```
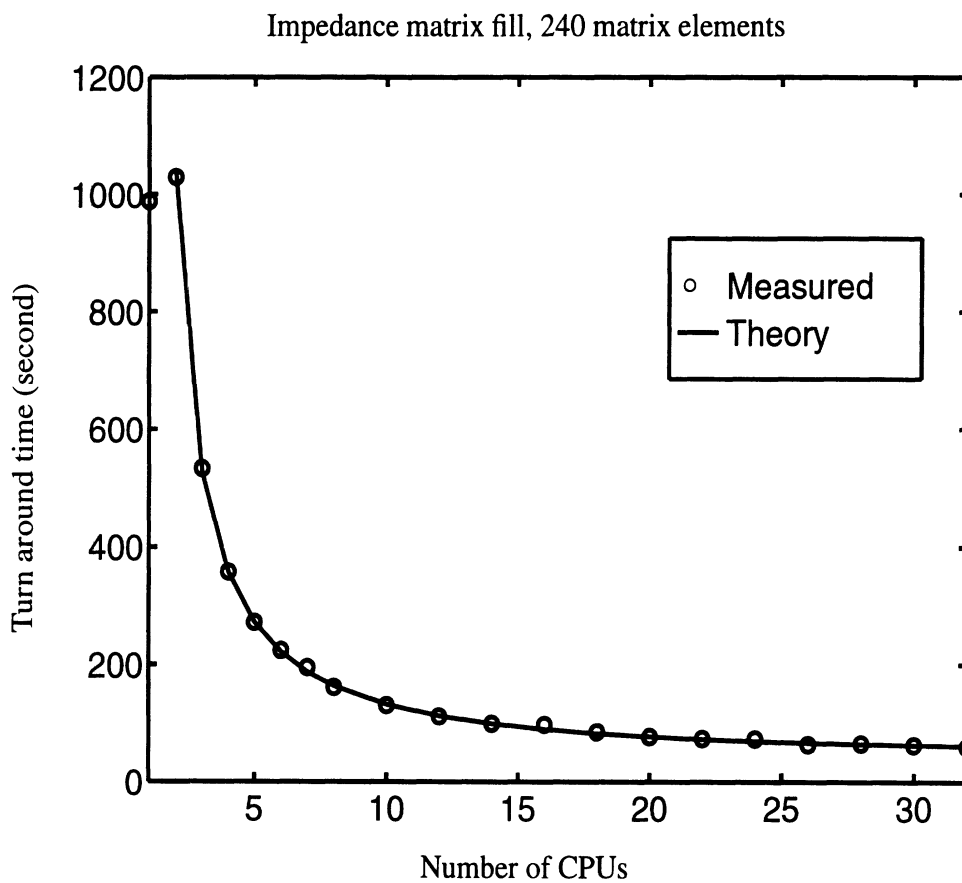
Figure 23: The measured turn around time of the impedance matrix fill process. The theoretical result is plotted by curve-fitting the measured data to **??**

Parallelizing Model of Fast Wavelet Transform

—▶ Data path

Impedance Matrix

CPU 1

CPU 2

⋮

CPU N

Transformed Impedance Matrix

• Evenly divided by N.
• Send each share to each CPU.

• Perform FWT.

• Gather results from each CPU.
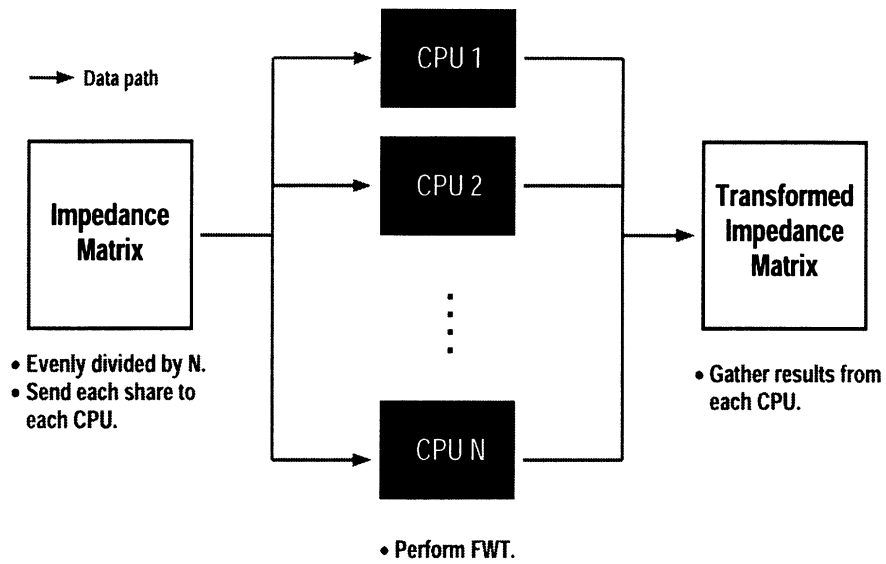
Figure 24: A static allocation scheme for the FWT process.
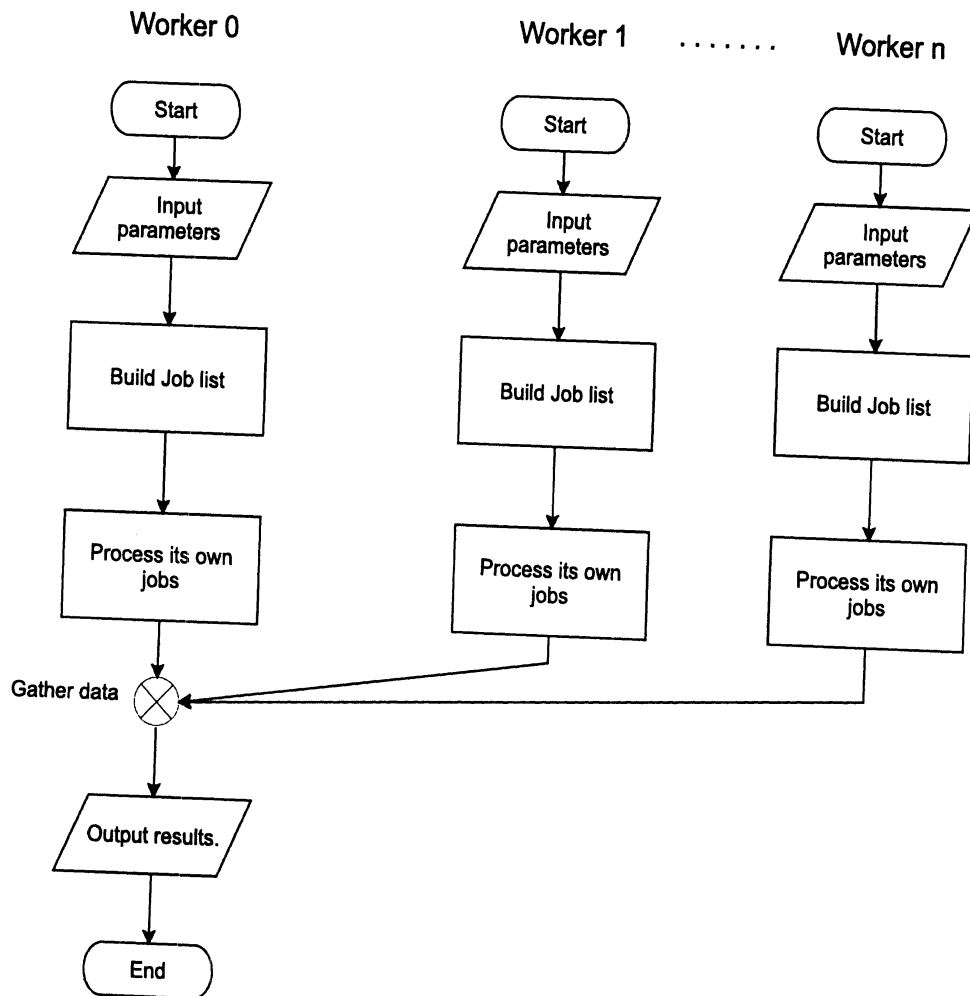
Figure 25: The flow chart of a static allocation scheme for the FWT process.

Fast wavelet transform, 3568 matrix elements
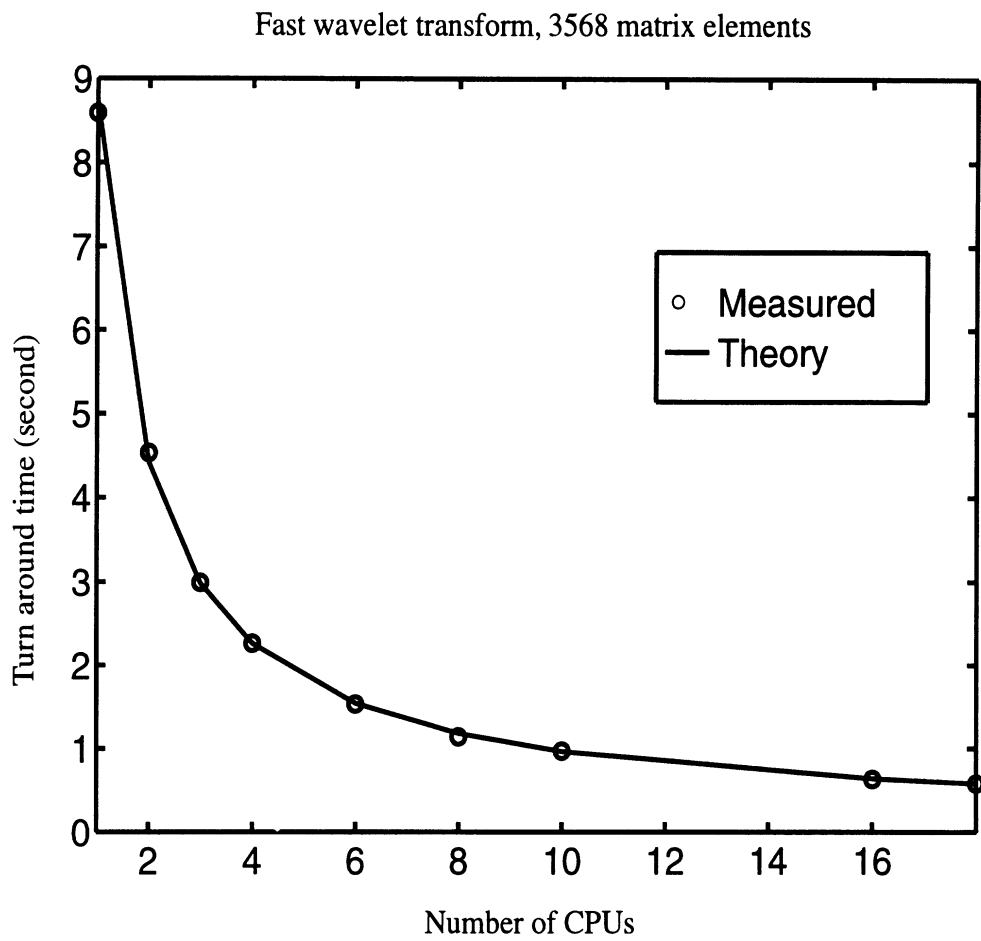
Figure 26: The measured turn around time of the FWT process. The theoretical result is plotted by curve-fitting the measured data to **??**

F Publications

References

[1] J.-G. Yook, J. Cheng, D. Chen and Linda katehi, "Parallel Electromagnetic Solvers for High Frequency Antenna and Circuit Design," *DoD HPCMP User Group Meeting*, San Diego, CA. 1997.

[2] J.-G. Yook, J. Cheng and Linda katehi, "Parallel Electromagnetic Solvers for High Frequency Antenna and Circuit Design," *DoD Mission Success Story from High Performance Computing.*

[3] J.-G. Yook, "Electromagnetic Modeling of High-speed High-frequency Interconnects," *Ph.D. Dissertation*, The University of Michigan, Ann Arbor, Michigan, 1996.

[4] J. Cheng, "Theoretical Modeling of MMICs Using Wavelets, Parallel Computing and a Hybrid MoM/FEM Method," *Ph.D. Dissertation*, The University of Michigan, Ann Arbor, Michigan 1998.

[5] G. Ponchak, D.-H. Chen, J.-G. Yook and Linda katehi, "Characterization of Plated Via Hole Fences for Isolation between Stripline Circuits in LTCC Packages," *IEEE MTT-S 1998 Symposium.*

[6] E. Yasan, J.-G. Yook and Linda katehi, " Generalized Method for Including Two Port Networks in Microwave circuits Using the Finite Element Method," *ACES 97(presented).*

[7] E. Yasan and Linda katehi, "An FEM based Method on Full Wave Characterization of Distributed Circuits Including Linear and Nonlinear Elements," *IEEE AP-S/URSI 1998 Symposium.*

[8] J.-G. Yook, D.-H. Chen, J. Cheng and Linda katehi, "Electromagnetic Solvers for High Frequency Circuits," *DoD HPCMP Presentation*, Nov. 1997.

[9] D.-H. Chen, J.-G. Yook, and Linda katehi, ""Electromagnetic Solvers for High Frequency Circuits," *DoD HPCMP Presentation*, Nov. 1998.

[10] D.-H. Chen and Linda katehi, ""Parallel Electromagnetic Solvers for High Frequency Antenna and Circuit Design," *DoD HPCMP Progress Report*, Jan. 1999.

PARALLEL ELECTROMAGNETIC SOLVERS FOR HIGH FREQUENCY ANTENNA AND CIRCUIT DESIGN

J.-G. Yook, J. Cheng and L. Katehi
Radiation Laboratory
Department of Electrical Engineering and Computer Science
The University of Michigan, Ann Arbor, MI 48109-2122, U. S. A.
Tel: 313-764-0608, Fax: 313-647-2106

DoD partner : Barry S. Perlman, Army Communications - Electronics Commands.

Computer Resource : IBM SP2 [MHPCC]

Research Objective : The purpose of this effort is development of linearly scalable parallel electromagnetic solvers for large array antenna and complicated microwave/millimeter-wave circuits which have not been successfully characterized by other means. Fast and accurate characterization of these electromagnetic structures are of critical importance for a successful DoD mission in digitizing the battlefield and developing secure communication systems.

Methodology : For parallel electromagnetic tools, we have developed wavelet-based method of moment (MoM) and tetrahedral finite element method (FEM) codes for arbitrary three-dimensional structures, and a message passing interface (MPI) has been utilized for parallelization on distributed memory parallel computers. Furthermore, fast wavelet transform and thresholding techniques are applied to achieve accelerated computation of the MoM solution. The linear scalable performance of the parallelized MoM and FEM is also investigated for real time design and optimization of the large array antenna and high frequency circuits.

Results : Preliminary results of the parallel impedance matrix filling and fast wavelet transform for MoM and task parallelization strategy for FEM show linearly scalable performance improvement. This truly scalable parallel MoM and FEM code performs successfully due the minimal communication overhead between the computing nodes and is not subject to the bandwidth of the network or switches. The number of unknowns of the problem ranges from 15,000 to 20,000 in the MoM case and from 150,000 to 200,000 in the FEM case. Figures below shows three-dimensional electric field distributions at far region from the 6×6 rectangular patch array antenna which are computed on parallel computers very efficiently.

Significance : Design and optimization of large electromagnetic structures, such as array antennas and high density circuits and packages, are of critical importance in the development of the advanced sensors and tactical communication systems. Through our research, we have demonstrated linearly scalable parallel strategies for various numerical electromagnetic codes and solved various class of problems which were not possible or extremely time consuming with conventional method and computers. This project has been funded by NASA Lewis Research Center, Army Research Office and the DoD High Performance Computing Program.

Figure: Far field radiation patterns for 6×6 rectangular patch array antenna. Authors : Jong-Gwan Yook, Juiching Cheng and Linda P.B. Katehi in the University of Michigan. Tel : 313-764-0608.

CO-FIRED CERAMIC PACKAGE FOR A KA-BAND MIMIC PHASE SHIFTER

Jong-Gwan Yook and Linda P. B. Katehi
Radiation Laboratory
Department of Electrical Engineering and Computer Science
The University of Michigan, Ann Arbor, MI 48109-2122, U. S. A.
Tel: 313-764-0502, Fax: 313-747-2122 Email:yookjong@engin.umich.edu

DoD partner : J. Harvey, Army Research Office, RTP, NC.

Computer Resource : IBM SP2 [MHPCC]

Research Objective : The purpose of this effort is the full-wave characterization of Microwave/Millimeter wave packages for discrete MMIC components. While these packages find widespread use in MMICs, their modeling has been limited by the large size and complexity of the problem leading into long design cycles, low yield and high cost.

Methodology : To model the MMIC package we have parallelized a full-wave finite element (FEM) code on the distributed memory parallel computer, IBM SP2, in Maui High performance Computing Center (MHPCC). Among the many parallelization schemes, we have selected "task parallelization" based on the considerations that FEM is a frequency domain technique and each frequency point needs to be computed independently in order to obtain the complete package response over the desired frequency spectrum.

Results : Preliminary results of the "task parallelization" strategy show linearly scalable performance improvement. This truly scalable parallel FEM code performs successfully due the minimal communication overhead between the computing nodes and it is not subject to the bandwidth of the network or switches. The number of unknowns of the problem ranges from 150,000 to 200,000 and the global matrix equations are simultaneously built and solved at all frequency points within an hour. The same code would normally require 40 hours of CPU time if it were run in serial computer.

Significance : Hermetic packages are frequently utilized in microwave integrated circuits to provide protection from a hostile environment, reduced electromagnetic interference and minimal radiation leakage. A variety of packages based on a cofired ceramic technology have developed for use in high frequency application by DoD. The presented effort has allowed, for the first time, the complete and accurate high-frequency characterization of a MMIC package and the understanding of the electromagnetic interference it produces in the form of parasitic resonances. This package has been developed by Hughes at Torrance under a contract from NASA Lewis Research Center in Cleveland, OH.
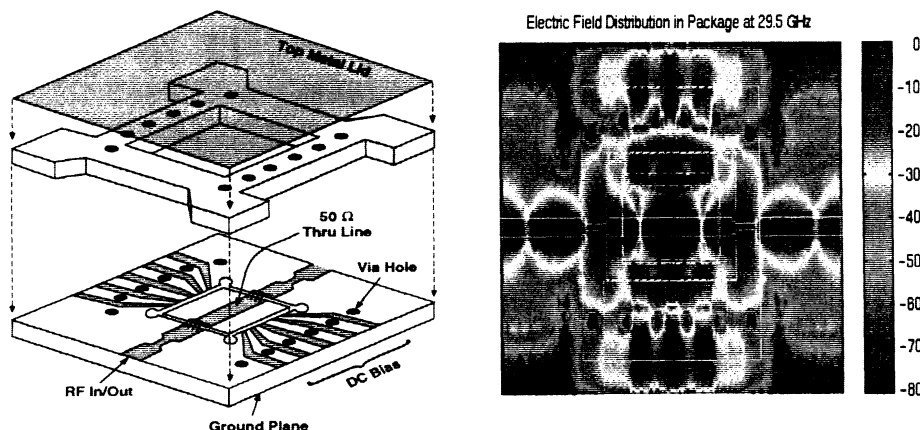
Figure: The 18 - 40 GHz MMIC package for phase shifter chip and electric field distribution in the package. Authors : Jong-Gwan Yook and Linda P.B. Katehi in the University of Michigan. Tel : 313-747-1796.

W-Band Coplanar Waveguide Probe Structures

Emmanouil M. Tentzeris, Jong-Gwan Yook, and Linda P. B. Katehi
Radiation Laboratory
Department of Electrical Engineering and Computer Science
The University of Michigan, Ann Arbor, MI 48109-2122, U. S. A.
Telephone : 313-764-0502 Fax : 313-747-2122 Email : yookjong@engin.umich.edu

DoD partner : J. Harvey, Army Research Office, RTP, NC.

Computer Resource : Convex SPP-1 [NCCOSC San Diego]

Research Objective : Significant attention is being devoted now-a-days to the analysis and design of W-band waveguide structures which are used either to probe the modal propagation inside the waveguides or as active-element mounts. This effort aims at the full-wave characterization of these highly complex waveguide probe structures.

Methodology : We have applied the Finite Difference Time Domain (FDTD) technique in the calculation of the S-parameters of a W-band coplanar waveguide-to-rectangulat waveguide probe. The FDTD code has been parallelized on the Convex SPP-1 [NCCOSC] using "task parallelization".

Results : A parametrical study has been performed in an effort to maximize the coupling between the probe and the waveguide over the widest possible frequency range. A waveguide absorber based on an analytical Green's function has been developed to minimize the reflections over a wide band of frequencies. As an application, a membrane coplanar waveguide-to-rectangular waveguide probe has been characterized and designed for less than -20 dB return loss from 75 GHz to 115 GHz. The mesh size is $480 \times 477 \times 52$ and it would require about 250 hours of CPU time if the FDTD code were to run on an HP 735 Workstation, and 72 hours in a Cray C90 supercomputer. The parallelized version of the same program on Convex SPP-1 requires about 31 hours CPU time for completion.

Significance : The presented effort has allowed, for the first time, the complete and accurate high-frequency characterization and design of a W-band back-to-back waveguide probe configuration. Until recently, W-band waveguide probes for diode mounting or waveguide probing have only been designed experimentally through very long and costly design cycles.
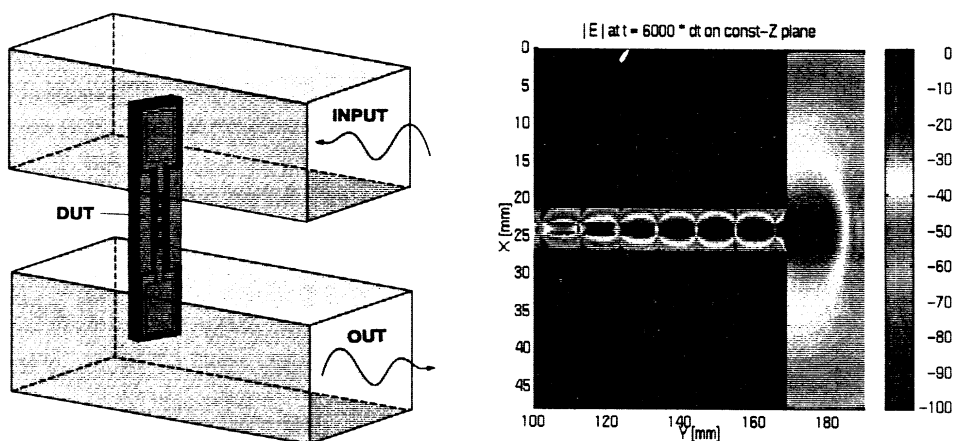
Figure: The membrane coplanar waveguide probe and the electric field distribution for the structure . Authors : Emmanouil M. Tentzeris, Jong-Gwan Yook, and Linda P.B. Katehi in the University of Michigan. Tel : 313-747-1796.

Parallel Electromagnetic Solvers for High Frequency Antenna and Circuit Design

J.-G. Yook, D. Chen, J. Cheng and L. Katehi
Radiation Laboratory
Department of Electrical Engineering and Computer Science
The University of Michigan, Ann Arbor, MI 48109-2122
Tel: 734-764-0608, Fax: 734-647-2106

B. Perlman
US Army Communications-Electronics Commands(CECOM)
Command/Control & System Integration Directorate
AMSEL-RD-C2
Ft. Monmouth, N.J. 07703
Tel: 723-427-4883

Introduction

The purpose of this effort is development of linearly scalable parallel electromagnetic solvers for large scale array antennas and complicated microwave/millimeter-wave circuits which have not been successfully characterized by other means. Fast and accurate characterization of these electromagnetic structures are of critical importance for a successful DoD mission in digitizing the battlefield and developing secure communication systems.

Methodology

For parallel electromagnetic tools, we have developed wavelet-based method of moment (MoM) and tetrahedral finite element method (FEM) codes for arbitrary three-dimensional structures, and a message passing interface (MPI) has been utilized for parallelization on distributed memory parallel computers. Furthermore, fast wavelet transform and thresholding techniques are applied to achieve accelerated computation of the MoM solution. The linear scalable performance of the parallelized MoM and FEM is also investigated for real time design and optimization of the large array antenna and high frequency circuits.

Results

Preliminary results of the parallel impedance matrix filling and fast wavelet transform for MoM and task parallelization strategy for FEM show linearly scalable performance improvement. This truly scalable parallel MoM and FEM code performs successfully due the minimal communication overhead between the computing nodes and is not subject to the bandwidth of the network or switches. The number of unknowns of the problem ranges from 15,000 to 20,000 in the MoM case and from 150,000 to 200,000 in the FEM case. Figures below shows three-dimensional electric field distributions at far region from the 6×6 rectangular patch array antenna which are computed on parallel computers very efficiently.

Significance

Design and optimization of large electromagnetic structures, such as array antennas and high density circuits and packages, are of critical importance in the development of the advanced sensors and tactical communication systems. Through our research, we have demonstrated linearly scalable parallel strategies for various numerical electromagnetic codes and solved various class of problems which were not possible or extremely time consuming with conventional method and computers. This project has been funded by NASA Lewis Research Center, Army Research Office and the DoD High Performance Computing Program.

Figure 1: Far field radiation patterns for 6×6 rectangular patch array antenna

PARALLEL ELECTROMAGNETIC SOLVERS FOR HIGH FREQUENCY ANTENNA/CIRCUIT DESIGN

Barry S. Perlman
Army Research Laboratory
Sensors and Electronics Directorate
Fort Monmouth, NJ 07703

Jong-Gwan Yook*, Juiching Cheng
Donghoon Chen, and Linda P. B. Katehi
Radiation Laboratory
The University of Michigan, Ann Arbor, MI 48109
yookjong@engin.umich.edu

Abstract

In this paper, several different parallelization strategies for the method of moment (MoM) and the finite element method (FEM) are implemented on a distributed memory parallel computer (IBM SP2) having 48 CPUs. For the portability of the parallel codes on various platforms, standard message passing paradigm (MPI) has been adapted. Having in mind that a major bottleneck of the parallelized codes is the interprocessor communication overhead, data independence is fully exploited for efficient parallelization and as a result near linear scalability has been achieved.

I. Introduction

High-frequency radar systems for communication, detection and surveillance incorporate MMIC modules which are characterized by high density and substantial geometrical complexity. In most cases these modules are packaged for electrical and/or environmental protection and the resulting 3D structures exhibit a considerable complexity that impedes design and influences electrical performance due to unwanted parasitics. The design of these complex three-dimensional monolithic circuit (MMIC modules) with hundreds of vias and lines interconnecting a large number of active and passive circuit components to a rather large number of radiating elements, has been a problem of critical importance to DoD. The design and characterization of these circuits requires numerical approaches which can fully characterize the excited electromagnetic fields. Among the various techniques, the method of moments has demonstrated superiority in solving radiation problems but it has been hindered by long computational times and is limited, for this reason, to small circuits not exceeding more than a few components and interconnecting lines. In this paper, a novel technique based on the multiresolution expansion and the hybrid combination of the integral equation technique and the finite element method is parallelized to solve very large problems.

II. Parallelization Strategies

In this section, several different parallelization strategies for MoM and FEM have been presented. In the former case, parallel MoM impedance matrix generation and parallel fast wavelet transform (FWT) are

Parallelization Model of Impedance Matrix Fill   **Parallelizing Model of Fast Wavelet Transform**

(a)   (b)
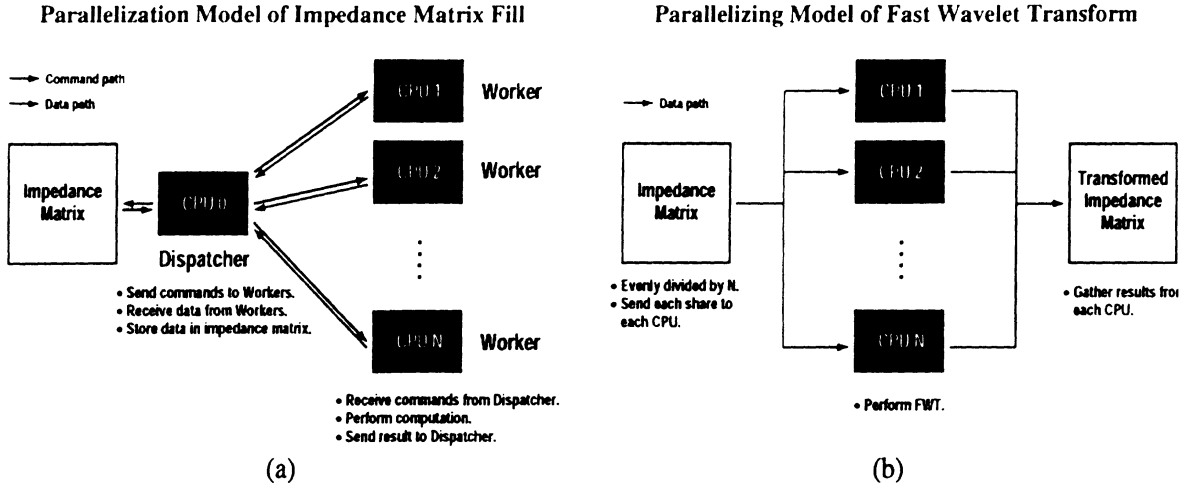
Figure 1: Parallelization schemes for MoM: (a) Parallel impedance matrix filling. (b) Parallel fast wavelet transform.

implemented, while parallelization of iterative linear equation solver and frequency parallelization schemes are tested for the later case.

A. Parallel MoM Matrix Element Generation

In method of moments, each matrix element is produced by the integration of a source function and a test function with an integration kernel. When the closed form representation is not available, numerical integration, which is time-consuming, must be used. However, the procedure of the integration of each matrix element fits quite well to the Single Instruction Multiple Data (SIMD) parallelization model, enabling the utilization of parallel computers to speed up the process. Because the computation time of each matrix element can vary in a great range, an algorithm that dynamically assigns jobs to each CPU is devised as illustrated in figure 1(a). In this algorithm, one CPU is reserved as a dispatcher to send jobs to and gather results from other CPUs. Jobs are sent whenever there are free CPUs. To achieve performance gain, the communication time between the CPUs must be much smaller than the computation time which is true in most impedance matrix calculation.

B. Fast Wavelet Transform

In order to take the advantage of multiresolution analysis [1], the MoM matrix is further transformed by FWT to its equivalent representation in wavelet bases. The FWT also fits to SIMD model, but comparing to the generation of MoM matrix elements, the computation time for each element is much smaller and the total number of iterations is much higher. If the same algorithm as the MoM matrix element generation is used, communication overhead will be too high. Instead, another algorithm is devised to reduce the communication overhead as shown in figure 1(b). In this algorithm, jobs are evenly divided to each CPU. Only one communication is needed when each CPU completes its entire job list and sends the results back to the designated CPU for further processing.

C. Task Parallelization

2

(a)   (b)
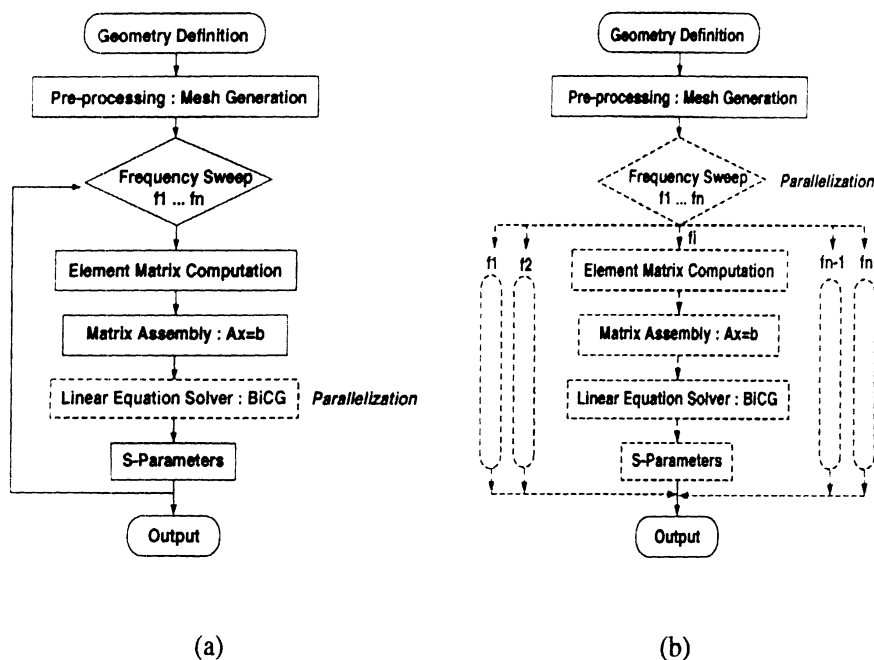
Figure 2: Parallelization schemes for FEM: (a) Parallelization of linear equation solver- BiCG. (b) Task parallelization.

The generation of the matrix entries in the finite element method is in general a much easier and faster process compare to that of the MoM [2, 3]. Under most practical situations, FEM matrix generation takes less than 10% of total FEM solution time. As a result, the parallelization of linear equation solver may result in an efficient method (refer fig. 2(a)). On the other hand, based on the property of the frequency domain finite element method, each frequency point can be parallelized with minimum inter-process communication overhead which might lead to scalable FEM code as shown in figure 2(b). In the following section, the performance of two different parallelization schemes for FEM is investigated and the speedup curves are presented.

III. Numerical Results

A. Parallelized MoM Code for Antenna Applications

In order to demonstrate the performance gain of the parallelization models discussed in the previous section, the impedance matrix of a 6 × 6 microstrip patch array antenna is calculated and solved by taking the FWT. The individual patch size, the dielectric constant of the substrate, and the thickness of the substrate is 59.5 mm × 50 mm, 2.62, and 1.59 mm, respectively. The rooftop function is used as the basis function of the field expansion. The number of cells are 16 × 16 on each patch and the resulting total number of unknowns is 17280 for the whole array. The radiation patterns for E_ϕ and E_θ are calculated at 1.536 GHz.

Figure 3(a) and (b) show the measured computation time v.s. number of CPUs and theoretical result for both the impedance matrix filling process and FWT using the models presented in Section II. As can be seen from the figures, the measured result matches very well to the theoretical prediction. The radiation patterns of the antenna are computed as shown in figure 4 for E_ϕ and E_θ plane patterns. The thresholding is taken after

3

the FWT and the resulting sparse matrix is solved with iterative linear equation solver, such as biconjugate gradient method.

Impedance Matrix Fill, 240 matrix elements

Time(i) = P + Comm x N + Comp x N / (i - 1), for i >1

P: preprocessing time.
Comm: commnunication time.
Comp: computation time.
i: number of CPUs.
N: number of matrix elements.

Number of CPUs

Note: the turn around time of 2 CPUs is higher than 1 CPU. This is due to the higher preprocessing time of parallelized program and the communication cost. Also note that, due to the programming model, one CPU is always reserved for coordinating other CPUs, which leaves only one CPU to perform the computation when only two CPUs are used.

(a)

Fast Wavelet Transform, 3568 matrix elements

Time(i) = O + Comm x N + Comp x N / i

O: overhead.
Comm: communication time.
Comp: computation time.
i: number of CPUs.
N: number of matrix elements.

Number of CPUs

Note: the overhead includes the extra function calls for measuring time and parallel processing.

(b)

Figure 3: Parallelization performances for MoM: (a) Parallel impedance matrix generation, (b) Parallel fast wavelet transform.

A. Parallelized FEM Code for Packaging Applications

To measure the performance of the parallelized Bi-CG routine on distributed memory machine, two different size of problems are solved. As shown in figure 5(a), parallelization efficiencies are minimal, even though the larger problem size shows slightly better result. With this observation, the task parallelization scheme is tested as shown in figure 5(b) and reveals excellent result. The poor performance of the parallel Bi-CG routine is mainly due to heavy communication overhead. On the other hand, the linearly scalable performance of the task parallelization scheme is coming from the minimum data dependency between the CPUs. As an application of the parallelizaed FEM code, we have characterized two typical microwave/millimeter-wave packages and the internal electric field distributions are calculated as presented in figure 6.

IV. Conclusions

In this paper, single instruction multiple data (SIMD) model have been fully implemented for the finite element method and the method of moment using the MPI standard on distributed memory machine. Due to the data independence between the processes, linearly scalable parallel codes are achieved. In particular, matrix element generation in MoM has been parallelized in view of its heavy computational burden. In the FEM code, frequency parallelization scheme has been implemented after the observation that the performance of the parallelized linear equation solver has been poor.
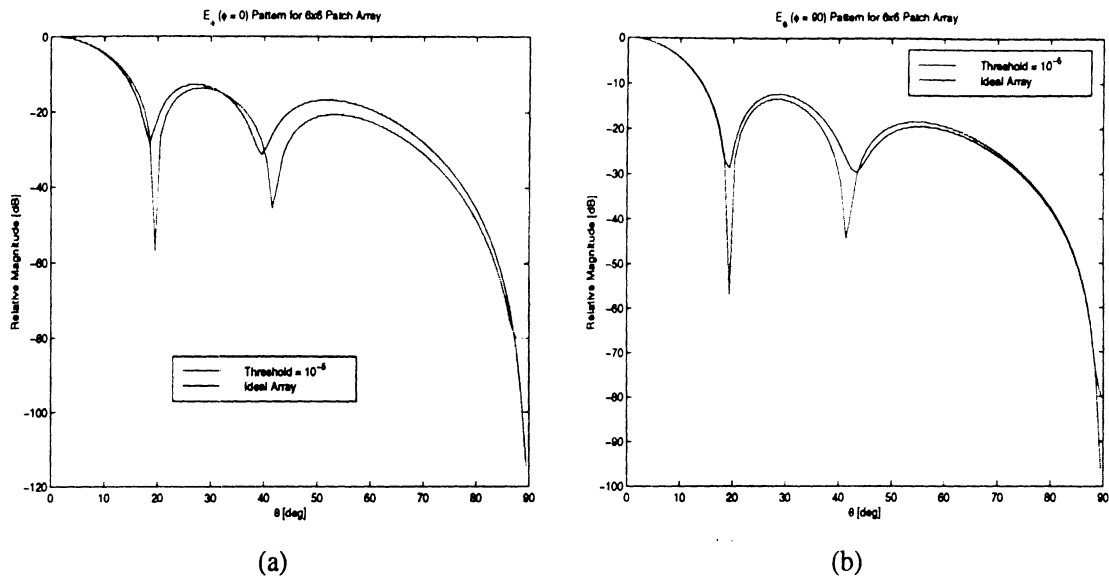
Figure 4: Radiation patterns for 6×6 rectangular patch array: (a) E_ϕ pattern, (b) E_θ pattern

Acknowledgment

References

[1] Kazem F. Sabet, Jui-Ching Cheng and Linda P. B. Katehi, "Efficient Wavelet-based Modeling of Printed Circuit Antennas and Arrays," submitted to *IEEE Transactions on Antennas and Propagation*.

[2] Jong-Gwan Yook and Linda katehi, "Characterization of MIMICs Packages Using A Parallelized 3D FEM Code," *1996 ACES Symposium, Monterey, CA.*, pp. 954-961.

[3] Jong-Gwan Yook and Linda katehi, "Parallelization of the Finite Difference Time Domain Code on Shared Memory Machine," *PIERS 1996, Innsbruck, Austria.*

5
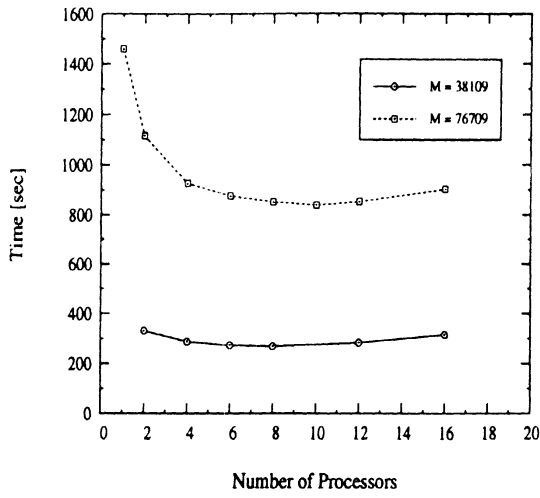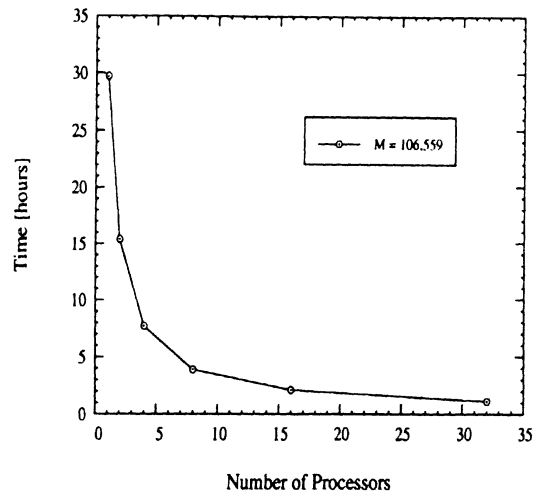
Figure 5: Parallelization performances for FEM ("M" is the number of unknowns to be solved): (a) Parallel Bi-CG routine, (b) Frequency parallelization scheme.
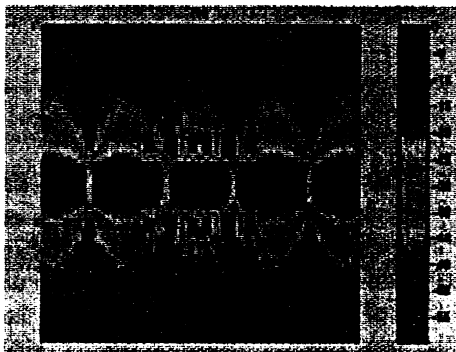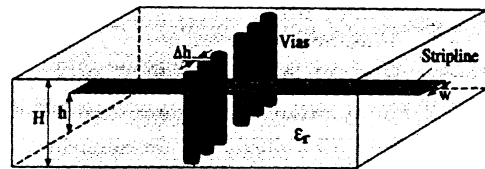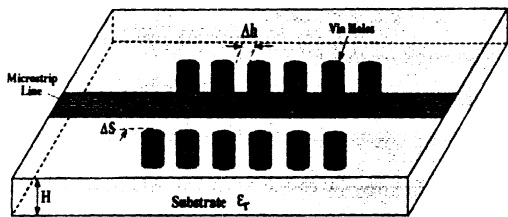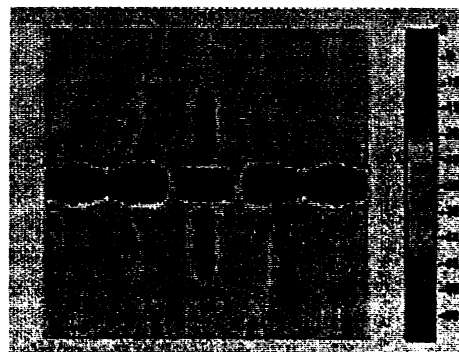
(a)   (b)

Figure 6: Two different packaging structures and electric field distributions inside of the structures.

Characterization of Plated Via Hole Fences for Isolation Between Stripline Circuits in LTCC Packages

George E. Ponchak[1], Donghoon Chen[2], Jong-Gwan Yook[2], and Linda P. B. Katehi[2]

1. NASA Lewis Research Center, 21000 Brookpark Rd., MS 54/5, Cleveland, OH 44135
2. University of Michigan, 3240 EECS Building, Ann Arbor, MI 48109-2122

Abstract

Reduced coupling between adjacent striplines in LTCC packages is commonly accomplished by walls made of plated via holes. In this paper, a 3D-FEM electromagnetic simulation of stripline with filled via fences on both sides is presented. It is shown that the radiation loss of the stripline and the coupling between striplines increases if the fence is placed too close to the stripline.

Introduction

Smaller packages with more circuitry are required for the advanced RF systems being built today and planned for tomorrow. These new packages house a variety of high density circuits for data processing, biasing, and memory in addition to the RF circuits. While the size is being reduced and the complexity increased, the cost of the package must also decrease. To accomplish these contradictory goals, new packaging technologies are required.

Low Temperature Cofired Ceramics (LTCC) is an ideal packaging technology. The material has a moderate dielectric constant, $4<\varepsilon_r<8$, which permits wider strips and thus lower conductor loss than circuits on Si, GaAs, or Alumina. In addition, the loss tangent is on the order of 0.002 at 10 GHz which yields an acceptably low dielectric loss. LTCC packages are comprised of many 0.1-0.15 mm thick ceramic layers with transmission lines on each layer. This increases the level of integration by allowing bias, digital routing, and RF transmission lines and interconnects to be built up in three dimensions.

The multilayer character of these circuits leads to RF transmission lines which are not of microstrip type but of stripline type. Even with the high levels of integration LTCC offers, designers are required to decrease the spacing between striplines to meet the new size and cost requirements. In doing so, coupling between adjacent striplines severely limits the overall
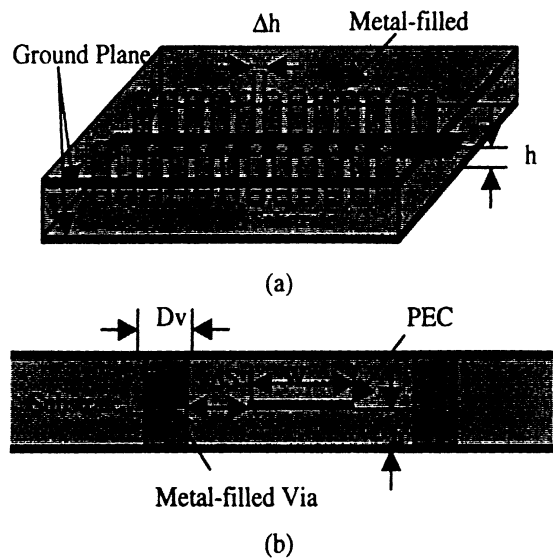
Fig. 1 (a) Stripline with a continuous filled via fense on both sides (b) Cross section.

packaged circuit performance. As a solution to this problem, package designers have included filled via fences adjacent to the stripline to confine the electromagnetic fields around the center strip, partition the package and reduce electrical couplings [1-2].

In this paper, we utilize a 3D-Finite Element Method (FEM) [3] to evaluate stripline structures in the vicinity of filled via fences. It is shown for the first time that filled via fences increase the radiation loss of the stripline and decrease the coupling between adjacent striplines. Design guidelines are given to minimize these parasitic effects which degrade overall performance.

Results

The cross section of the stripline structure is shown in Figure 1. Throughout this paper: the relative These values are all standard for typical LTCC

A GENERALIZED METHOD FOR INCLUDING TWO PORT NETWORKS IN MICROWAVE CIRCUITS USING THE FINITE ELEMENT METHOD

Eray Yasan, Jong-Gwan Yook and Linda P. Katehi

Radiation Laboratory

Dept. of Electrical Engineering and Computer Sci.

The University of Michigan, Ann Arbor, MI 48109-2122, U.S.A.

Tel: 313-764-0502, Fax: 313-747-2106, Email: eray@engin.umich.edu

Abstract

This paper discusses the methodologies required to introduce basic passive elements into an FEM modelled microstrip circuit. Three different approaches have been investigated and are presented herein. The first two methods use the basic principles of circuit theory while the third employs the so called zeroth order approximation or volume current method. One of the EM-circuit method uses the voltage-current relations applying at the passive element(s) in the circuit. This is done through the impedance of that element and requires a modification of the functional of the FEM equations. The second method uses the S-parameters of the passive element(s) to provide the required circuit relation. By using these methods the effect of the presence of the passive element(s) on the microstrip circuit can be observed.

1 Introduction

The Finite Element Method (FEM) has been established during the past ten years as an accurate and versatile frequency-domain technique for passive circuit problems. Despite the capability of the technique to treat a broad variety of circuit geometries, it has been limited to only distributed elements that are mostly passive and linear. To be able to make the technique applicable to more complete microwave and millimeter wave circuits, its capability needs to be extended to handle passive and active elements. Some studies about these issues have been made by using different techniques such as FDTD, TLM and FEM [1]-[3]. The techniques presented herein are divided into circuit element methods and volume current methods. In the following, a short description of each technique is given.

1.1 Circuit Method # 1

This method uses circuit concepts such as the current-voltage $(I - V)$ relations through the nodes connected to the element[6]. From circuit theory the following relations for the resistor, capacitor and inductor hold respectively

$$V = RI \qquad V = j\omega LI \qquad I = j\omega CV. \qquad (1)$$

In terms of field quantities the voltage and current are expressed in the following way

$$V = \int \mathbf{E} \cdot dl \qquad (2)$$

$$I = \oint_c \mathbf{H} \cdot dl \qquad (3)$$

where the integral is evaluated along the element for the voltage and around the element for the current flowing through the nodal points. Since tetrahedral based FEM is used throughout the analysis, lumped elements are located along the edges of the tetrahedrons.

1.2 Circuit Method # 2

In the second circuit method, S-parameters of the lumped elements are known and given to the system a priori. In order to use $(I - V)$ relations, S-parameters are converted to Z-parameters. Referring to Fig.1, the following relations hold

$$V_1 = Z_{11}I_1 + Z_{12}I_2 \qquad (4)$$

$$V_2 = Z_{21}I_1 + Z_{22}I_2 \qquad (5)$$

In the microstrip case V_1 is the voltage between the signal line and the ground. If this is a symmetric microwave circuit, then V_1 is equal to V_2. I_1 and I_2 are the currents flowing through the conductors towards the element as shown in Fig. 1. In terms of field expressions V_1 and V_2 are the line integrals of electric fields evaluated through the edges from conductors to the ground. I_1 and I_2 are the closed line integrals of magnetic fields around the conductors.

1.3 Volume Current Method

The third method [7] uses the relation

$$\mathbf{J}_i = \sigma \mathbf{E} \qquad (6)$$

in order to account for the lumped elements' contribution by introducing fictitious conductivity regions in the volume. The conductivity σ in these regions is given by

$$\sigma = l/(Z_L s) \qquad (7)$$

where Z_L, s and l represent load impedance in ohms(Ω), cross-sectional area and length of the load respectively.
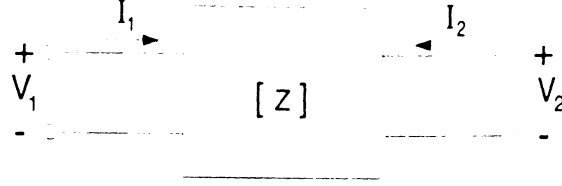
Figure 1: Two port network with Z parameters

2 FEM Formulation

Starting with Maxwell's equations, the following wave equation is weighted according to Galerkin's method and discretized

$$\nabla \times \nabla \times \mathbf{E} - \omega^2 \mu\epsilon\mathbf{E} = -j\omega\mu\mathbf{J}_i \tag{8}$$

where $\mathbf{J}_i$ is the impressed current source. Discretization is done in a conventional way using tetrahedral elements. The following weak form of Maxwell's equations is obtained

$$\int\int\int_v [(\nabla \times \mathbf{E})\cdot(\nabla \times \mathbf{P}) - \omega^2\mu\epsilon\mathbf{E}\cdot\mathbf{P}]dv = \oint_s j\omega\mu(\mathbf{H}\times\mathbf{P})\cdot\hat{n}ds - \int\int\int_v j\omega\mu\mathbf{P}\cdot\mathbf{J}_i dv \ . \tag{9}$$

Expanding the electric field as a summation of linear basis functions and choosing the weighting function as the same edge basis function give

$$\mathbf{E} = \sum_{i=1}^{6} a_i\mathbf{W}_i \tag{10}$$

$$\mathbf{P} = \mathbf{W}_j \ , \ j = 1,...,6 \tag{11}$$

where a_i are the unknowns to be determined, and $\mathbf{W}$'s are the first order edge based Whitney functions. For the circuit method #1 the first term on the right hand side of the FEM equation (9) is expressed in such a way that the effect of the lumped element is included. The resulting term in the FEM equations becomes

$$\frac{-j\omega\mu}{Z_L} \oint_s [\mathbf{e}_{12}\cdot\mathbf{E}\delta(\mathbf{r}-\mathbf{r}_o)][\int_1^2 \mathbf{E}\cdot d\mathbf{l}]ds \tag{12}$$

where $\mathbf{e}_{12}$ is the unit vector pointing from node 1 to node 2 along which the element is placed and Z_L is the load impedance.

According to the circuit method #2, having additional set of equations from $I - V$ relations enables us to write another matrix equation having N unknowns not necessarily being equal to the number of additional equations. By careful examination, elimination of some of the

unknowns. especially through the edges along which the element is located, by use of these equations decreases the size of the original FEM matrix. This matrix equation is solved using iterative matrix-solving algorithms.

The third method uses the second term on the right hand side of the FEM equation (9) in order to introduce the effect of the lumped element to the equations. The term takes the form

$$\frac{-j\omega\mu l^2}{Z_L} \int \int \int_v \mathbf{E} \cdot \mathbf{E} dv \ . \tag{13}$$

Similar to the first method, this term only contributes to the diagonal elements in the FEM matrix. The most efficient way to solve these matrix equations is found to be the Pre-Conditioned Conjugate Orthogonal Conjugate Gradient (COCG) Method.

3   Results

A shielded symmetric two port microstrip structure shown in Fig. 2 was examined. Using circuit method # 1 and volume current method, the case of 100Ω between the lines was studied. The S parameters obtained out of these two methods are shown in Fig. 3. For S_{11} the results agreed with theoritical ones ($|S_{11}| = |S_{22}| = -6.02$dB) quite reasonably but for S_{12} they are degraded in the high frequency region. This might arise because of circuit discontinuity at the element and also insufficient discretization. For circuit method # 2, the same geometry with a PEC wire is used in place of the resistor(Fig. 4). The results are shown in Fig. 5 and are in good agreement with the regular FEM results.

A variety of results involving complex arrangement of passive elements will be presented and discussed at the conference.

4   Conclusions

Three different approaches have been proposed and applied to the shielded two port microstrip geometry. These approaches can be applied to similar geometries which include inductors and capacitors as well. Generalization of these approaches might lead us to analyze structures having active lumped elements and to utilize harmonic balance technique with FEM.

References

[1]   T. Shibata and H. Kimura,"Computer-aided engineering for microwave and millimeter-wave circuits using the FDTD technique of field simulations,"Int. Journal of Microwave and

Millimeter-Wave Computer-Aided Engineering. Vol.3, No. 3 pp. 238-250. 1993.

[2] V.A. Thomas, M.E. Jones.M. Piket-May, A. Taflove and E. Harrigan."The use of SPICE lumped circuits as sub-grid models for FDTD analysis." IEEE Microwave Guided Wave Ltters,vol. 4. pp. 141-143, May 1994.

[3] A. Jahnsen and V. Hansen,"Spectral analysis of multiport microstrip circuit with active and passive lumped elements,"EMC, p. 1053,1990.

[4] R.H. Voelker and R. Lomax, "A Finite Difference Transmission Line Matrix method incorporating a nonlinear device model," IEEE Trans. Microwave Theory Tech., vol.38, March 1990,pp.302-312.

[5] K. Guillouard, M.-F. Wong, V. Fouad Hanna, J. Citerne, "A new global Finite Element analysis of microwave circuits including lumped elements," Digest of the 1996 IEEE Microwave Theory Tech. Symposium,vol. 1.

[6] E. Yasan , J.-G. Yook and L. Katehi, "Modeling the interface between fields and devices using the Finite Element Method," Digest of 1996 Progress In Electromagnetic Research Symposium (PIERS).

[7] Jong-Gwan Yook, "Electromagnetic modeling of high-speed high frequency intercon-nects," PhD Thesis,The University of Michigan 1996.
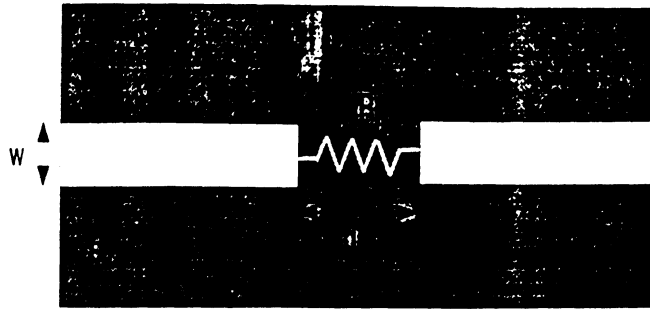
Figure 2: Shielded microstrip circuit with $Z_o = 50\Omega$, $\epsilon_r = 10.5$ w= $0.34mm$ $R = 100\Omega$ h=0.38mm
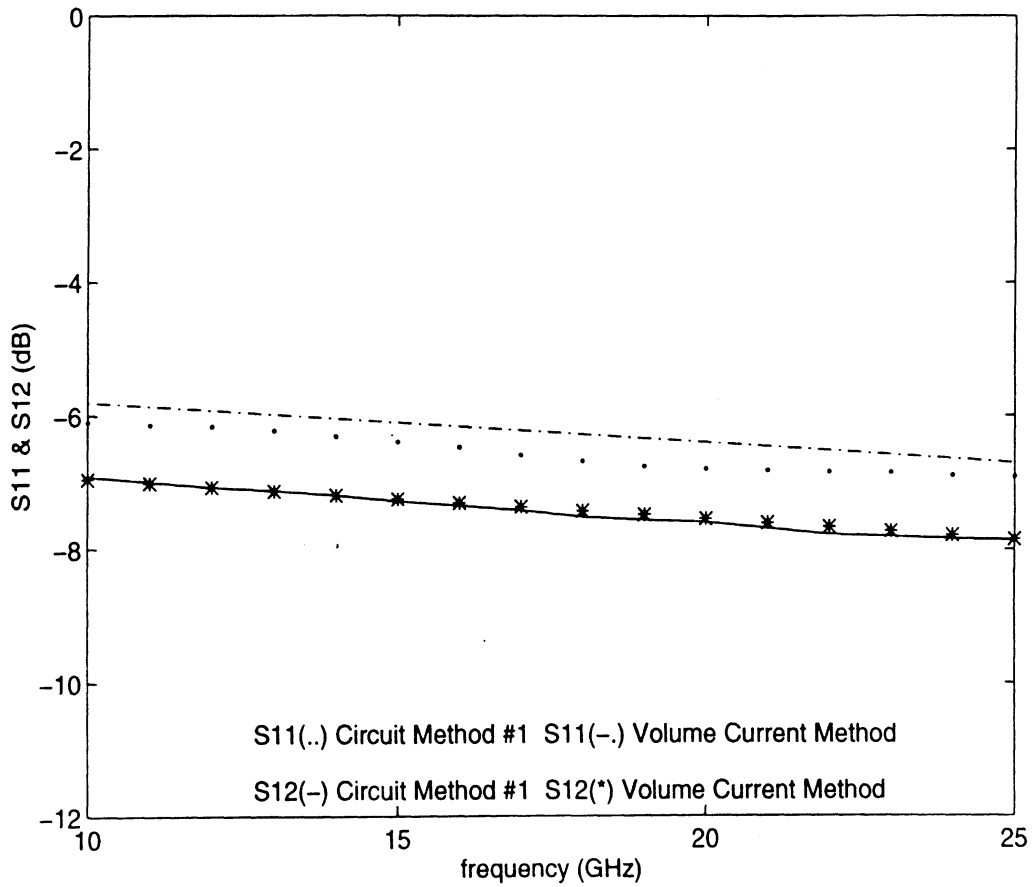
Figure 3: S-parameters of the shielded microstrip circuit with a resistor
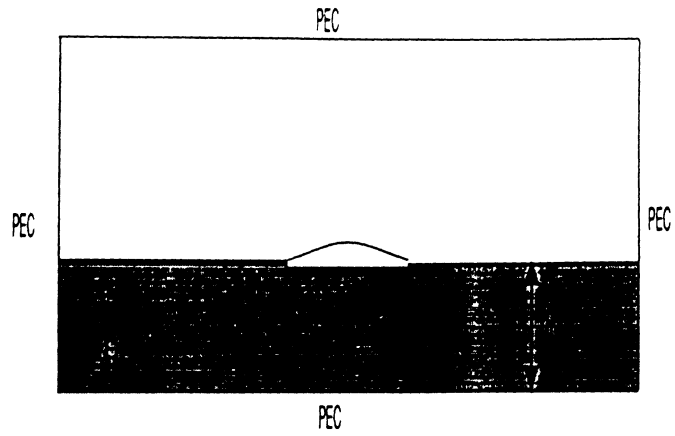
Figure 4: Shielded microstrip circuit with a PEC wire between the conductors
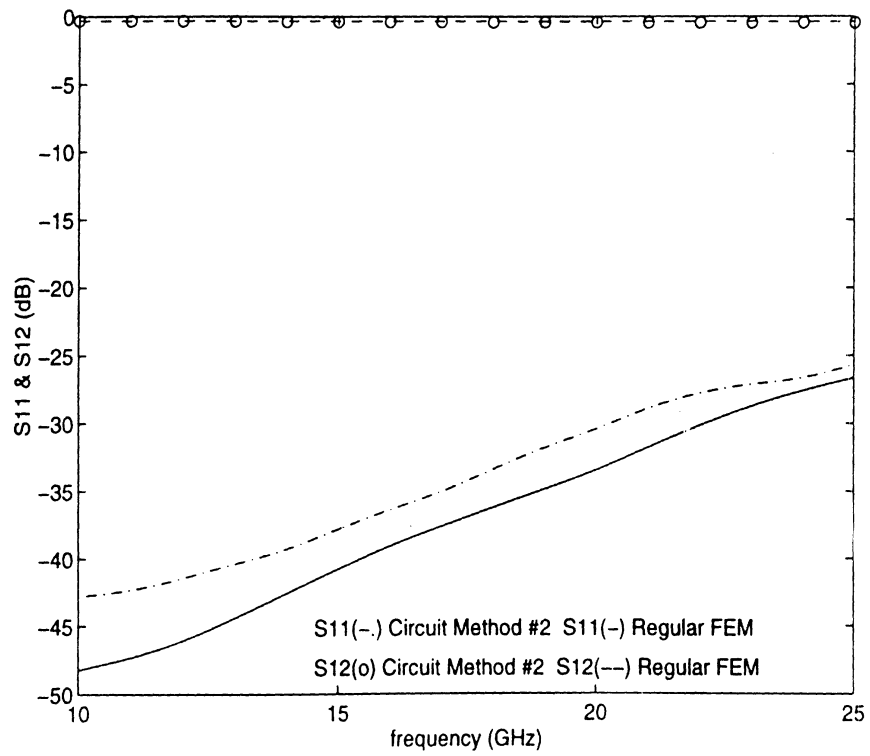
Figure 5: S-parameters of the shielded microstrip circuit with a PEC wire

An FEM Based Method on Full Wave Characterization of Distributed Circuits Including Linear and Nonlinear Elements

Eray Yasan* and Linda P. Katehi

Radiation Laboratory

Dept. of Electrical Engineering and Computer Sci.

The University of Michigan, Ann Arbor, MI 48109-2122, U.S.A.

Tel: 313-764-0502, Fax: 313-747-2106, Email: eray@engin.umich.edu

Theoritical characterization of microwave circuits including linear and nonlinear elements has been an interest in many ways using numerical techniques including Finite Element Method (FEM). Since the lenghts of elements connected to the microwave circuit are very short so that Kirchoff's laws can be applied, the conventional scheme to find S parameters by adding extra line lengths is no more applicable. In this case the circuit is treated as a combination of inner (internal) ports where the linear or nonlinear elements are connected and the outer (external) ports where the input and output of the circuit are taken. Work has been done in time domain using "Compression Approach"(J. Kunish,M. Rittweger, S. Heinen and I. Wolff,Proc. 21st European Microwave Conf.,1296-1301,1991).

The linear passive part of the circuit is analyzed using the FEM. The ports are excited one at a time while the others are left open to derive the appropriate voltages and currents at all ports. The linear part of the circuit is thus characterized by the impedance matrix (Z-matrix). To reduce the computational cost, circuit symmetries are used and assuming circuit lossless, S parameters can be found using the simple relation

$$\left([Z] + [I] \right)^{-1} \left([Z] - [I] \right) = [S] \, .$$

Following the computation of scattering matrix, a simulation software such as HP EEsof Libra and connecting the linear or nonlinear elements to the inner ports yields the input and output S-parameters of the microwave circuit.

As an example a microstrip line with a gap where a lumped element is connected has been analyzed. Simple lumped elements like resistors,capacitors and inductors have been connected and the resulting circuits have been modeled successfully. A diode mixer on a coplanar waveguide (cpw) designed for higher power handling capability has been analyzed using the above method in connection with Harmonic Balance Method (HBM). Results from these studies will be presented and discussed extensively.

electromagnetic field while the wider spaced via holes permit a significant leakage of power. Note that ΔS/h=1 in both of these field plots.

In case where we need to locally improve isolation, the continuous via fence may be replaced by a short via fence as shown in Figure 5 [2]. Figures 6 (a) and (b) show the simulated performance for this line. It is seen that the scattering parameters and radiation loss vary with ΔS/h in the same way as the continuous via fence. However, upon comparison with Figures 2 and 3, there is 5 dB degradation in the line characteristics. Figure 7 shows that this is due to the perturbation of the fields upon reaching the via fence on either side of the strip.

The electromagnetic fields that escape the confinement of the via fences and result in radiation loss cause coupling between adjacent striplines as shown in Figure 8. Figure 9 shows the magnitude of the total electric fields for two striplines separated by a via fence with ΔS/h=0.615 and Δh/h=0.764 (h=0.7366mm). The stripline on the left has an imposed voltage on it while the stripline on the right is coupled. Separation of the field into its components shows that electric field in the plane of the strips is approximately 10 dB greater than the electric field normal to the strips near the via fence. The large magnitude of this parallel field component is due to the small via size and large value of Δh/h, resulting − 10 dB coupling between the strips. Although perfect conductors were assumed in this study, the current distribution on the strip with a close via fence is expected to cause an increase in conductor loss compared to the conventional stripline case.

Conclusions
It has been shown that when filled via fences are placed too close to the stripline, radiation loss increases resulting in coupling between adjacent striplines. To minimize the radiation loss, the via fence should be kept at least four times the ground plane separation away from the strip, or ΔS/h>2. Furthermore, the use of via fences locally only where isolation is required, can actually degrade the stripline characteristics by causing a large perturbation in the electric fields that normally extend on either side of the strip.

References
1. J. W. Gipprich, "EM modeling of via wall structures for high isolation stripline," Digest for Workshop WWFC, Interconnect and Packaging Technologies and Issues, IEEE Int. Microwave Symp., San Diego, CA, pp. 78-114, June 1994.
2. J. Gipprich, C. Wilson, and D. Stevens, "Multilayered 3-D packaging issues," Digest for Workshop WFC, Interconnects and Packaging for RF Wireless Communications Systems, IEEE Int. Microwave Symp., Denver, CO, June 8-13, 1997.
3. J.-G. Yook, N. Dib, and L. Katehi, "Characterization of High Frequency Interconnects using Finite Difference Time Domain and Finite Element Methods, " IEEE Trans. Microwave Theory Tech., pp. 1727-1736, vol. 42, Sep. 1994.

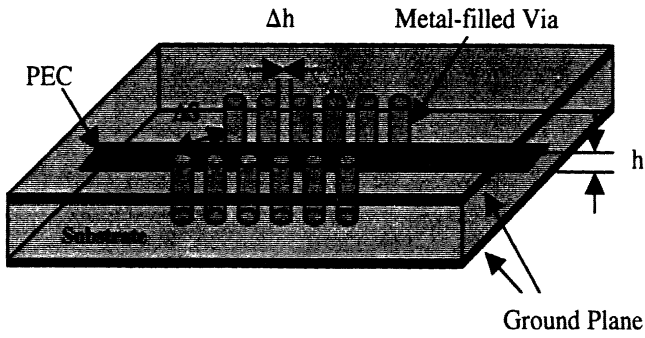Fig. 9 Electric field distribution of two striplines separated by a continuous fence f=10GHz, ΔS/h=0.45, and Δh/h=0.5).

Fig. 5 Stripline with a short section of a filled via fence on both sides.
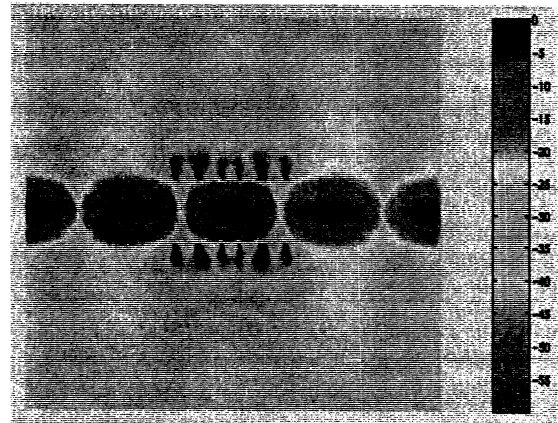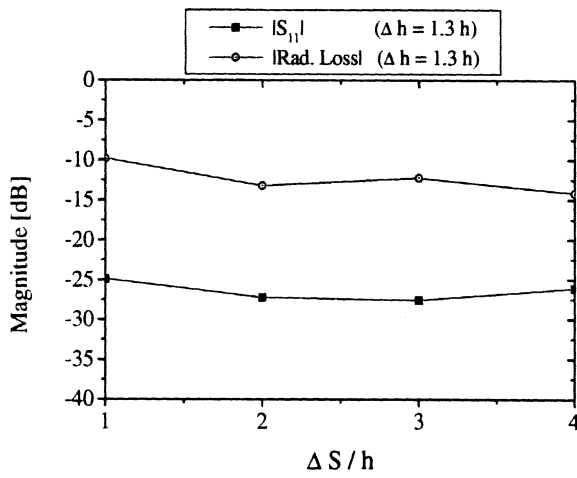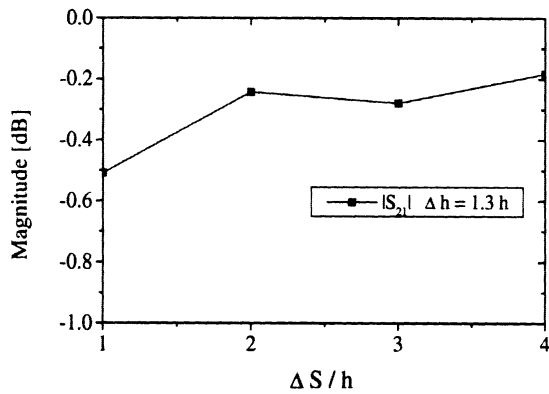

Fig. 7 Electric field distribution of stripline with a short via fence at 25GHz with $\Delta S/h=1$ and $\Delta h/h=1.3$.

(a)

(b)

Fig. 6 (a) Return loss and radiation loss, $1-|S_{11}|^2-|S_{21}|^2$, of stripline with a short via fence as a function of $\Delta S/h$, $\Delta h/h=1.3$, (b) Insertion loss of stripline with a continuous via fence as a function of $\Delta S/h$, $\Delta h/h=1.3$.
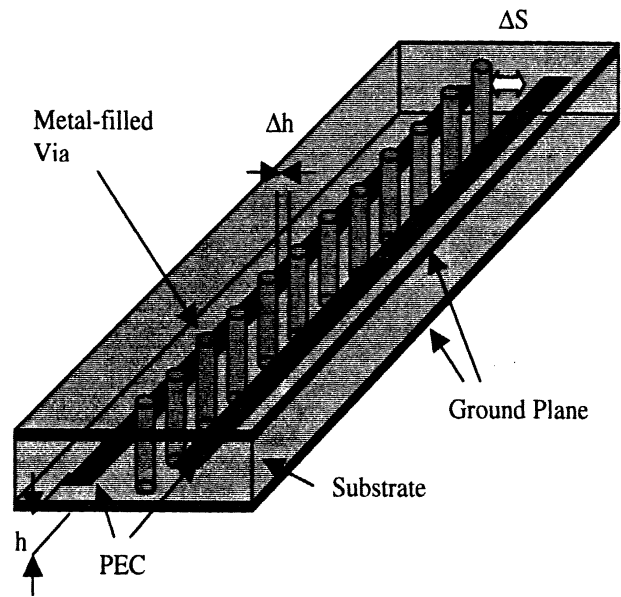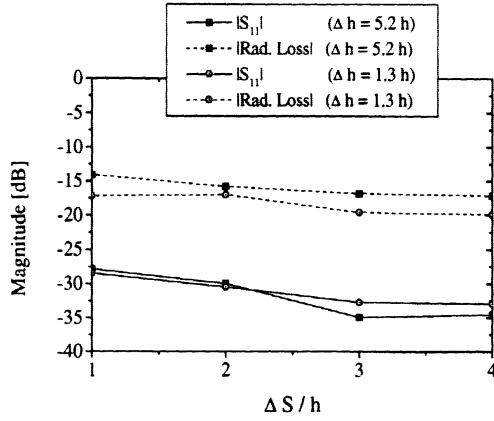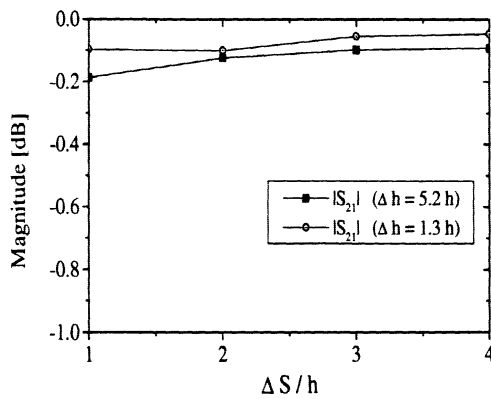

Fig.8 Adjacent striplines separated by via fences.

(a)

(b)

Fig. 2 (a) Return loss and radiation loss, $1-|S_{11}|^2-|S_{21}|^2$, of stripline with a continuous via fence as a function of $\Delta h/h$ and $\Delta S/h$, (b) Insertion loss.
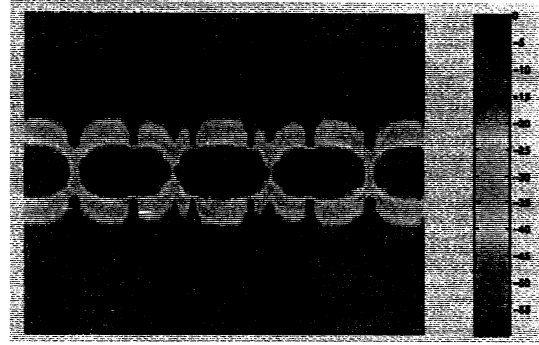

Fig. 3 Electric field distribution of stripline with a continuous via fence at 25GHz with $\Delta S/h=1$ and $\Delta h/h=5.2$.
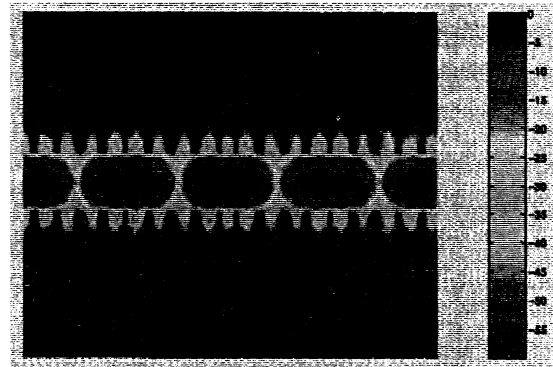

Fig. 4 Electric field distribution of stripline with a continuous via fence at 25GHz with $\Delta S/h=1$ and $\Delta h/h=1.3$.

diameter, Dv, is 0.25 mm; the width, W, of the stripline is 0.19 mm to yield a 50 Ohm characteristic impedance; and the thickness, h, is 0.25 mm. The distance between the stripline and the vias is kept greater than 0.25 mm and the via-to-via spacing ranges between 1.3 and 5 times the via diameter. These values are all standard for typical LTCC processes and thus make these results directly applicable to the packages being designed today.

The first structure investigated is a single stripline with a via fence on both sides of the strip as shown in Figure 1. This is a typical structure to ensure suppression of the parasitic parallel plate waveguide modes. The transmission lines are first analyzed over the frequency range of 10 to 40 GHz. It is found that the scattering parameters do not vary by more than a few percent over this frequency range as long as $2\Delta S+W<\lambda_d/2$ where λ_d is the wavelength in

the dielectric. This condition is necessary to avoid the excitation of dielectric filled rectangular waveguide modes. Based on this finding, the results are presented as a function of the line geometry with the average of the scattering parameters plotted. Figures 2 (a) and (b) show the magnitude of S_{11}, S_{21}, and the radiation loss, $1-|S_{11}|^2-|S_{21}|^2$, as a function of the transmission line geometry. It is seen that the reflection coefficient, the insertion loss, and the radiation loss all decrease as the separation between the strip and the via holes, $\Delta S/h$, increases. Reduction of the parasitic effects levels off as $\Delta S/h$ approaches 2. Furthermore, it is seen that the insertion loss decreases as the distance between the via holes decreases. Field distribution for a stripline with large narrow via hole spacing are shown in Figures 3 and 4 respectively. These plots indicate that the closely spaced via fence completely confines the

CEN4/ ELECTROMAGNETIC SOURCE FREQUENCY CIRCUIT

- **Jong-Gwan Yook and Linda P.B. Katehi**
  The University of Michigan

- **Barry Perlman** Army Research Lab

- **Jim Harvey** Army Research Office

- **Leo Di Dominico** Army Research Lab

- **Contributors :**
  Jui-Ching Cheng and Donghoon Chen
  The University of Michigan

H PCMO

CEN4/ ELECTROMAGNETIC SOURCE FREQUENCY CIRCUIT

➤ **Goal**

➤ Real Time Design and Optimization of Large Scale
Electromagnetic Problems with Emphasis on Three-
Dimensional MMICs/Antennas

➤ **Approach**

➤ Develop Computationally Efficient Codes by Use of MRA
(Multi-Resolution Analysis)

➤ FWT (Fast Wavelet Transform) for Accelerated
Computations

➤ Develop Code Parallelization Schemes for Maximum Speed

H PCMO

Relevance to Army/DoD and Impact

➤ **BCIS-DS** (Battlefield Combat Identification

Systems-Dismounted Soldier)

- Need for Better Design
- Need for Faster Turnaround
- Need for Lower Cost
- Need for Better System Evaluation

H PCMO

Relevance to Army/DoD and Impact (cont.)

➤ **LongBow** Point-to-Point Communications

- Need for Conformal Flat Array Design
- Mixed Analog/Digital Circuits
- Need for Single Iteration Designs and Verification

H PCMO

Relevance to Army/DoD and Impact (cont.)

➤21st Century Land Warrior-

Digitized Battlefield

- Need for Conformal Small High-Efficiency Antennas for PCS

- Need for Very High-Density Low Weight   Circuit Designs

H PCMO

CEN4/ Goal : Three-Dimensional Integration

Radiating Elements

Coupling Slots

Feeding Network

Source Layer
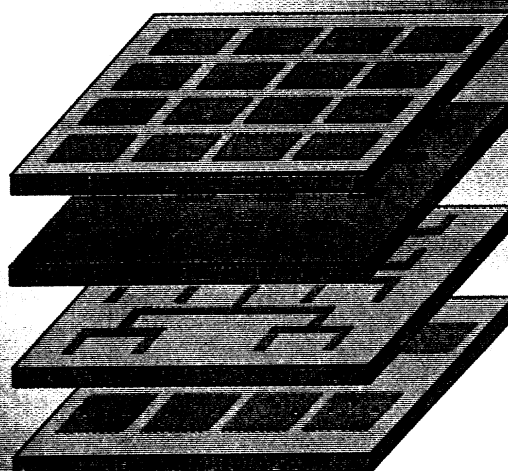
H PCMO

CEN4/ Goal - Size and Memory Budget

- **Microstrip Patch Array Layer: 6 x 6 Elements**
  - 9,500 unknowns
  - 9,500x9,500 matrix = 90,250,000 entries
  - 99.9% sparsity : 902,500 non-zero elements
- **Coupling Slot Layer:** 6x6 slots
  - 540 unknowns
  - 540x540 matrix= 291,600 entries
  - 85% sparsity: 43,740 non-zero elements
- **Distribution Layer:**
  - 9,000 unknowns
  - 9,000x9,000 matrix=81,000,000 entries
  - 99.9% sparsity:810,000 nonzero elements
- **Total Budget with Coupling Terms:**
  - 19,040 unknowns
  - 362,521,600 matrix entries
  - 1,756,240 nonzero elements

H PCMO

CEN4/ Goal - Size and Memory Budget

- **Parallelization Strategies**
  - Parallel Computation of Matrix Entries Using FWT -
  - compute 45,000 nonzero elements
  - Parallel Matrix Solver
  - Frequency Parallelization
- **Computational Requirements**
  - Required Core Memory > 512 Mbyte
  - Required Communication Latency < 10 μsec
  - Required Bandwidth > a few hundred Mbytes/sec
  - Preferred Computers: IBM SP2, Cray T3D, Cray Y-MP,
  - C90, SGI Powerchallenge

H PCMO

- Separate Problem Domain into Subdomains
- Replace Green's Function with FEM Solution in Areas where Green's Function is Unknown
- Match Boundary Conditions Between Domains
- Apply Galerkin's Moment Method
    - Build Impedance Matrix
        - Apply FWT and Thresholding
- Solve the Resulting Sparse Matrix Equation

H PCMO

Match boundary conditions
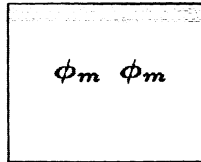
Green's function: unknown
Use FEM to replace the
Green's function

$\delta\Omega$

Ω_{in}

Ω_{out}

Green's function: known
Use the Green's function

H PCMO

FWT and Thresholding

Elements to be computed: 45,105

$$\phi_m \quad \phi_m$$

Matrix Size: 9504x9504

FWT

Sparsity: :99.7

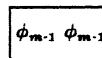| $\phi_0 \phi_0$	$\psi_0 \psi_1$	· · · · · ·
$\psi_1 \psi_0$	$\psi_1 \psi_1$	· · · · · ·
· · ·	·	
· · ·	·	$\psi_{m-1} \psi_{m-1}$

Parallel FWT

Parallelized F.W.T.

$$\phi_m \quad \phi_m$$

$\phi_{m-1} \quad \phi_{m-1}$

$\phi_{m-1} \quad \psi_{m-1}$
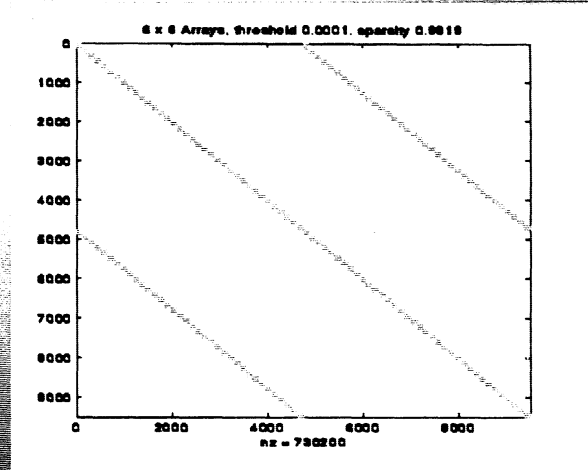
$\psi_{m-1} \quad \phi_{m-1}$

$\psi_{m-1} \quad \psi_{m-1}$
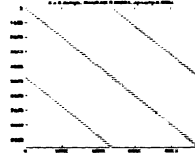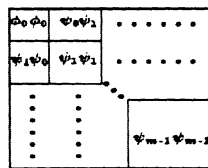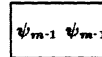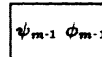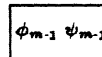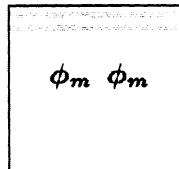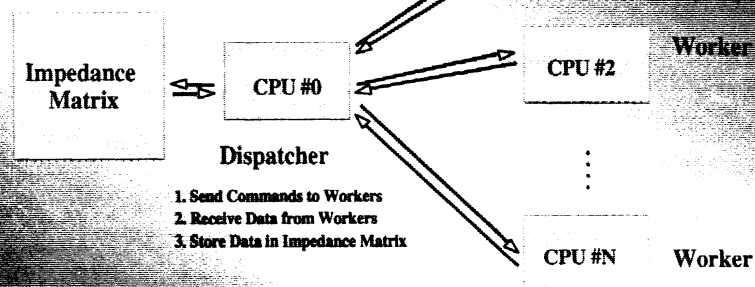
CEN4/ Array layer: **Near matrix-diagonalization**

Thresholding = 0.001: Sparsity=99.19%

H PCMO

CEN4/ Parallelization Model of Impedance Matrix Fill
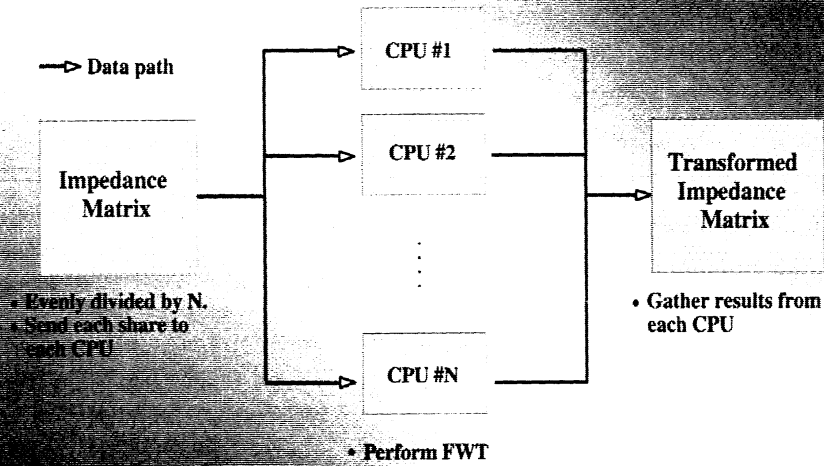
— ▷ Command path
— ▷ Data path

Impedance Matrix

CPU #0

Dispatcher

1. Send Commands to Workers
2. Receive Data from Workers
3. Store Data in Impedance Matrix

CPU #1   Worker

CPU #2   Worker

CPU #N   Worker

1. Receive Commands from Dispatcher
2. Perform Computation
3. Send Result to Dispatcher

H PCMO

CEN4/ Parallelization Model of Fast Wavelet Transform

—▷ Data path

Impedance Matrix

CPU #1

CPU #2

⋮

CPU #N

Transformed Impedance Matrix

- Evenly divided by N.
- Send each share to each CPU

- Gather results from each CPU
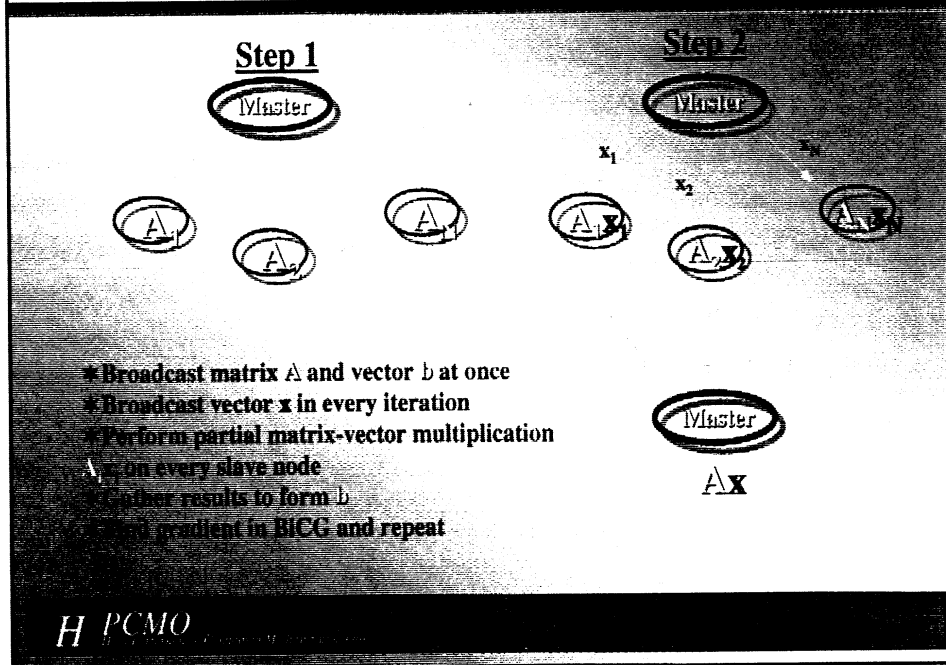
- Perform FWT

H PCMO

CEN4/ Parallelization of Linear Equation Solver

- Per frequency point, 80 to 90% of solution time is spent in the linear equation solution routine
- In the BiCG routine, more than 90% of time is spent by matrix-vector multiplication
- This approach resolves memory and time requirements due to problem size and complexity
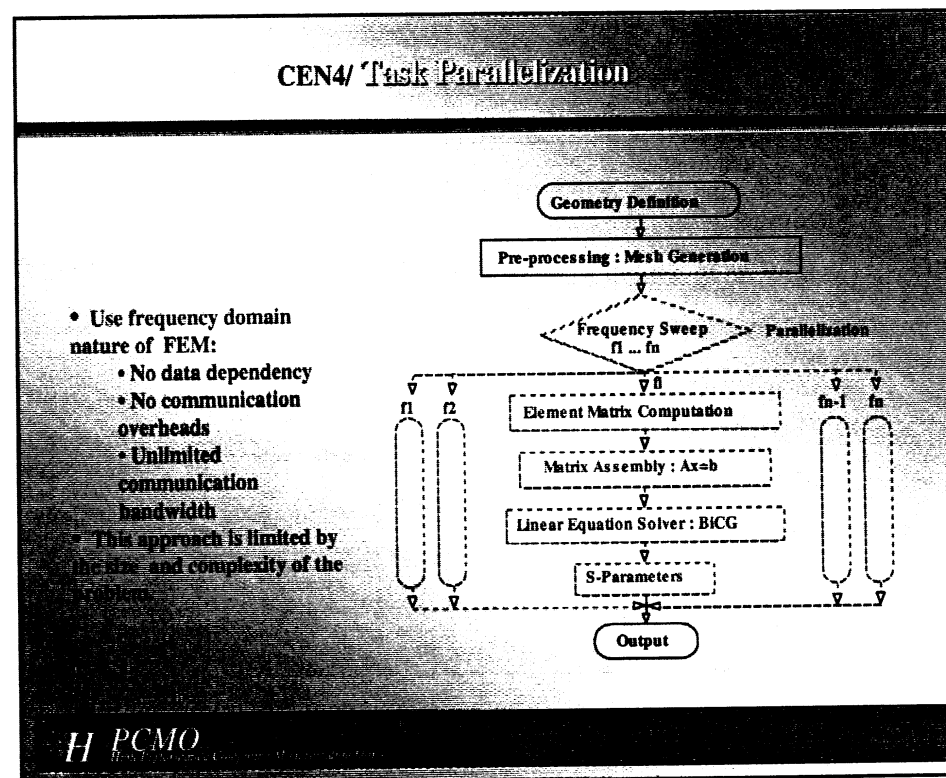- It performs frequency computations serially

Geometry Definition

Pre-processing : Mesh Generation

Frequency Sweep f1 ... fn

Element Matrix Computation

Matrix Assembly : Ax=b

Linear Equation Solver : BiCG   Parallelization

S-Parameters

Output
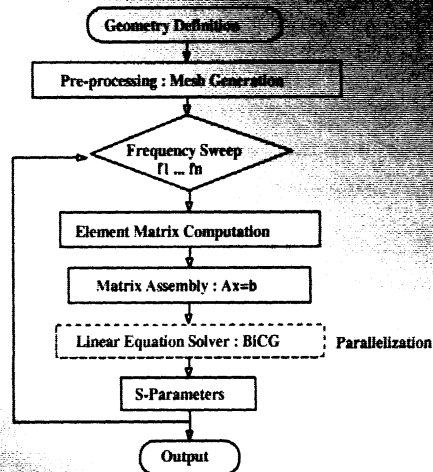
H PCMO

CEN4/ Approach: Parallel Matrix Multiplication

Step 1

Master

A_1 A_1 A_1

A_1x A_2x A_Nx

Step 2

Master

x_1

x_2

x_N

Master

Ax

*Broadcast matrix A and vector b at once
*Broadcast vector x in every iteration
*Perform partial matrix-vector multiplication
$A_i x$ on every slave node
*Gather results to form b
*Find gradient in BICG and repeat

H PCMO

CEN4/ Task Parallelization

Geometry Definition

Pre-processing : Mesh Generation

Frequency Sweep
f1 ... fn

Parallelization

* Use frequency domain
nature of FEM:
  * No data dependency
  * No communication
  overheads
  * Unlimited
  communication
  bandwidth
*This approach is limited by
the size and complexity of the
problem

f1   f2

fn-1   fn

fl

Element Matrix Computation

Matrix Assembly : Ax=b

Linear Equation Solver : BICG

S-Parameters

Output

H PCMO

Impedance Matrix Fill for Single Patch Antenna
(240 matrix elements, Toeplitz Matrix)

Time(i) = P + Comm x N + Comp x N / (i - 1), for i >1

P: preprocessing time.
Comm: commnunication time.
Comp: computation time.
i: number of CPUs.
N: number of matrix elements.

Number of CPUs
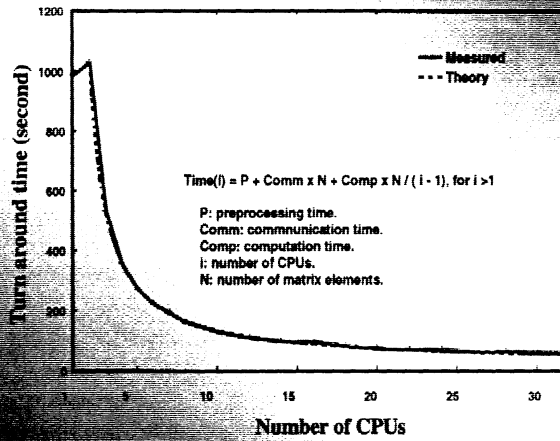
H PCMO

Fast Wavelet Transform for Single Patch Antenna
(3568 matrix elements, Not Toeplitz Matrix)

Time(i) = O + Comm x N + Comp x N / i

O: overhead.
Comm: communication time.
Comp: computation time.
i: number of CPUs.
N: number of matrix elements.
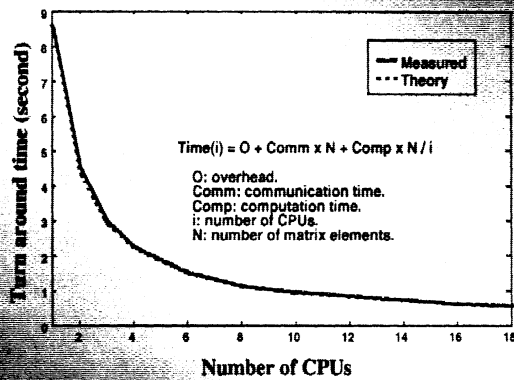
Number of CPUs

includes the extra function calls for measuring time and
processing.

H PCMO

CEN4/ 3X3 Patch Array Radiation Patterns: E
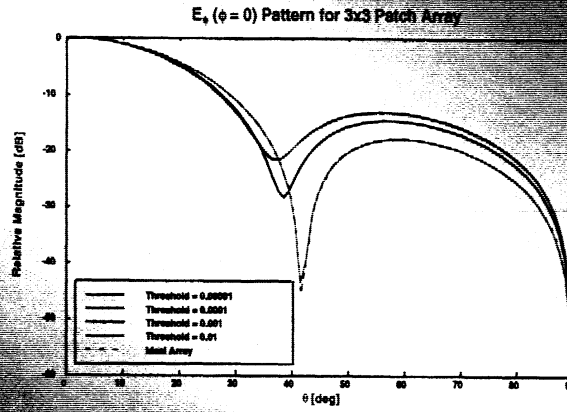
E_ϕ (ϕ = 0) Pattern for 3x3 Patch Array

* Number of Unknowns = 2376
* Total Number of Matrix Entries = 5,645,376
* Computation Time = 1.5 hours on 32 CPUs

H PCMO

CEN4/ 3x3 Patch Array Radiation Patterns: E
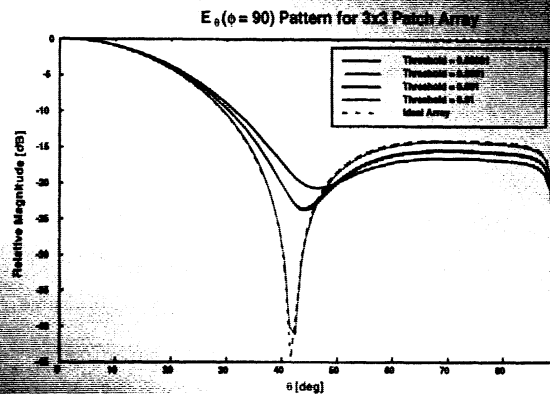
E_θ (ϕ = 90) Pattern for 3x3 Patch Array

* Number of Unknowns = 2376
* Total Number of Matrix Entries = 5,645,376
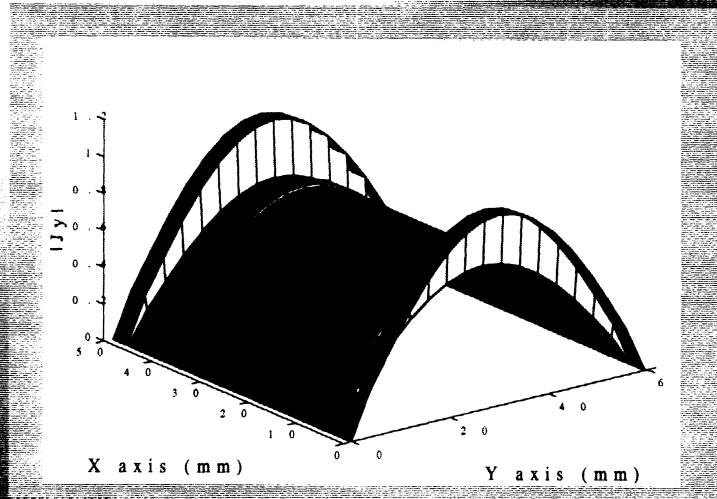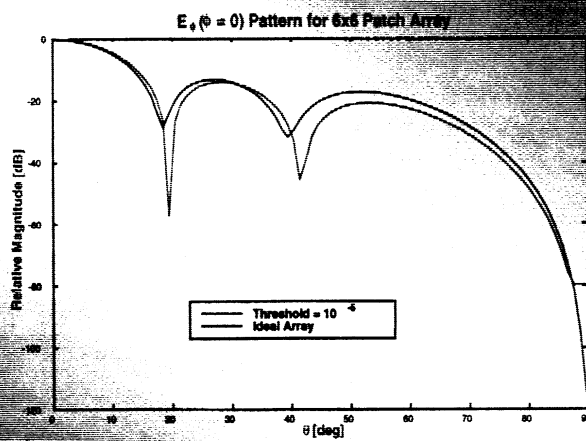* Computation Time = 1.5 hours on 32 CPUs

H PCMO

CEN4/ Current Distribution on a Patch
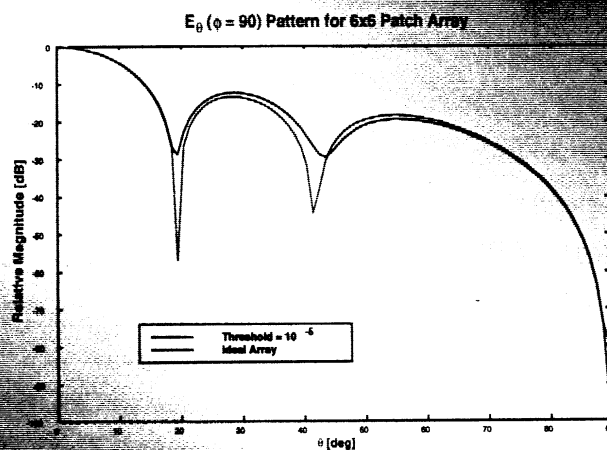
H PCMO

CEN4/ Near Field Distribution

H PCMO

CEN4/ 6x6 Patch Array Radiation Patterns: E

E_ϕ (ϕ = 0) Pattern for 6x6 Patch Array

Threshold = 10^{-6}
Ideal Array

* Number of Unknowns = 17,280
* Total Number of Matrix Entries = 298,598,400
* Computation Time = 4 hours on 32 CPUs

H PCMO

CEN4/ 6x6 Patch Array Radiation Patterns: E

E_θ (ϕ = 90) Pattern for 6x6 Patch Array

Threshold = 10^{-6}
Ideal Array

* Number of Unknowns = 17,280
* Total Number of Matrix Entries = 298,598,400
* Computation Time = 4 hours on 32 CPUs
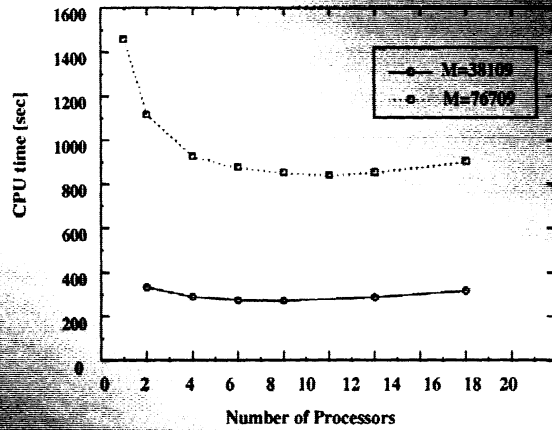
H PCMO

Parallel Matrix-Vector Multiplication

This Approach is Limited by:
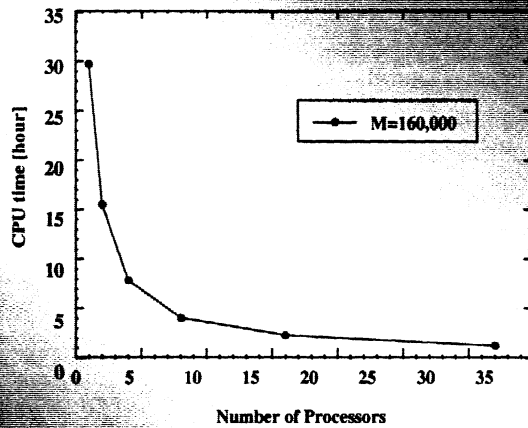*Communication Latency (40µsec)
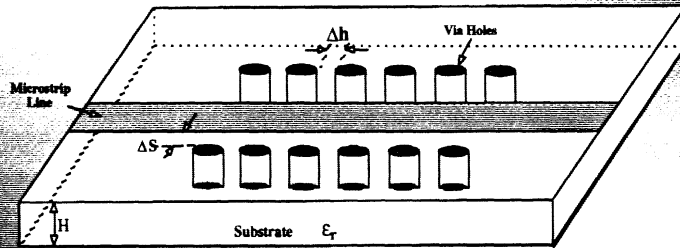*Bandwidth of Switch
*Node Synchronization

H PCMO

Task (Frequency) Parallelization

Linearly scalable parallelization limited by the size and complexity of problem

H PCMO

- Operating Frequency Range = 5 to 40 GHz
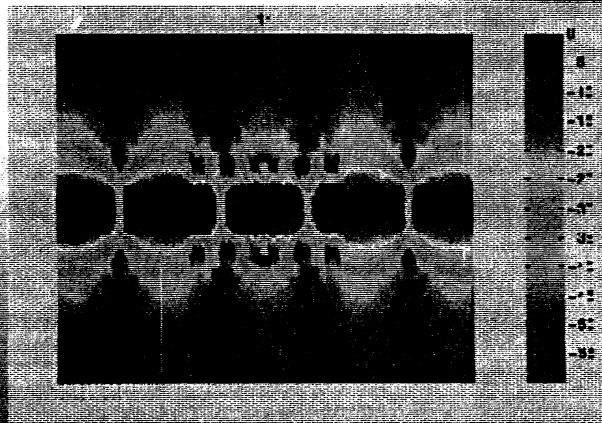- Number of unknowns = 150,000
- Solution time = 2.0 hours

$\varepsilon_T = 5.3$ $\Delta h = 0.4$ mm $\Delta S = 0.25$ mm

$H = 0.25$ mm $W = 0.414$ mm

H PCMO

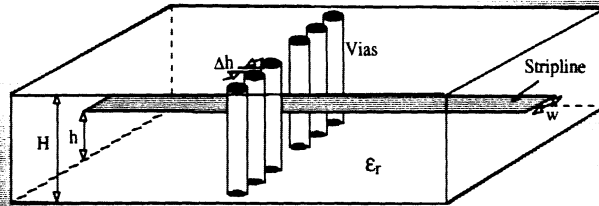**Operating Frequency = 33 GHz**

H PCMO

- Operating Frequency Range = 5 to 40 GHz
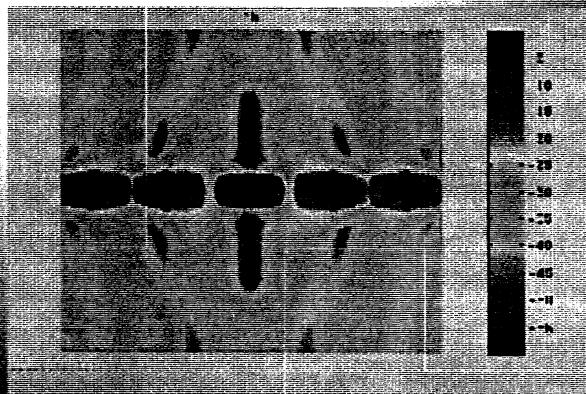- Number of Unknowns = 100,000
- Solution Time = 1.3 hours

$\varepsilon_r = 5.3$

$\Delta h = 0.326$ mm

$\Delta S = 0.25$ mm

H = 0.5 mm

h = 0.25 mm

W = 0.19 mm

H PCMO

Operating Frequency = 28 GHz

H PCMO

➤ **Milestones and Conclusions**

➤ Completion of a Frequency Parallelized Code 12/96

➤ Modeling of a 2in x 2in Ka-Band Single Layer Power Combining Network - About 10^5 Unknowns 12/96

➤ Completion of a Matrix Element Parallelized Code 12/97

➤ Modeling of a 3in x 3in Ka-Band Double Layer 3-D Co-Fired Ceramic Circuit- About 5×10^5 Unknowns 12/97

➤ Completion of a Fully Parallelized Code 12/98

➤ Modeling of a 4in x 4in Ka-Band Multi-Layer 3-D Co-Fired Ceramic Circuit Including Interconnects, Filters and Radiating Structures - About 10^6 Unknowns 12/98
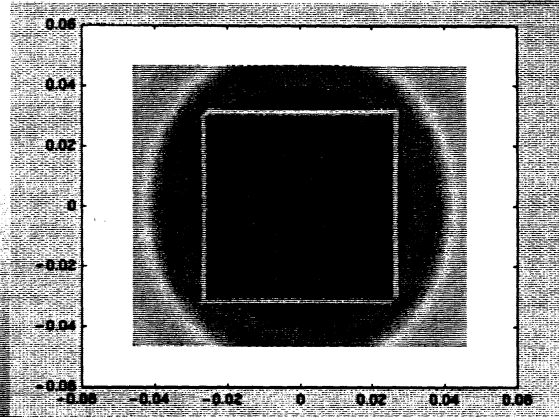
H PCMO

➤ **Teaming**

➤ ARL, Univ of Michigan, NASA Lewis Research Center, Air Force Wright Patterson Laboratory

➤ **POC**

➤ Leo DiDomenico, ARL, (908) 427-2377
ldomenico@ftmon.arl.mil

➤ Linda P.B. Katehi, UofM, (313)647-1796
katehi@eecs.umich.edu

H PCMO

CEN4/ Near Field Distribution for Single Patch Antenna

H PCMO

CEN4/ ELECTROMAGNETIC SOLVE...
FREQUENCY CIRCUITS

Dr. Linda Katehi
Jong-Gwan Yook,
and Donghoon Chen

The University of Michigan

Barry Perlman
CECOM

Jim Harvey
Army Research Office

Leo DiDomenico
Army Research Lab

H PCMO

CEN4/ ELECTROMAGNETIC SOLVERS FO...
CIRCUITS

GOALS

- Design and optimize large scale electromagnetic structures with emphasis on three-dimensional MMIC's and antennas.
- Show that code is capable of efficiently solving for fields that commercial solver can not process easily.
- Demonstrate performance against actual hardware.

H PCMO

IMPACT

- Quick analysis time for designers will reduce development cost.

- New capability for exploration of exotic structures such as multi-layer fractal antennas for ultra-broad broadband EW.

- Conformal & small high-efficiency antennas for mounted and dismounted solder systems.

H PCMO

APPROACH

- Use Hybrid method (Finite Element Method for for antenna feeding network and Method of Moment for patch array antenna)

- Develop code parallelization schemes and optimize code (memory and speed optimization) for maximum speed and large scale problem

H PCMO

STATUS AND SCHEDULE

• Completion of frequency and excitation parallelized code for 3-D double layer 2x2 array patch antenna 9/98

• Optimization of the speed of code (FEM solver & MOM numerical integration routine), and about 45% memory saving FEM code 10/98

• Modeling of 3-D double layer 2x2 array patch antenna - about half million unknowns 11/98

• Completion of code parallelization for solving 1.5 million unknowns   (An increase of 200% over current value) 6/99

• Modeling of 3-D double layer multi-array patch antenna - about 1~1.5 million unknowns 6/99

• Modeling of 3-D multi-layer high frequency circuit - about 1.5 million or more unknowns 12/99

H PCMO

LEVERAGING

This effort can greatly contribute to a number of other projects presently under study:

- DARPA/HUGHES (1996-1999) ($1M)

  "W-Band Power Cube"

- JPL (1998-2003) ($2.5M)

  "System on a chip"

Both of these efforts require full-wave characterization of fairly complex 3-dimensional circuits. The use of the parallelized codes developed by this project can provide for the first time theoretical solutions to these

H PCMO

CEN4/ ELECTROMAGNETIC SOLVER
FREQUENCY CIRCUITS

CAPABILITY IMPROVEMENT

1996

- Frequency parallelization of FEM code (Electric field based, fortran77)

- Modeling of 3-D single layer high frequency circuits - about 100,000 unknowns

1997

- Parallelization of FWT (Fast Wavelet Transform) code

- Parallelization of impedance matrix calculation code

- Modeling of 3-D single layer 6x6 patch array antenna using parallelized FWT and impedance matrix calculation code.

H PCMO

CEN4/ ELECTROMAGNETIC SOLVER
FREQUENCY CIRCUITS

CAPABILITY IMPROVEMENT (cont.)

1998

- Frequency and source parallelization of FEM code for 3-D double layer array patch antenna (Magnetic field based, C++)

- Modeling of 3-D double layer high frequency circuits - about 500,000 unknowns

1999

- Code parallelization for solving 1~1.5 million unknowns

- Modeling of 3-D multi-layer high frequency circuit - about 1.5 million or unknowns

H PCMO

PROGRAMS

Program name	Function	Lang-uage	Programing modle/libraray	Interface	Target platforms	Program developer
Array_FEM.cpp	FEM calculation for array feeding network	C++	MPI Standard	ACSII files	IBM SP2	Juiching Cheng, Donghoon Chen donghoon@engin. umich.edu
Array_MOM.cpp	Method of moment calculation for patch antenna	C++	MPI Standard	ACSII files	IBM SP2	Juiching Cheng, Donghoon Chen donghoon@engin. umich.edu
Array_HYBRID.cpp	Combine FEM, MOM results to get final solution	C++	MPI Standard	ACSII files	IBM SP2	Juiching Cheng, Donghoon Chen donghoon@engin. umich.edu

---

Teaming

- ARL, Univ. of Michigan, NASA Lewis Research Center, Air Force Wright Patterson Laboratory

POC

- Leo DiDomenico, ARL, (734) 764-4239
  leoddd@engin.umich.edu
- Linda P.B. Katehi, UofM, (313)647-1796
  katehi@eecs.umich.edu

CEN4/ Slot coupled array antenna

Example of the type of structure that can be efficiently solved.

2x2 Array antenna

Coupling Slots

Feeding Network
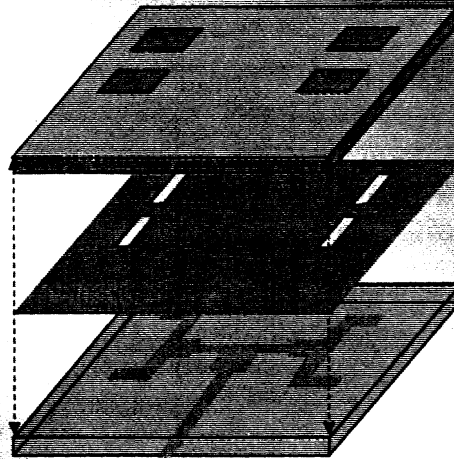
H PCMO

CEN4/ Dimensions
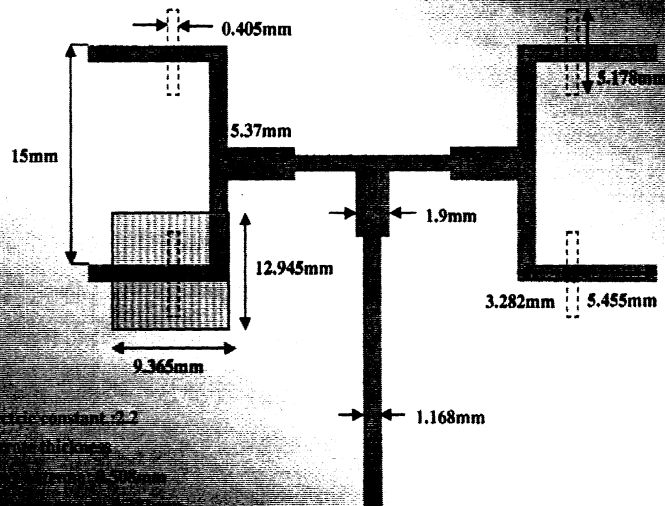
0.405mm

5.178mm

5.37mm

15mm

1.9mm

12.945mm

3.282mm   5.455mm

9.365mm

1.168mm

Dielectric constant: 2.2

H PCMO

CEN4/ ELECTROMAGNETIC SOLVERS FOR FREQUENCY CIRCUITS

Performance Measure
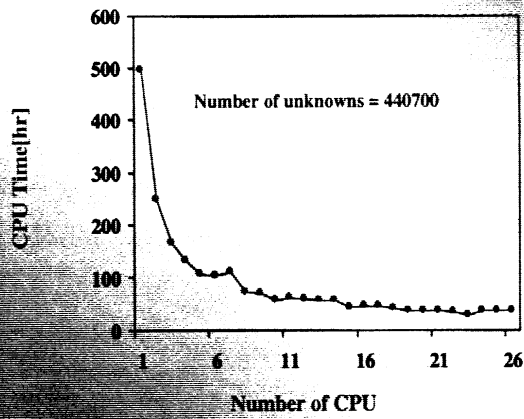
Number of unknowns = 440700

H PCMO

CEN4/ Magnetic Field Distribution in Feeding Network

Operating Frequency = 10 GHz

TOTAL MAGNETIC FIELD DISTRIBUTION

H PCMO

CEN4/   Magnetic Field Distribution in Feeding Network

Operating Frequency = 10 GHz

TOTAL MAGNETIC FIELD DISTRIBUTION
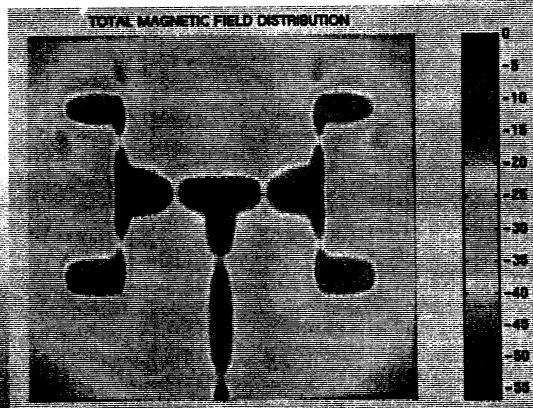
H PCMO
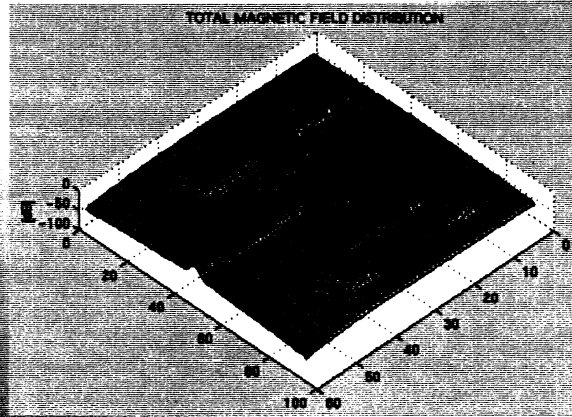
CEN-Project # 4, Parallel Electromagnetic Solvers for High Frequency Antenna and Circuit Design
January 1999

Scope

This document is an update of the progress of CEN-Project # 4 for Electromagnetic Solvers based on parallel processing and multi-resolution analysis.

NOTE: The information in this report supersedes all previous monthly reports.

The following paragraphs will identify a software system for accurate and computationally efficient codes for the solution of large scale electromagnetics problems with an emphasis on planar circuits for high frequency applications. The codes will be developed for use in both stand-alone and parallel processing environments.

Identification

The required software system is an analysis program for accelerated numerical computations in electromagnetics where there exists large computational domains and/or computationally intensive tasks. The output of the software will provide critical information that a designer may use to develop complex RF systems. Typical outputs would include: current distributions, scattering parameters, and field distributions.

The overall objective of the system is to use multi-resolution analysis (MRA) in computational electromagnetics to achieve large sparsity in the integral equation (IE) matrix formulation. Multi resolution expansions in integral based formulation leads to the generation highly sparse linear systems whose solution is fast and efficient with minimal memory usage. In addition, the application of wavelet techniques to the method of moments (MOM) will allow the modeling of large-scale electromagnetics problems to be undertaken. It is expected that matrix sparsities on the order of 99.99% or better will be achievable with the MRA method. A large number of the computations associated with the MRA are in the form of nested loops where similar types of calculations are being performed many times. Therefore, parallelization of the code will also be performed in order to improve the speed and efficiency of this electromagnetics solver.

From a users point-of-view the output of this development effort will be software that will be able to analyze in real-time complex three-dimensional monolithic circuits (MMIC modules) with hundreds of vias and lines interconnecting a number of active and passive circuit components to a large number of radiating elements.

Module Definitions

Open - Space Radiation Problems

1) IMP_SORT This module uses the symmetries or anti-symmetries of the impedance matrix to sort out a list of unique matrix elements. In non-parallized version only.

2) IMP_MAT, IMP_MAT.P : This module (in regular and parallel versions) generates the elements of the impedance matrix for a microstrip patch fed by a slot using the single layer greens function. This program creates a vector of unique non-zero elements.

3) FWT, FWT.P : This module applies the fast wavelet transform to generate the interactions (impedance matrix) for a given module.

4) MAT_SOLVE, MAT_SOLVE.P : This module performs thresholding of the matrix, prepares the matrix for solution and solves it using either Gaussian elimination or BiCG as requested by the user.

5) MoM_POST: This module plots the data calculated by the previous modules in a variety of ways (near field, far field, S-Parameters, ect.)

6) MoM_LIB: This is a library module that contains supporting functions for the above modules.

Circuit Problems

1) FEM_MESH: Generates a tetrahedron mesh using bricks.

2) FEM_MAT, FEM_MAT.P : Generates the FEM matrix for shielded circuit problems.

3) FEM_MAT_ABS, FEM_MAT_ABS.P : Generates FEM matrix for open circuit problems.

4) FEM_SOLVE_BiCG, FEM_SOLVE_BiCG.P : Solves the FEM matrix for lossy circuit problems using a conjugate Orthogonal Conjugate Gradient.

5) FEM_SOLVE_CG, FEM_SOLVE_CG.P : Solves the FEM matrix for lossy circuit problems using a Conjugate Gradient method.

6) IMP_LOAD, IMP_LOADP : Creates the FEM matrix for circuit problems with lumped elements.

7) FEM_POST_FIELD :   Plots field values in a variety of ways as requested by user.

8) FEM_POST_SCAT : Plots scattering parameters.

Module Progress Matrix

| MODULE	Start Date	1st version complete	1st version debug	2nd version complete	2nd version debug	3rd version complete	Complete
IMP_SORT	3/1/96	5/1/96	7/1/96	9/1/96	NA	NA	Y
IMP_MAT.P	7/15/96	2/25/96	4/1/96	3/4/97	3/18/97	NA	Y
FWT.P	5/1/96	6/1/96	8/2/96	3/25/97	4/3/97	NA	Y
MAT_SOLVE.P	5/15/96	6/25/96	10/20/96	12/17/96	NA	NA	Y
MoM_POST	5/25/96	6/15/96	7/15/96	9/30/96	12/1/96	NA	Y
MoM_LIB	7/15/96	6/25/96	8/20/96	12/1/96	2/1/97	NA	Y
FEM_MESH	5/6/95	12/3/95	3/5/96	5/15/96	NA	NA	Y
FEM_MAT.P	3/1/96	4/1/96	5/15/96	11/1/96	NA	NA	Y
FEM_MAT_ABS.P	4/20/95	12/1/95	4/16/96	9/12/96	3/1/97	NA	Y
FEM_SOLVE_CG.P	7/1/95	8/30/95	11/30/95	1/15/96	NA	NA	Y
FEM_SOLVE_BiCG.P	1/1/96	3/20/96	5/1/96	9/13/96	NA	NA	Y
IMP_LOAD.P	4/23/96	7/2/96	12/1/96	1/15/97	NA	NA	Y
FEM_POST_FIELD	2/13/96	4/17/96	6/18/96	10/17/96	10/10/97	10/30/97	Y
FEM_POST_SCAT	2/15/96	5/1/96	7/1/96	10/25/96	9/30/97	11/20/97	Y
IMP_SORT_SLOT	8/15/96	10/11/96	11/29/96	1/19/97	NA	NA	Y
IMP_MAT_SLOT.P	9/25/96	12/1/96	2/27/97	3/11/97	**12/15/98**		Y
MoM_FEM_MAT.P	12/15/96	2/28/97	4/15/97	6/3/97	**2/19/98**	**5/30/98**	Y
MoM_FEM_MAT_ABS.P	3/12/97	3/27/97	4/15/97	5/26/97	**8/30/98**	**12/26/98**	
MoM_FEM_MAT_SOLVE.P	6/3/97	**12/27/97**	**2/25/98**	**5/30/98**	**8/18/98**	**1/4/99**	
FEM_LUMPED	7/20//97	9/30/97					
FEM_LUMPED.P	10/15/97						
MoM_FEM_LUMPED.P	12/20/96						
MoM_FEM_HARM.P							
MoM_FEM_POST_FIELD	9/3/97	9/21/97	**10/10/97**	**12/20/97**	2/20/98	NA	Y
MoM_FEM_POST_SCAT	3/15/97	3/29/97	4/4/97	5/12/97	5/26/97	**1/30/98**	Y
MoM_FEM_ARRAY.P	9/15/97	**12/30/97**	**3/1/98**	**11/20/98**			
MoM_FEM_ARRAY_SORT	10/7/97						
MoM_FEM_ARRAT_MAT.P	10/3/97	**3/15/98**	**6/30/98**	**11/20/98**			
MoM_FEM_ARRAY_MAT_SOLV.P							
MoM_FEM_ARRAY_HARM.P							
MoM_FEM_ARRAY_POST	10/15/97	**3/1/98**	**7/1/98**	NA	NA	NA	Y
FEM_SOLVE_QMR	3/15/97	4/20/97	6/30/97	NA	NA	NA	Y
FRM_SOLVE_CGS	3/10/97	4/10/97	6/15/97	NA	NA	NA	Y

Summary of Progress

1) MOM PART

- New integration scheme/routine is applied for better convergence.
  As a result, calculation time for numerical integration becomes shorter than before.

- The scheme of generating only non-zero unique element of MoM matrix is applied and
  the speed-up is achieved more than two times.

- New parallelization of MoM matrix generation routine is implemented.
  The new version includes new MPI commands to improve calculation time and optimize
  parallelized MoM codes. As shown in the following diagram, the non-zero unique MoM
  matrix elements are assigned to and generated from each processor, and gathered into
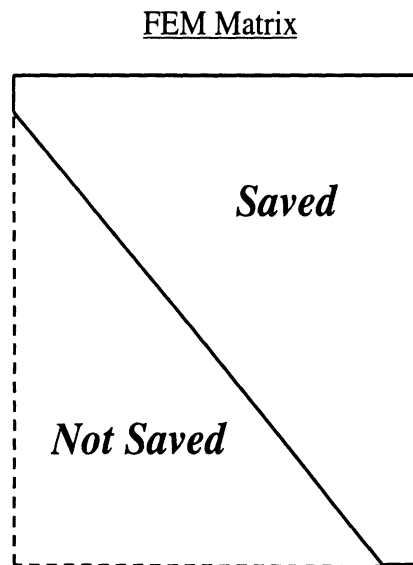 root processor.
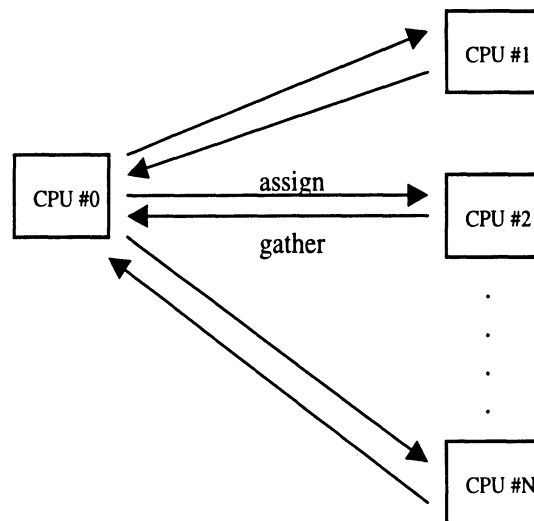
2) FEM PART

- When the feeding network of array structure is solved by FEM, the magnetic sources are
  placed in coupling slots and impedance matrix is calculated for each magnetic source. In this
  aspect, parallelization of solving FEM problem for each magnetic source is necessary and it is
  implemented using task parallelization scheme.
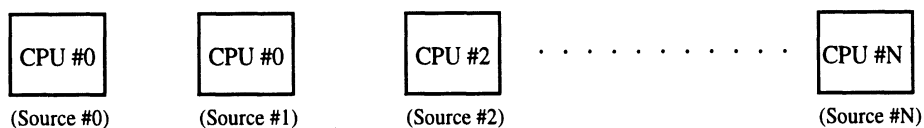
- As FEM matrix elements have symmetry property, we can save about 40% of memory by storing diagonal and upper triangle element of FEM matrix. With this FEM matrix storage scheme, we could solve about half million unknowns.

FEM Matrix

- In order to solve more than half million unknowns, we needed to parallelize FEM routine further more in addition to the above scheme. We found out two major parts of work should be completed : FEM matrix must be decomposed to processors and communication setup between processors when matrix to vector or vector to vector multiplication/addition is occurred in iterative FEM solver. After implementing this parallelization scheme, we could solve 1 million unknows. We are making more effort to solve more than 1 million unknowns and 1.5 million unknowns will be tested very soon. Following is the FEM matrix decomposition scheme applied in this project.

FEM Matrix
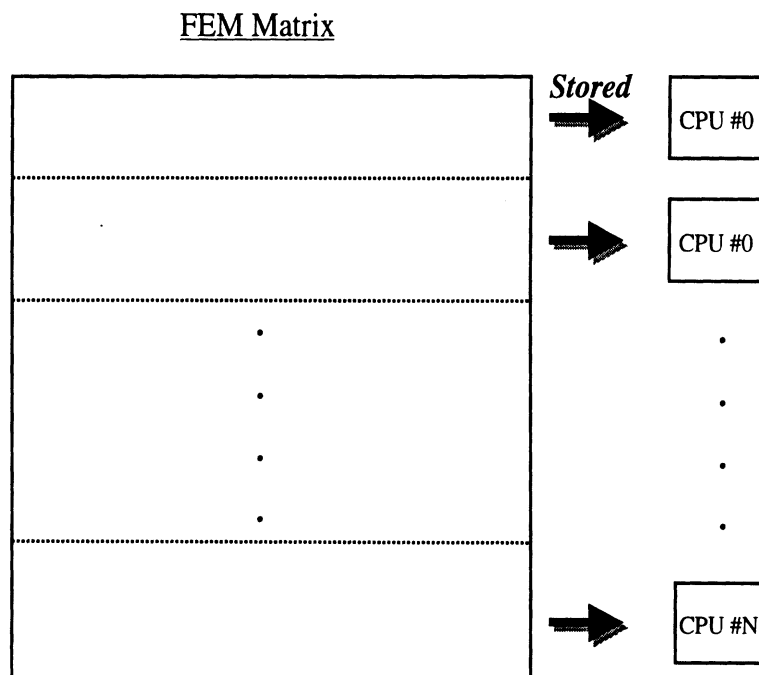
3) Application of progress on Modules

- IMP_MAT_SLOT.P

A new scheme has been applied in evaluating integrals involving singularities when MoM an impedance matrix is generated. The scheme mostly involves a new pole extraction method for the Green's functions which have a singularity over the defined integration range. This implementation is important in for the reduction of computation time, since the new scheme improves convergence when integration is numerically calculated.
Toplize property of MoM matrix element can be used for reducing MoM matrix computation time, because all of the matrix element can be known with non-zero unique matrix elements. The new version of code determines non-zero unique matrix element and computes them. The achieved speed-up with this scheme is more than two times, which is quite significant.
As a result of the above two schemes the MoM part is much improved in terms of computation time.

- MoM_FEM_MAT.P

This was an effort for saving computer memory and produced an improvement in the software's efficiency. An advantage in memory required was achieved by utilizing the fact that the FEM matrix has a symmetry property, the new program stores half of the actual FEM matrix. As a result, the size of memory needed to store FEM matrix is reduced by half. This is a sizable advantage in memory when the size of problem becomes large. We could generate FEM matrix for half million meshes with this scheme.
Further effort was made recently for generating FEM matrix for 1 million meshes. It involves FEM matrix decomposition to processors: root processor divides FEM matrix domain and assigns matrix domains to processors, and each processor generates assigned part of FEM matrix.
The scheme is successfully implemented and we can generate FEM matrix for 1 million meshes. 1.5 million mesh case is under test now.

- MoM_FEM_MAT_ABS.P

This module is an extension of MoM_FEM_MAT.P for open FEM problem. We can adapt same memory saving scheme as before and achieve same improvement as was the case of MoM_FEM_MAT.P. FEM matrix for half million meshes can be generated with this scheme. Similarly, FEM matrix decomposition scheme is applied to open FEM problem and the new code can generate FEM matrix for 1 million meshes.

- MoM_FEM_MAT_SOLVE.P

When the FEM part of a computation is being simulated, most of the solution time is consumed in solving for the FEM matrix elements. It is very important to speed up FEM iterative solver to reduce the resulting CPU time to solve a problem. Most of the operations in the FEM solver are by nature of the physics and computation algorithm of the form of multiplication's and additions of vectors with vectors and vectors with matrices. Therefore, a smart management strategy of the memory for matrix-vector multiplication and the iterative loops was realized using an

assortment of techniques that are utilized under the optimal condition for a particular algorithm. Currently these improvements have allowed computations at twice the previous rate.

When 1 million unknowns are to be solved, the decomposed FEM matrixs are generated from each processor. These matrixs in each processor must be communicated with other processors when multiplication/addition of vector with vector or vector with matrix is occurred in iterative FEM solver. This communication time takes most of FEM computation time when the problem size becomes large. Therefore, careful communication schemes should be applied to reduce overall FEM computation time for large FEM problem. Using most effective communication schemes between processors, the FEM iterative solver is optimized for least communication time. As a result, 1 million unknowns can be solved with this least communication time scheme.

- MoM_FEM_POST_FIELD

When the field distribution of FEM part is plotted, we need to control the plot, for example, by zooming to a certain area, flipping up/down or left/right, and smoothing. The new program is quipped with all these functions using MATLAB's internal functions. In addition, the program can be customized by the user.

- MoM_FEM_ARRAY.P

The FEM solver for the patch antenna problem has been optimized. Most of the optimization involved the efficient management of iteration loops and arithmetic for vector/matrix operations. As a result of this optimization, the speed of the FEM solver has been improved by an additional two times. When the array antenna problem is simulated by hybrid computational techniques, a number of sources are placed in the slot for FEM simulation. The feeding network is simulated for each source using FEM. Therefore, in addition to frequency parallelization, source parallelization is also necessary. To this end, the new program is source parallelized. As a result, the program may be both frequency and source parallelized at the same time.

FEM matrix decomposition scheme and effective communication setup between processors in iterative solver are applied to array antenna problem to solve large size of array feeding network. Currently, 1 million unknowns in array feeding network section can be solved using new FEM routine.

- MoM_FEM_ARRAY_MAT.P

The memory saving scheme of the FEM matrix is adopted in the new program for the ARRAY antenna problem. Using symmetry properties of the FEM matrix, we store only half of the FEM matrix when the feeding network of array antenna is solved by FEM. Considering the large size of typical problems in this case, we can save significant amounts of memory with this new technique.

FEM matrix of 1 million meshes of array feeding network can be generated using FEM matrix decomposition scheme. 1.5 million case is under testing now.

- MoM_FEM_ARRAY_POST

The post-processing file for field distribution of feeding network in array antenna system is customized for easy and convenient use of third parties. The field distribution of feeding networks can be rotated, flipped, smoothed, and magnified.

- FEM_LUMPED

In this program, we have implemented a combination of full-wave electromagnetic simulator (FEM) *and active circuit elements*. This is an extension of the previous work on the inclusion of passive lumped element into FEM tool. As an example, a single diode mixer with a strip-line configuration has been designed and solved using the program. This enhancement of capability of the code allows the user the ability to simulate any type of two port active circuits in full-wave electromagnetic solver. We are currently working on the generalization of this code to simulate multi-port active circuits.

Requirements Traceability Matrix (Module vs. Requirement)

MODULE	Analyzer	Partitioner	Simulation	User Interface	Parallelizing
IMP_SORT		X		X	
IMP_MAT.P	X		X		X
FWT.P	X		X		X
MAT_SOLVE.P			X		X
MoM_POST			X	X	
MoM_LIB					
FEM_MESH		X		X	
FEM_MAT.P	X		X		X
FEM_MAT_ABS.P	X		X		X
FEM_SOLVE_CG.P	X		X		X
FEM_SOLVE_BiCG.P	X		X		X
IMP_LOAD.P	X		X		X
FEM_POST_FIELD			X	X	
FEM_POST_SCAT			X	X	
IMP_SORT_SLOT		X			
IMP_MAT_SLOT.P	X		X		X
MoM_FEM_MAT.P	X		X		X
MoM_FEM_MAT_ABS.P	X		X		X
MoM_FEM_MAT_SOLVE.P	X		X		X
MoM_FEM_LUMPED.P	X		X		X
MoM_FEM_HARM.P	X		X		X
MoM_FEM_POST_FIELD			X	X	
MoM_FEM_POST_SCAT			X	X	
MoM_FEM_ARRAY.P	X		X		X
MoM_FEM_ARRAY_SORT		X			
MoM_FEM_ARRAT_MAT.P	X		X		X
MoM_FEM_ARRAY_MAT_SOLV	X		X		X
E.P.					
MoM_FEM_ARRAY_HARM.P	X		X		X
MoM_FEM_ARRAY_POST				X	

Fault Profiling

Fault profiles will be provided for each module after the module design has officially stabilized. For a module to be considered stabilized the schedule of events table must show a module as complete. Any problems with the module after the completion of the module will therefore be considered a fault. Additional information may be provided on the resolution of significant coding errors if this information is considered significant by the primary researcher, however, these errors will not be considered module faults. In summary, "errors" are associated with modules before the module completion and "faults" are associated with modules after the module completion.

No faults or errors to report for this period.